Proceedings of the I·R·E

MAY, 1944

VOLUME 32 NUMBER 5

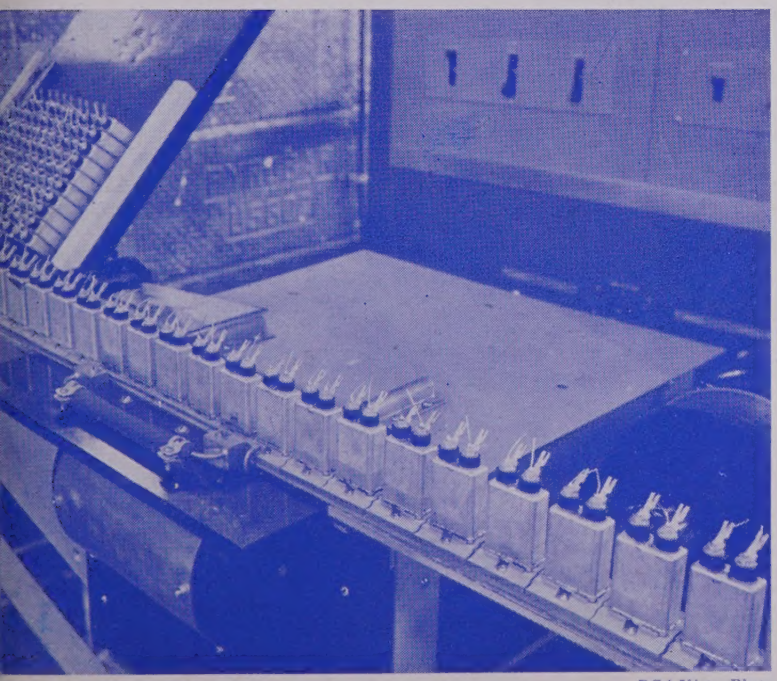

RCA Victor Photo

DENSER-CAN-BASE SOLDERING SPEEDED UP 2500 PER CENT ELECTRONICALLY

Institute of Radio Engineers

WHY AMPEREX

WATER AND AIR COOLED

TRANSMITTING and RECTIFYING TUBES

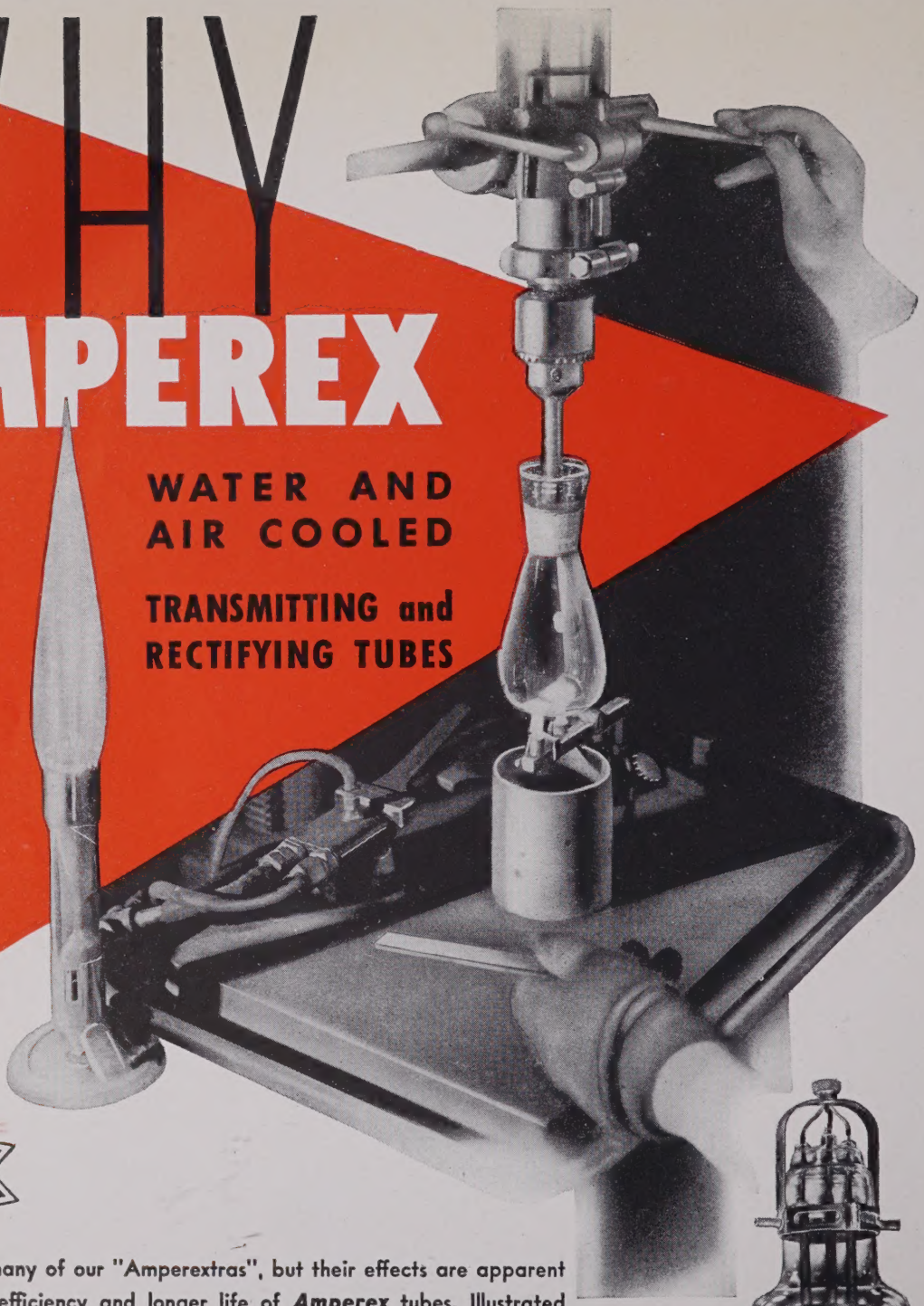

ARMY E NAVY

You can't see many of our "Amperextras", but their effects are apparent in the quality, efficiency and longer life of ***Amperex*** tubes. Illustrated is a highly specialized method of glass fabrication. Among our other novel techniques are sealing operation on rotating fires, precise welding, unique way of sealing glass to copper, extremely careful chemical cleaning. These operations are characteristic of the standards of ***Amperex***—the scientific laboratory on an enlarged scale.

Still Your Best Investment . . United States War Bonds

AMPEREX ELECTRONIC PRODUCTS

79 WASHINGTON STREET BROOKLYN 1, N. Y.

Proceedings of the I·R·E

Published Monthly by

The Institute of Radio Engineers, Inc.

VOLUME 32 — *May, 1944* — NUMBER 5

Entered as second-class matter October 26, 1927, at the post office at Menasha, Wisconsin, under the Act of February 28, 1925, embodied in Paragraph 4, Section 538 of the Postal Laws and Regulations. Publication office, 450 Ahnaip Street, Menasha, Wisconsin. Editorial and advertising offices, 330 West 42nd St., New York 18, N. Y. Subscription $10.00 per year; foreign, $11.00.

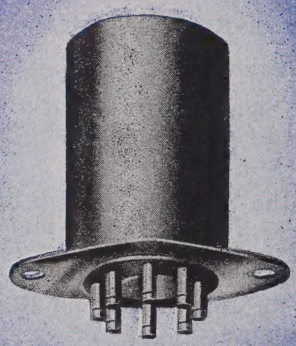

UTC OUNCER

NOW AVAILABLE HERMETICALLY SEALED

The UTC Ouncer type transformer is one of the most popular units in military equipment at the present time.

UTC glass-metal seals have been production proven for over a year. Additional developments have now made it possible to employ this type of sealing in the miniature Ouncer unit . . . 7/8" diameter.

Should you have limited space requirements, this transformer (the smallest hermetically sealed unit now available) can be supplied to specifications.

United Transformer Co.

150 VARICK STREET • NEW YORK 13, N. Y.

EXPORT DIVISION: 13 EAST 40th STREET, NEW YORK 16, N. Y., CABLES: "ARLAB"

Commercial leaders in the radio-and-electronic industry have been invited to present their views on timely subjects to the readers of the PROCEEDINGS OF THE I.R.E. as "guest editorials" which are published in the form in which they are received. It is believed that such editorials will promote vigorous and sound engineering effort.

The President of the Philco Corporation has risen to that post after successfully undertaking direct responsibility for the conversion of his company's operations from civilian to war production and for the handling of its war work. An expression of his viewpoint follows.

The Editor

Radio Looks to the Future

JOHN BALLANTYNE

The radio industry has literally performed engineering and production miracles to do what has been asked of it in this war emergency. The industry is now producing Army and Navy radio and electronic equipment at the rate of $3,200,000,000 annually, an output as great as that of the entire automobile industry in 1939. This is more than six times the "normal" peacetime production of all types of radio receiving sets, radio-phonographs, vacuum tubes, and broadcast equipment in the United States.

Such a tremendous increase in production had, of course, to be preceded by a vast amount of research engineering. Many of radio's assignments are common knowledge, communications equipment to link infantry forces, tanks, airplanes, and ships into one gigantic web of fighting power; walkie-talkie sets for paratroopers and front-line forces; and high-powered transmitting and receiving equipment to hurl messages back and forth with the speed of light between headquarters in Washington and the distant battle areas.

In addition to all these, there are even more important uses of radio-and-electronic equipment that cannot be described while the fighting is on. Many of the "secret weapons" now in use by the United Nations are the result of new practical applications given to radio and electronic principles.

No wonder this has been called a "radio war," for radio is helping in countless different ways to give our fighting forces tremendous advantages over the Axis. That is why the lights in our radio laboratories are burning through the night and why many of the production lines in our radio plants are on a "round-the-clock" basis.

When the full story of this war can be told and radio's part in winning it becomes public knowledge, every single person in the industry will be entitled to take pride in the job that has been done and thankful that they were privileged to participate in it.

What of the future? The next great advance in radio and electronics that will touch all our lives will be television, the magic doorway to the future. You all know the tremendous effect that the addition of sound had in the development of the motion-picture industry. It increased by many times the scope, the dramatic quality, and the influence of motion pictures on the public.

The greatest of all human senses, however, is sight. Human beings place far greater value on their sight than their hearing. Television adds sight to sound; it adds the motion picture to the radio voice and certainly that is a far more vital contribution to radio than the addition of sound was to the movies.

Even before the war television had been developed to such a point that it was possible to provide pictures of greater clarity and detail than are afforded by home movies. Undoubtedly much of the research and engineering work that is now being done by the radio industry as its contribution to the war effort will have collateral benefits for television when there is time to make the necessary applications.

All the evidence now at hand indicates that television will progress rapidly to become one of the nation's important industries as soon as the war is won and technical personnel and materials are available to erect transmitting stations, build receivers, and produce acceptable programs for the public.

Television is going to provide a new and better kind of service for the public; and it is going to create thousands of new jobs in research, engineering, production, sales, service and installation, and programming. With this vision ahead of it, the radio industry can look forward to the future with confidence in the realization that its accomplishments to date, brilliant as they are, represent but a preview of what is to come.

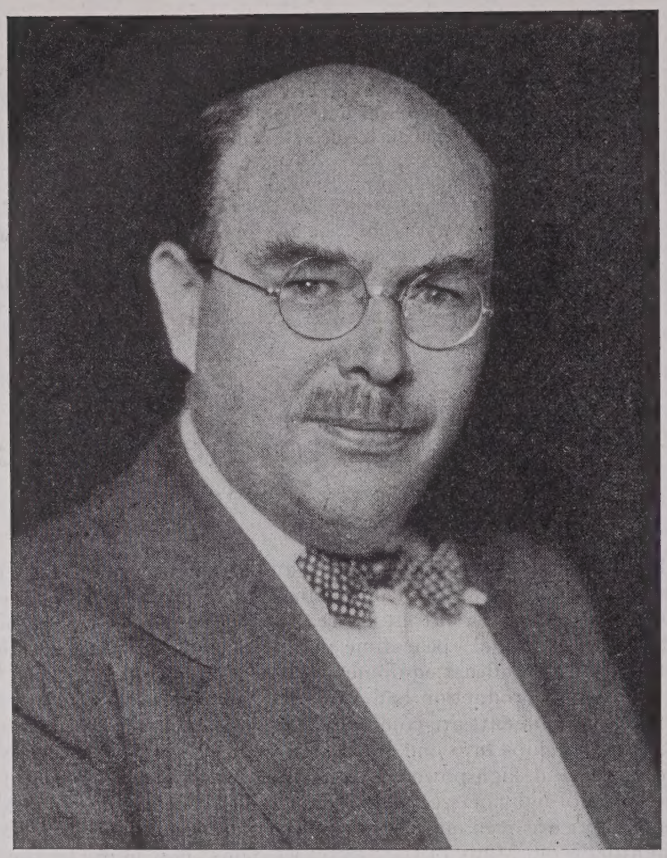

L. C. F. Horle

BOARD OF DIRECTORS—1944

Lawrence C. F. Horle was born in Newark, New Jersey, on May 27, 1892. In 1914 he received the M.E. degree from Stevens Institute of Technology. Following graduation, Mr. Horle became a member of the faculty of the physics department of Stevens, where he remained until 1916, devoting a large part of his time to investigations of vacuum-tube characteristics and development of vacuum-tube circuits. In 1916 and 1917 he was a design engineer of the Public Service Corporation of Newark. The war years of 1917 to 1920 saw him Expert Radio Aide in the Navy Department, in charge of the radio development laboratory at the Washington Navy Yard.

Following his Naval service, he became chief engineer of the de Forest Radio Company and remained in this capacity until 1921. From 1921 to 1924 he was consulting engineer for the Department of Commerce Radio Laboratories, National Bureau of Standards, Washinggon, D. C. In 1924 he became associated with the Federal Telephone and Telegraph Company as chief engineer, becoming vice-president in charge of engineering in 1927. Since 1929 he has been a practicing consultant, specializing in industrial standardization in the communications field, serving since 1941 as civilian consultant to the Army Communications and Co-ordination Board of the Chief Signal Officer, United States Army.

Mr. Horle was elected to Associate membership in the Institute in 1914, transferred to the Member grade in 1923, and to Fellow grade in 1925. He has served on various committees and in 1940 he was president of the Institute of Radio Engineers. He is now a member of the Board of Directors.

He is a Fellow of the American Institute of Electrical Engineers and of the Radio Club of America.

Certain important radio-and-electronic developments are published in a form not readily available to or usable by many readers of the PROCEEDINGS. The Institute deems it desirable to publish at this time English translations of certain of the corresponding papers. Through the appreciated courtesy of the publishers of the original source, the *Journal of Technical Physics* (Russian), the following paper has been placed at the disposal of our readers. Thanks are also expressed to the translator of the paper, A. M. Gurewitsch for his extensive and voluntary efforts.

The Editor

A Metal Triode for Ultra-High-Frequency Operation*

N. D. DEVIATKOV†, NONMEMBER, I.R.E., M. D. GUREVICH†, NONMEMBER, I.R.E., AND N. K. KHOKHLOV†, NONMEMBER, I.R.E.
TRANSLATED BY A. M. GUREWITSCH‡, ASSOCIATE, I.R.E.

Summary—**The metal tube here described (designated type DCM-1) is established as a practical design, suitable for production. It can be used as a converter in the wavelength range of 25 to 30 centimeters, and as an oscillator with a power output of 1 to 5 watts in the wavelength range of 30 to 60 centimeters. It can also be employed as an amplifier with an amplification coefficient[1] K of 3 to 4 at a wavelength of 25 centimeters, or with a K of 6 to 7at λ of 40 centimeters. If used as a regenerative amplifier, a K of 10 can be secured at λ of 25 centimeters, and a K of 15 at λ of 40 centimeters.**

WAVES in the decimeter region find increasing application. The main difficulty of operation below 50 centimeters wavelength was the lack in the Union of Soviet Socialist Republics, of tubes operating efficiently with sufficient power output. In the United States, the appearance of three-electrode tubes of the type described by Samuel[2,3] enabled the designing of a number of radio devices. Recently, greater attention has been devoted to an entirely new principle, namely that of velocity modulation. But it may prove more convenient and practical in some instances to use triodes.

Triodes operating at negative grid potential are of great interest in the decimeter region because they offer the possibility for the solution, in a more conventional fashion, of a considerable number of technical problems. Although the vacuum-tube manufacturing art has made considerable progress and has developed new methods permitting the production of rather complex tube devices, the development of triodes operating in the decimeter region with a power from 4 to 6 watts for oscillators and amplifiers has not been sufficiently advanced in the U.S.S.R. until recently[4,5]. This limitation was caused by the existence of numerous difficulties which were encountered in the construction and engineering fields. In the period 1938–1939, tubes of the type DC 21 were developed by us. The characteristics of this tube made it of major interest for radio engineering applications in the decimeter region. However, the difficulties in the way of mass production of this tube were excessive.

Accordingly, the problem was faced of redesigning the DC 21 tube for mass production. It was decided that the most convenient procedure was to adopt standard methods of radio tube production, and to utilize the general ideas embodied in the American metal tubes which are being produced in large quantities by our factories. After preliminary experiments, the tube shown in Figs. 1 and 2 was developed.

The glass seals on both ends of the metal cylinder enable the connection of coaxial lines. The tube, as thus redesigned, was designated as type DCM-1.

The cathode and grid are mounted as a single unit, after which the plate is sealed in. This process is carried out on a special sealing machine. Experimental operations developed a method of setting the plate-grid distance at a desired value of 0.2 millimeter or 7.8 mils. As will be seen, this tube is a simple triode. The cathode is an oxide-coated disk, of a diameter of 5 millimeters. The heater is a flat spiral. The grid is made of tungsten wire 0.05 millimeter in diameter (approximately 2.0 mils). The distance from wire to wire in the grid is 0.2 millimeter or 7.8 mils. The grid is supported by two nickel disks, each having a central 7-millimeter opening. The grid mesh is welded to these disks, and the disks are then welded to the supporting cylinder. The cathode is attached to a cylinder which in turn is welded to connectors passing through a glass seal (so that the grid and cathode form a unit structure). One side of the

* Decimal classification: R330. Translated from and reprinted by permission of the *Journal of Technical Physics* (Russian), vol. 11, no. 8, pp. 756–761; 1941. English translation received by the Institute, August 17, 1943.

† Leningrad, U.S.S.R.
‡ Electronics Laboratory, General Electric Company, Schenectady, N. Y.

[1] K is defined in the text.

[2] A. L. Samuel and N. E. Sowers, "A power amplifier for ultra-high frequencies," PROC. I.R.E., vol. 24, pp. 1464–1483; November, 1936; *Bell Sys. Tech. Jour.*, vol. 16, pp. 10–34; January, 1937.

[3] A. L. Samuel, "A negative grid triode oscillator and amplifier for ultra-high frequencies," PROC. I.R.E., vol. 25, 10, pp. 1243–1252; October, 1937.

[4] Tsvetkovskii and Dzhibelli, *Izvestiia Elektropromyshlennosti Slabago Toka*, (*Bulletin of the Electrical Weak Current Industry*), Number 5, 1939.

[5] N. D. Deviatkov, E. N. Danil'tsev, and V. K. Khokhlov, Izvestiia Elektropromyshlennosti Slabago Toka, (*Bulletin of the Electrical Weak Current Industry*), Number 2, 1940.

filament is connected to the body of the tube, while the other terminal of the filament is brought out as a separate wire which is placed within the cathode cylinder. The anode is shaped as a flat-ended cone (conical frustrum) at the end of a cylinder. To improve heat conduction, the anode is solidly filled with copper.

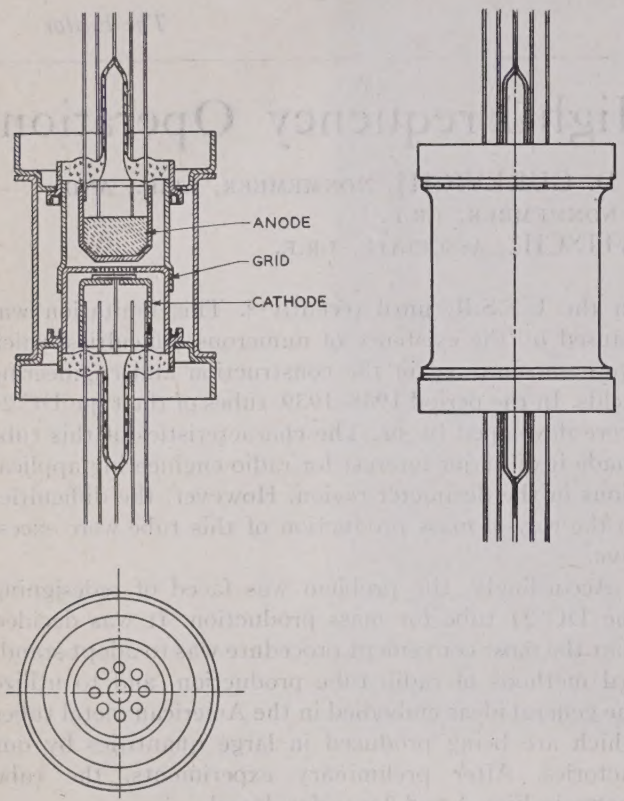

Fig. 1—Cross section of the DCM-1 triode.

Test Results of the DCM-1

The DCM-1 tube was tested in three ways: first as an oscillator; second as an amplifier; and third as an amplifier with regenerative feedback. The static characteristics of the tube are shown in Figs. 3 and 4. Maximum plate dissipation is between 9 and 10 watts. The average interelectrode capacitances are $C_{gp}=2$ micromicrofarads, $C_{gk}=1.8$ micromicrofarads, and $C_{pk}=0.2$ micromicrofarads. The oscillation circuit consists of two coaxial lines which are tunable by means of plungers (forming an end-to-end oscillator) (see Figs. 5 and 6). The plate resonator has an opening through which power can be withdrawn by means of a line connection. Feedback is obtained by the variable capacitance shown in Fig. 5. The DCM-1 tube operates with high stability as an oscillator at 1500 megacycles ($\lambda=20$ centimeters). However, because of capacitance effects, the plate resonator cannot be operated at quarter wave, and it is difficult to obtain the necessary coupling for an appreciable power output. At frequencies of 1200 megacycles ($\lambda=25$ centimeters) and lower frequencies, the operation is more satisfactory.

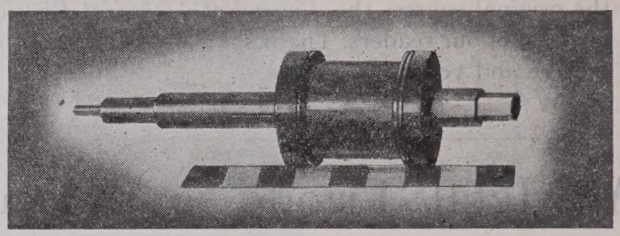

Fig. 2—Over-all view of the DCM-1 triode.

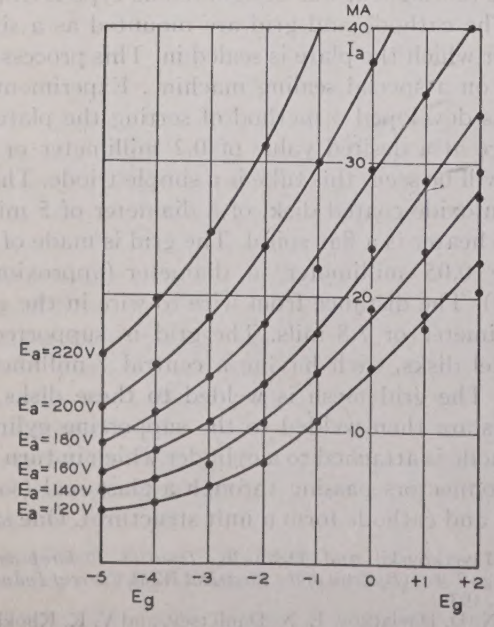

Fig. 3

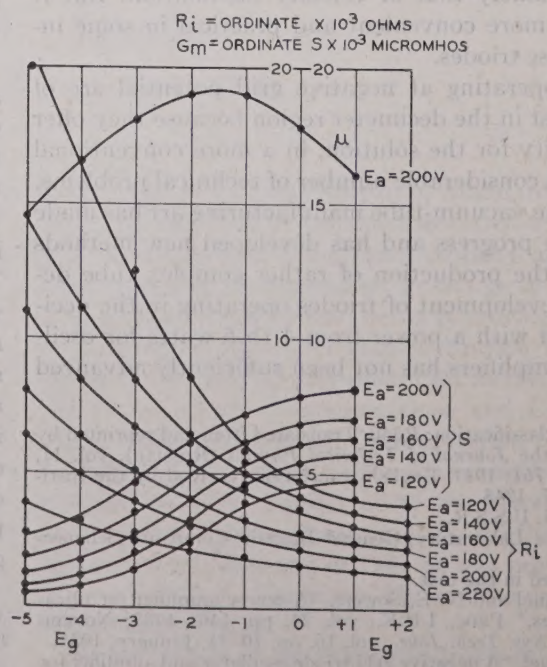

Fig. 4

Static characteristics of the DCM-1.

The power output was measured using incandescent lamps. Tube efficiency is shown as a function of wavelength and power input in Fig. 7. It will be seen that, with increased power input, the efficiency increases as expected. Power input is naturally limited by the heat capacity of the plate. If used with concentric type resonators, the DCM-1 tube can regenerate at different modes. Highest efficiency was obtained at quarter-wave operation. As an example, at $\lambda = 42$ centimeters, the cathode-grid line was changed from $\frac{1}{4}\lambda$ to $\frac{3}{4}\lambda$. It was found necessary to increase the input by 12 per cent.

The transition from $\frac{1}{4}\lambda$ to $\frac{3}{4}\lambda$ is even more detrimental in the plate-grid resonator. At $\lambda = 42$ centimeters, it was necessary to increase the input power by 30 per cent in order to secure the same output. For wavelengths below 30 centimeters, the efficiency rapidly falls off, and it is impossible to operate the tube at the $\frac{3}{4}\lambda$ mode because the requisite input power is greater than the tube can safely dissipate. From the preceding data, it is concluded that $\frac{3}{4}\lambda$ operation is less practical than operation at $\frac{1}{4}\lambda$.

The DCM-1 tube can also be used as a converter from $\lambda = 25$ centimeters or more, and as an oscillator from $\lambda = 30$ centimeters or more.

The use of the DCM-1 tube as an amplifier will next be considered. The signal was introduced between the grid and the cathode, and the amplified signal appeared between the plate and the grid. The circuit was the same as shown in Fig. 5, which circuit was used as an oscillator, except that the feedback was removed. The measurements were made as follows. A signal was obtained from an oscillator operating between 1500 and 2000 megacycles. The signal was modulated at 800 cycles. It was received by a dipole which was connected to a line terminating in a loop and passing into the cathode-grid space of the amplifier. The output was

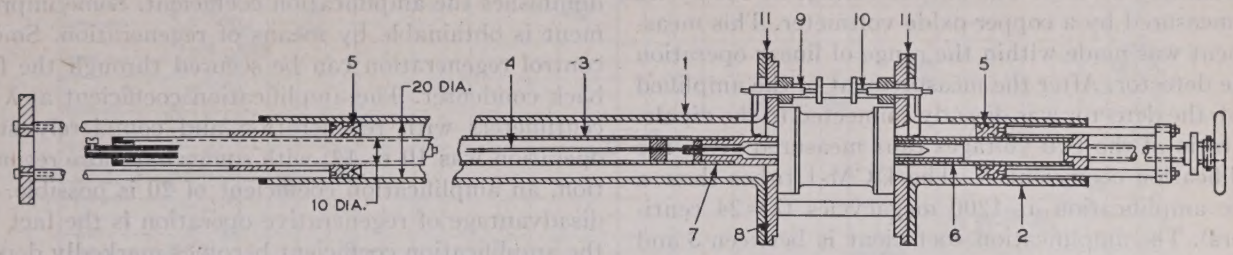

Fig. 5—Cross section of the circuit used in conjunction with DCM-1.
1—Outside tubing of the grid-cathode resonator.
2—Outside tubing of the plate-grid resonator.
3—Inside tubing of the grid-cathode resonator.
4—Heater connection of the cathode.
5—Tuning pistons for the plate-grid and the grid-cathode resonator.
6—Plate connection.
7—Cathode connection.
8—Grid connection.
9—The movable plate of the feedback condenser.
10—The fixed plate of the feedback condenser.
11—By-pass condenser.

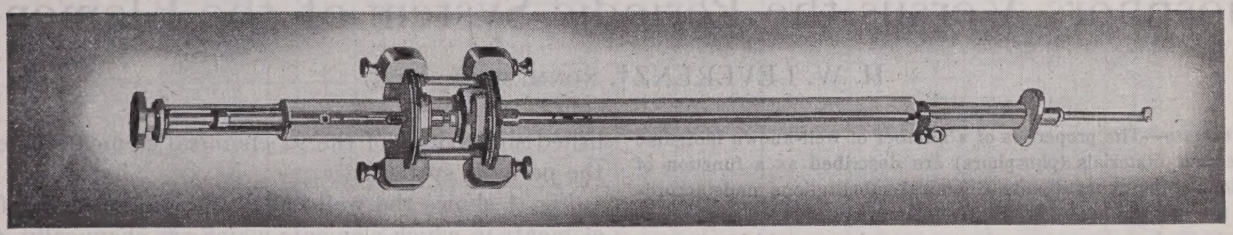

Fig. 6

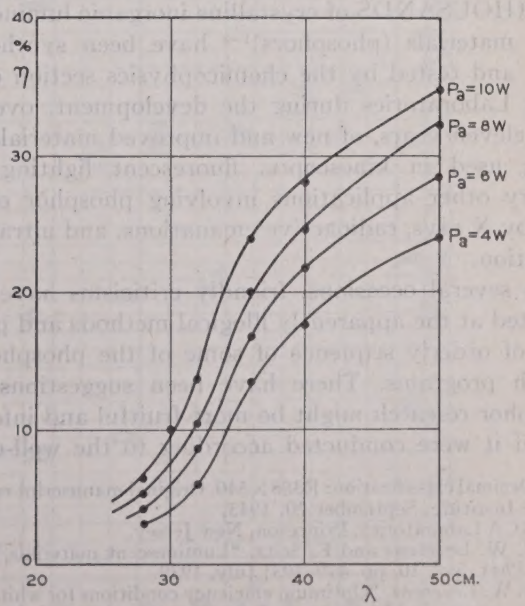

Fig. 7—The efficiency as a function of wavelength with power output as parameter.

withdrawn by a loop-terminated line, and detected by a Barkhausen detector. The detected signal was amplified with two stages of the metal 6F5 tubes, with voltage amplification of 2000. The output voltage at 800 cycles was measured by a copper-oxide voltmeter. This measurement was made within the range of linear operation of the detector. After the measurement of the amplified signal, the detector was directly connected to the dipole. The ratio of the two voltages thus measured gives the amplification coefficient K. The DCM-1 tubes show a stable amplification at 1200 megacycles ($\lambda = 24$ centimeters). The amplification coefficient is between 3 and 4. The operating grid voltage was zero, the plate voltage 200 to 220 volts, and the plate current 30 to 40 milliamperes. With increasing wavelength, the amplification coefficient increases. Some improvement in the amplification coefficient is obtainable by a modification of the plate resonator corresponding to an auto-transformer connection.

Amplification with Regeneration

A marked disadvantage of the tubes used at high frequencies is their low input impedance which in turn diminishes the amplification coefficient. Some improvement is obtainable by means of regeneration. Smooth control regeneration can be secured through the feedback condenser. The amplification coefficient at $\lambda = 25$ centimeters with regeneration and completely stable operation was 10 to 12; with somewhat more regeneration, an amplification coefficient of 20 is possible. One disadvantage of regenerative operation is the fact that the amplification coefficient becomes markedly dependent upon plate voltage. For instance, for a variation of plate voltage from 5 to 10 per cent, the amplification coefficient may change from unity to that corresponding to regeneration. Regenerative amplification may be used in receivers. In heterodyne receivers, however, it is advisable to separate the regenerative amplifier from the converter by a buffer stage.

Phosphors Versus the Periodic System of the Elements*

H. W. LEVERENZ†, NONMEMBER, I.R.E.

Summary—**The properties of a number of well-known inorganic luminescent materials (phosphors) are described as a function of variations of their constituents. Chemical substitutions made according to the ordered series in the periodic system of the elements are shown to produce many anomalous energy changes which appear as shifts in the spectral emission colors of phosphors. The anomalous energy changes indicate that the mechanisms of luminescence in solids cannot be given a simple interpretation.**

The relative cathodoluminescences of forty-five phosphors are codified and presented in tabular form for the convenience of cathode-ray tube engineers.

THOUSANDS of crystalline inorganic luminescent materials (phosphors)[1-3] have been synthesized and tested by the chemicophysics section of the RCA Laboratories during the development, over the past eleven years, of new and improved materials now being used in kinescopes, fluorescent lighting, and sundry other applications involving phosphor excitation by X rays, radioactive emanations, and ultraviolet radiation.

On several occasions, friendly criticisms have been directed at the apparently illogical methods and patent lack of orderly sequence of some of the phosphor research programs. There have been suggestions that phosphor research might be more fruitful and informative if it were conducted according to the well-established similarities of the 92 chemical elements listed in the periodic system.[4]

Fig. 1 shows the well-known periodic system of the elements in which elements which are chemically, optically, and physically similar are arranged in the same horizontal periodic group (0, 1A, 1B, 2A, etc.). For example, the chemically similar elements carbon (C), silicon (Si), germanium (Ge), tin (Sn), and lead (Pb) are classified in the given order in group 4B. Knowledge of the properties of one of the enumerated elements, viz., silicon (Si) and its compounds, affords qualitative information about the properties of the remaining members of the same periodic group, viz., C, Ge, Sn, and Pb. Without pursuing the point in detail, one could reasonably expect that intersubstitutions of chemically similar elements should change the properties of their resultant compounds in regular fashion as the atomic numbers of the substituted elements increase. However, such expectation of regularity must be qualified with mental reservations. Those who have plotted properties of elements and their compounds know that sometimes optimal properties are found within, rather than at the ends of, the periodic groups. The present article tends to add further exceptions to the periodic "rule" as applied to phosphors.

In order to make a fundamental, systematic study of the effect of changing chemical composition on the properties of phosphors, one might propose to commence the investigation with the alkali halides, viz.,

* Decimal classification: R388×540. Original manuscript received by the Institute, September 20, 1943.

† RCA Laboratories, Princeton, New Jersey.

[1] H. W. Leverenz and F. Seitz, "Luminescent materials," *Jour. Appl. Phys.*, vol. 10, pp. 479–493; July, 1939.

[2] H. W. Leverenz, "Optimum efficiency conditions for white luminescent screens in kinescopes," *Jour. Opt. Soc. Amer.*, vol. 30, pp. 309–315; July, 1940.

[3] H. W. Leverenz, "Cathodoluminescence as applied in television," *RCA Rev.*, vol. 5, pp. 131–176; October, 1940.

[4] H. W. Leverenz, "A convenient periodic chart of the elements," *Foote Prints*, vol. 12, pp. 22–24; June, 1939. (Published by The Foote Mineral Co., 16th and Summer Streets, Philadelphia, Pennsylvania.)

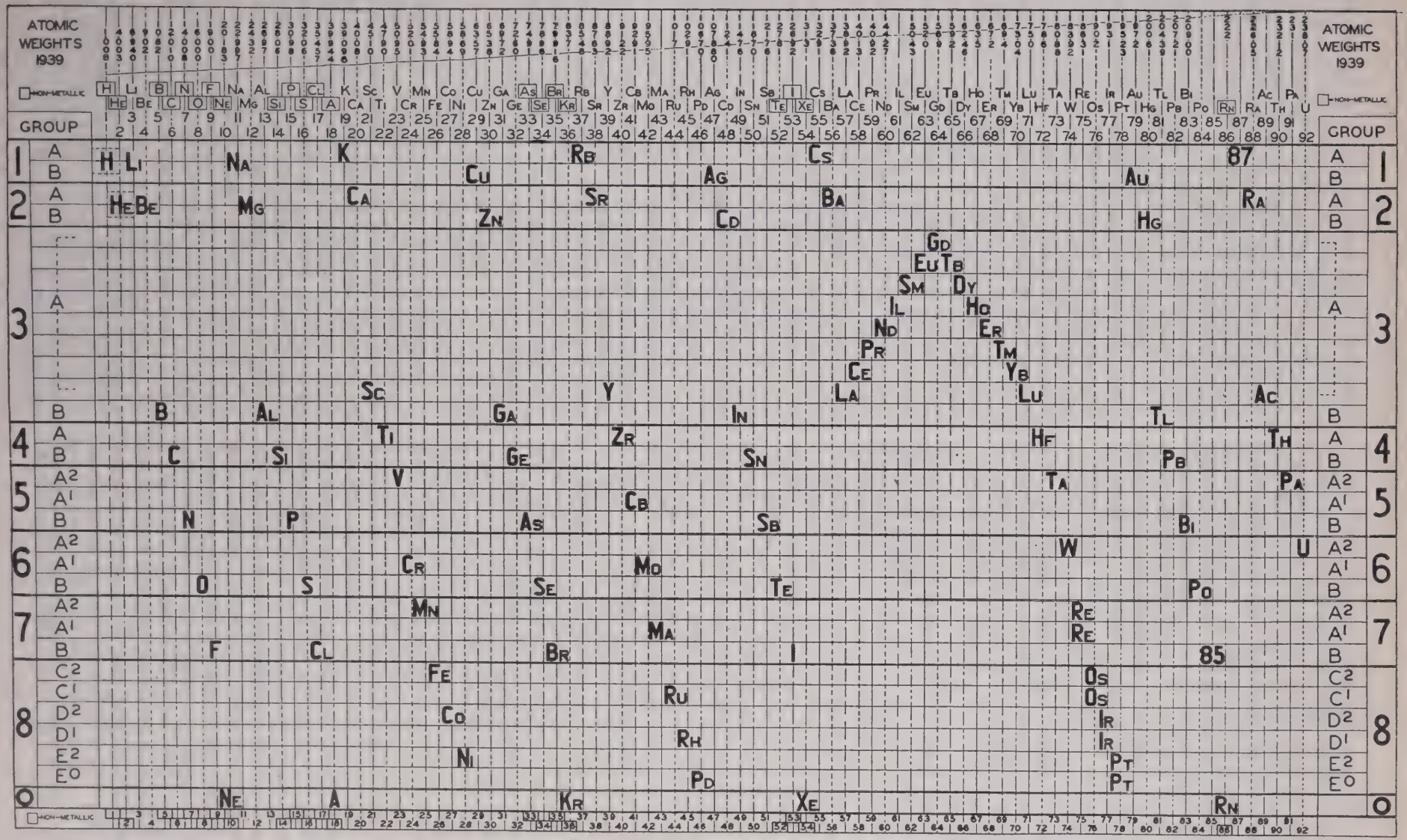

Fig. 1—The periodic system of the elements.

sodium or potassium chlorides (NaCl or KCl), which crystallize in simple cubic structures and are easily purified and synthesized. Although one finds that the alkali halides do luminesce, one also finds that they undergo complex microchemical transformations and become colored under excitation by ultraviolet, X rays, or cathode rays. Hence, these simplified compounds obfuscate investigation by alteration during testing.

Having failed to make the simple alkali-halide phosphors yield unambiguous information regarding the effects of varying chemical composition, it might be presumed that the investigator would select a well-known, stable, and efficient phosphor such as zinc sulphide or zinc silicate and would experiment with systematic chemical permutations according to the sequences given in the periodic table. Let us follow an imaginary chemist, Mr. Q, in such a well-ordered investigation.

Mr. Q spends some months reading the voluminous and polyglot literature of the past century covering zinc-sulphide and zinc-silicate phosphors. He finds much contradiction and confusion, but gains the rather certain information that, in order to make a good phosphor, (1) zinc sulphide requires about 0.01 per cent copper activator "impurity" and must be crystallized at 700 to 1300 degrees centigrade with a flux such as sodium chloride, and (2) zinc silicate requires about 1 per cent of manganese activator "impurity" and must be crystallized at 1000 to 1200 degrees centigrade but needs no flux.

Armed with this information, Mr. Q enters his laboratory and carefully purifies several pounds each of zinc sulphide (ZnS), zinc oxide (ZnO), and silica (SiO_2) in order to have basic ingredients which will be above reproach as to their compositions. Any or all of the standard chemical and physicochemical methods of purification may be applied, including: (1) fractional distillation or sublimation, (2) oxidation of impurity ions to yield more insoluble hydroxides, (3) electrochemical deposition by contact of aqueous salt solutions with zinc metal, (4) fractional precipitation in acid and alkaline solutions, (5) electrolysis, (6) fractional crystallization, (7) dialysis, (8) and selective solubility or adsorption. The choice and order of each purification step is often relatively immaterial, since practically the same purity of product may be achieved by very different procedures. Perhaps the chief caution which he should observe is that purification of sulphides is best carried out in neutral or acid solutions[5] to minimize the introduction of hydroxides or oxides, especially as caused by alkaline reaction with glass or quartz vessels.

Mr. Q's next step is to place separate small samples of the pure ZnS, ZnO, and SiO_2 in clean quartz or platinum crucibles and heat them to temperatures between 500 to 1500 degrees centigrade in an electric furnace. He finds all the crystallized substances have almost negligible luminescence under any excitation. However, by heating mixtures of (a) $2ZnO+SiO_2$ and (b) ZnS +2 per cent of purified NaCl at about 1000 degrees centigrade, Mr. Q obtains a weak blue luminescence from (a) ($=\alpha-Zn_2SiO_4$) and a strong blue luminescence from (b) ($=ZnS$). These two blue-emitting phosphors are the "grandfathers" of the two most important phosphor families, including phosphors emitting almost any color with either long, short, or intermediate persistences.

Mr. Q next activates a small sample of pure unheated ZnS, adding 0.01 per cent copper as a water-soluble salt. Evaporation and heating at 700 to 1300 degrees centigrade with 2 per cent sodium-chloride flux gives a phosphor (ZnS:Cu) having intense green luminescence. Reference to the periodic table, group 1B, shows copper to be the lightest member of the chemically similar series: copper (Cu), silver (Ag), and gold (Au). Since 0.01 per cent copper activator shifted the spectrum of ZnS toward the red, i.e., from blue to green, Mr. Q activates the next sample of pure ZnS with 0.01 per cent silver, adds the usual flux, and crystallizes the mixture in the expectation of getting a yellow- or orange-emitting phosphor. The first anomaly appears at this point when he discovers that the silver-activated zinc sulphide ZnS:Ag has an even deeper blue luminescence than the unactivated ZnS. Mr. Q may feel that the copper-activated material should have been considered as the reference point so that if activation with silver yielded a shift toward the blue, then the next and last activator element, gold, of the 1B series, should give a still farther shift to the blue, i.e., a violet emission. Unfortunately for his theory, his gold-activated phosphor, ZnS:Au, has a green-blue emission color intermediate to unactivated ZnS and ZnS:Cu. Fig. 2 shows[6] the spectral-distribution curves of the ZnS, ZnS:Cu, ZnS:Ag, ZnS:Au series of phosphors.

Score at the end of the first series of tests:

Expected results	— 0
Unexpected results	— 2

Since activators are present only in very small quantities in phosphors, Mr. Q reasons that permutations of the base material may be less ambiguous. Accordingly, he refers to the periodic table to find that beryllium (Be), magnesium (Mg), zinc (Zn), cadmium (Cd), and mercury (Hg) occur in the given order in group 2B. (Helium (He) is a member of Group 0.) Substitution of various percentages of the heavier cadmium for zinc in ZnS, with or without activation by Cu, Ag, or Au, gives an ordered progression of emission colors from the original blue to red[2] such as shown in the lower part of Fig. 3. Unfortunately, mercury sulphide sublimes at

[5] J. Einig, "The preparation of luminescent zinc sulphide," *Chemiker Zeit.*, vol. 3, p. 31, January, 1931; vol. 19, pp. 185–186; March, 1932.

[6] See footnote reference 1, page 487. A spectral shift toward the violet (shorter wavelengths) indicates an increase in the energy of the emitted light quanta, and, conversely, a spectral shift toward the red (longer wavelengths) indicates a decrease in energy of the emitted light quanta. Wavelength λ, frequency ν, and energy, E, are related by $\lambda\nu=c$ and $E=h\nu$, where c and h are constants ($c=3\times10^{10}$ centimeter per second^{-1}; $h=6.56\times10^{-27}$ erg second).

[2] *Op. cit.*, page 310.

583.5 degrees centigrade so that it is not suitable for substitution in the zinc-sulphide phosphor. Furthermore, substitution of beryllium (Be) or magnesium (Mg) for zinc merely decreases the phosphor's efficiency. Mr. Q, however, might tentatively assume the following "rule": "substitution of a heavier chemically similar element for a component of the base material will shift the emission spectrum of a phosphor toward the red. Conversely, substitution of a lighter chemically similar

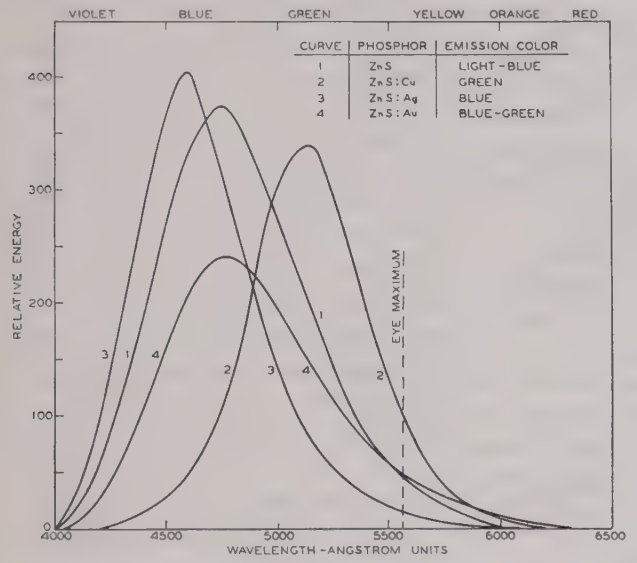

Fig. 2—Spectral distribution curves of some zinc-sulphide phosphors.

element for a component of the base material should shift the emission spectrum of a phosphor toward the blue."

To determine the effect of varying the nonmetallic constituent, sulphur, in zinc sulphide, Mr. Q investigates its neighbors in group 6B. Group 6B is, in order, oxygen (O), sulphur (S), selenium (Se), tellurium (Te), and polonium (Po). Preparation of ZnS (60 per cent) ZnSe (40 per cent) with or without silver or copper activator, substantiates the "rule," i.e., the emission colors of these zinc seleno-sulphides are green-yellows (see Nos. 3 and 4, Fig. 4). Increase in the selenium/sulphur ratio shifts the emission spectra farther toward the red; similar to the effect of increasing the cadmium/zinc ratio. Complete substitution of the lighter oxygen for sulphur, viz., by oxidation of zinc vapor, provides an unactivated phosphor which further substantiates the "rule" in that it emits a deep violet light. (See line 44, Fig. 5.) Partial substitution of small percentages of oxygen for sulphur in ZnS, however, unexpectedly gives a greener emission color than unactivated ZnS. In fact, the ZnS(O) phosphors behave much like ZnS:Cu phosphors in that they have uncommonly long persistences.[7] Substitutions of tellurium or polonium are unpromising because the two elements are quite metallic in character.

Score at the end of the second series of tests:

Expected results — 2
Unexpected results — 3

Although the "rule" has fared none too well with zinc-sulphide phosphors, Mr. Q now investigates its applicability to zinc silicate and its congeners. It will be remembered that ZnO and SiO_2 had almost negligible luminescences and their combination α-Zn_2SiO_4 had weak blue luminescence. In order to obtain a useful intensity of luminescence, Mr. Q activates the pure α-Zn_2SiO_4 with about 1 per cent of any manganese compound, such as MnO, which does not contain

CURVE	PHOSPHOR	TEMP. FOR 2hr.	RELATIVE VISUAL RESPONSE	NATURAL COLOR	COLOR OF LUMINESCENCE
1	ZnS:0.008% Ag	940°	18.5(1a)	WHITE	LIGHT BLUE
2	ZnS(80)CdS(20):0.01%Ag	"	27.0	LIGHT GREEN WHITE	VERY LIGHT BLUE GREEN
3	ZnS(60)CdS(40): "	"	66.3	VERY LIGHT GREEN	VERY LIGHT CREAM GREEN
4	ZnS(50)CdS(50): "	"	100.0(4a)	LIGHT YELLOW	LIGHT GREEN YELLOW
5	ZnS(40)CdS(60): "	"	63.7	LIGHT CREAM YELLOW	LIGHT YELLOW ORANGE
6	ZnS(20)CdS(80): "	"	9.4(6a)	TAN ORANGE	LIGHT RED
7	CdS:0.02% Ag	"	—	LIGHT BROWN ORANGE	RED

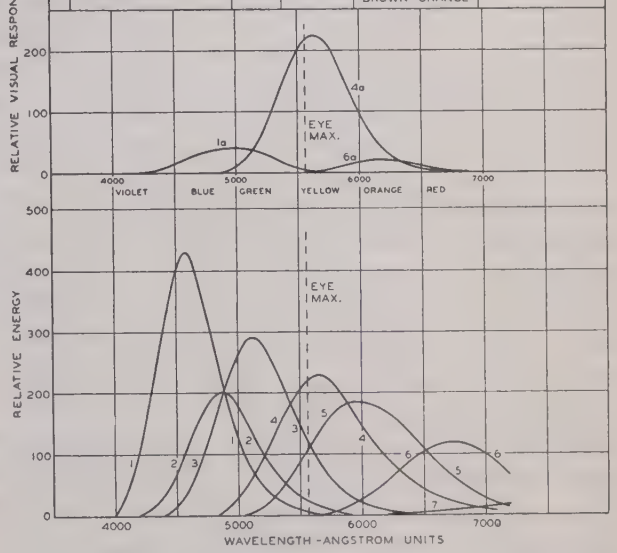

Fig. 3—Spectral distribution curves of some zinc-cadmium sulphide phosphors.

another metal. The crystallized α-Zn_2SiO_4:Mn, synthesized at 900 to 1500 degrees centigrade, has an intense green luminescence peaked at 5230 angstrom units as shown[8] in Fig. 6 and in lines 14 and 15, Fig. 4.

Using α-Zn_2SiO_4:Mn as a reference point, Mr. Q substitutes the heavier cadmium for the zinc and obtains, as expected, a shift of emission color to the red (compare No. 14, Fig. 4, and No. 24, Fig. 5). Mercury oxide decomposes at 100 degrees centigrade and, hence, prevents further substitution of heavier elements in group 2B. Turning to the lighter elements in group 2B, namely, magnesium Mg, and beryllium Be, Mr. Q finds that *complete* substitution of Mg for Zn in α-Zn_2SiO_4:Mn unexpectedly gives a deep-red-emitting phosphor (No. 40, Fig. 5), and *complete* substitution of Be for Zn

[7] A. A. Guntz, "Etude sur les sulfures de zinc phosphorescents," *Ann. de Chimie*, vol. 5, pp. 157–198, 363–420; 1926.

[8] *Op. cit.*, page 143.

No.	PHOSPHOR			RELATIVE CATHODO-LUMINESCENCE		SPECTRAL DISTRIBUTION CURVES (VIOLET | BLUE | GREEN | YELLOW | ORGE | RED; EYE MAX.; 4000 5000 6000 7000A°)	COLOR OF LUMINESCENCE	PHOSPHORESCENCE 0=VERY SHORT 5=VERY LONG	BEST Hg-LINE FOR ULTRAVIOLET EXCITATION	
	BASE MATERIAL	PER CENT ACTIVATOR	TEMP. °C	VISIBLE EFFICIENCY	PEAK ENERGY				3650A°	2537A°
1	ZnS(50)CdS(50)	0.01 Ag	940	235	240	5690	LIGHT GREEN-YELLOW	0	x	
2	ZnS	0.01 Cu	900	230	340	5280	LIGHT YELLOW-GREEN	3	x	
3	ZnS(60)ZnSe(40)	0.005 Cu	620	180	130	5680	LIGHT GREEN-YELLOW	3	x	
4	ZnS(60)ZnSe(40)	0.001 Ag	620	170	125	5560	LIGHT GREEN-YELLOW	2	x	
5	ZnS	0.01 Cu	1240	160	260	5160	LIGHT GREEN	5	x	
6	ZnS(50)CdS(50)	0.005 Ag	1200	160	170	5730	LIGHT YELLOW	1	x	
7	ZnS(60)CdS(40)	0.01 Ag	940	155	300	5100	LIGHT GREEN	0	x	
8	ZnS(40)CdS(60)	0.01 Ag	940	150	180	6000	LIGHT YELLOW-ORANGE	0	x	
9	ZnS	0.001 Cu	940	140	170	4700 5200	LIGHT BLUE-GREEN	3(G)	x	
10	ZnS(82)CdS(18)	0.006 Cu	1240	130	105	5690	LIGHT GREEN-YELLOW	5	x	
11	ZnS(73)CdS(27)	0.004 Cu	1240	130	100	6050	LIGHT YELLOW-ORANGE	3	x	
12	ZnS(90)CdS(10)	0.006 Cu	1240	125	115	5410	LIGHT YELLOW-GREEN	5	x	
13	ZnS	0.001 Cu	1200	120	100	4700 5200	LIGHT BLUE-GREEN	4(G)	x	
14	α-ZnC SiO_2	1 Mn	1200	110	110	5230	GREEN	2		x
15	α-2ZnO·SiO_2	1 Mn	1250	100	100	5230	GREEN	1		x
16	9ZnO·BeO·6SiO_2	1 Mn	1200	95	35	5300	LIGHT YELLOW-GREEN	3		x
17	ZnO BeO SiO_2 (w x y)	Mn_z	1000-1300	50-110	15-110	5230 6300	VARIABLE: GREEN TO RED-ORANGE	1-3		x
18	ZnS(50)CdS(50)	—	940	95	60	5800	LIGHT YELLOW-ORANGE	0	x	
19	ZnS	—	940	90	340	4700	LIGHT BLUE	2	x	
20	ZnS(50)CdS(50)	—	1200	85	80	5900	LIGHT YELLOW-ORANGE	0	x	
21	β-2ZnO·SiO_2	1 Mn	1600Q	80	65	5630	LIGHT GREEN-YELLOW	1		x
22	α-2ZnO·GeO_2	1 Mn	1100	65	60	5370	LIGHT YELLOW-GREEN	4	x	x
23	ZnS(80)CdS(20)	0.01 Ag	940	65	200	4880	LIGHT BLUE-GREEN	2	x	

4000 5000 6000 7000A°
EYE MAX.

Fig. 4—A compendium of properties of some high-efficiency phosphors.

No.	PHOSPHOR			RELATIVE CATHODO-LUMINESCENCE		SPECTRAL DISTRIBUTION CURVES	COLOR OF LUMINESCENCE	PHOSPHORESCENCE 0=VERY SHORT 5=VERY LONG	BEST Hg-LINE FOR ULTRAVIOLET EXCITATION	
	BASE MATERIAL	PER CENT ACTIVATOR	TEMP. °C	VISIBLE EFFICIENCY	PEAK ENERGY	VIOLET · BLUE · GREEN · YELLOW · ORGE · RED; 4000 5000 EYE MAX. 6000 7000A°			3650A°	2537A°
24	$CdO \cdot Si_1O_2$	1 Mn	1150	45	—	6050	LIGHT YELLOW-ORANGE	4		x
25	ZnS	0.008 Ag	940	45	380	4575	LIGHT BLUE	2	x	
26	$Zn_xO\ B_2O_3{}_y$	Mn_z	900	45	—	5450 6000	VARIABLE: LIGHT GREEN TO ORANGE	1-3		x
27	ZnS	0.032 Ag	940	35	400	4560	BLUE	3	x	
28	$CdO\ B_2O_3{}_y$	Mn_z	800	20-45	20-30	5400 6300	VARIABLE: CREAM COLOR TO ORANGE-RED	2.5		x
29	ZnS	—	1200	30	80	4700	LIGHT BLUE	1	x	
30	ZnS	0.02 Ag	1240	23	500	4350	BLUE-VIOLET	3	x	
31	ZnS(20) CdS(80)	0.01 Ag	940	22	120	6750	LIGHT RED	0	x	
32	$Zn_vO\ BeO\left(\begin{matrix}Ti\\Zr\\Th\end{matrix}\right)_w O_2Si_1O_2{}_y$	Mn_z	1000-1300	20-110	8-110	5650 5230	VARIABLE: GREEN TO WHITE	1-3		x
33	$MgO \cdot WO_3$	—	≈1000	20-40	7-14	4930	PALE BLUE	0		x
34	$ZnO \cdot Al_2O_3$	1 Mn	1600	21	41	5130	GREEN	0		x
35	$ZnO \cdot Ga_2O_3$	1 Mn	1600	20	35	5060	BLUE-GREEN	0		x
36	$CaO_x\ Si_1O_2{}_y$	Mn_z	900-1500	5-20	—	5600 6100	VARIABLE: YELLOW-GREEN TO ORANGE	1-3		x
37	$CdO \cdot Al_2O_3$	1 Cr	1150	18	—	4960 5890	CREAM COLOR	0		x
38	$CdO \cdot Al_2O_3$	1 Mn	1600	15	—	5890	LIGHT ORANGE-YELLOW	0		x
39	$CaO \cdot Al_2O_3$	1 Mn	1600	10	—	5470	LIGHT YELLOW-GREEN	0		x
40	$MgO_x\ Si_1O_2{}_y$	1 Mn	1000-1500	4-10	—	6860 6440	VARIABLE: LIGHT RED TO DEEP RED	1-4		x
41	$CaO \cdot WO_3$	—	≈1000	7	5	4300	PALE VIOLET	0		x
42	$ZnO \cdot WO_3$	—	≈1000	7	3	4930	PALE BLUE	0		x
43	CdS	0.02 Ag	940	<1	≈50		VERY DEEP RED	0	x	
44	ZnO	—	≈1000	<1	>3		VIOLET	0	x	
45	ZnS (NO FLUX)	—	800-1300	<1	?	?	DEEP BLUE	0	x	

4000 5000 EYE MAX. 6000 7000A°

Fig. 5—A compendium of properties of some low-efficiency phosphors.

in α-Zn_2SiO_4:Mn, again unexpectedly, gives a weak orange-red-emitting phosphor. Mr. Q further finds that partial substitution of Mg for Zn gives a phosphor which emits independent green and red bands instead of one single band. Partial substitution of beryllium for zinc, however, affords high efficiency, variable color, single bands in the most important phosphor system known. Colors from green to red-orange may be produced in the manganese-activated zinc-beryllium-silicate system (Nos. 16 and 17, Fig. 4).[1] It will be noted that neither total nor partial substitution of Be or Mg

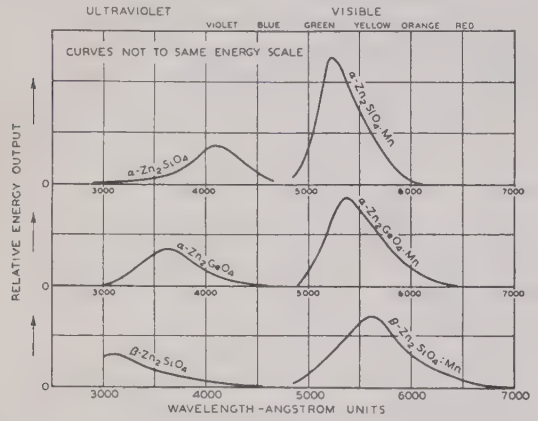

Fig. 6—Spectral-distribution curves of some zinc-silicate phosphors.

for Zn in α-Zn_2SiO_4:Mn obeyed the assumed "rule" that color shifts toward the blue with substitution of lighter elements in the same periodic group.

Score at the end of the third series of tests:

Expected results — 3
Unexpected results — 5

After considering group 4B substitutes for the silicon in α-Zn_2SiO_4:Mn, Mr. Q expects, and obtains, a shift toward the red by substituting the heavier chemically similar germanium (Ge) for silicon (Si) to produce green-yellow luminescing[1] α-Zn_2GeO_4:Mn (see No. 22, Fig. 4.) Since the substitution of a heavier, i.e., larger, for a lighter chemically similar element involves an expansion of the lattice, Mr. Q may decide to rephrase his rather battered "rule" to read "in general, an expansion of the crystal lattice shifts the emission color toward the red." To test this revised "rule" Mr. Q melts a small quantity of α-Zn_2SiO_4:Mn in a shallow platinum crucible at about 1600 degrees centigrade, removes it while still white hot, and quickly plunges it into cold distilled water.[8] He discovers that the green-emitting α-form of Zn_2SiO_4:Mn has changed to the yellow-emitting β-form which is chemically identical but has a crystallographically dissimilar lattice[1] (see No. 21, Fig. 4). The transition from α- to β-Zn_2SiO_4:Mn involves an expansion of the crystal structure and produces a shift toward the red in emission color, hence this experiment apparently substantiates the revised "rule" and may be counted as an expected result.

Score at the end of the fourth series of tests:

Expected results — 5
Unexpected results — 5

With the score improving, Mr. Q synthesizes manganese-activated zinc aluminate, $ZnAl_2O_4$:Mn, perhaps expecting the emission spectrum to be shifted toward the blue, because aluminum (Al) although in a different group (3B) is lighter than silicon (Si). The expectation, though unjustified, is rewarded since $ZnAl_2O_4$:Mn, as shown in line 34, Fig. 5, emits a peak wavelength 100 angstrom units nearer the blue than does α-Zn_2SiO_4:Mn.

Group 3B contains, in order, boron (B), aluminum (Al), gallium (Ga), indium (In), and thallium (Tl). Substitution of the lighter boron for aluminum disobeys the "rule" in that manganese-activated zinc borates have emission spectra which are on the red side of $ZnAl_2O_4$:Mn as shown in line 26, Fig. 5. Only the lightest base-material elements have given anomalies thus far, however, and Mr. Q expects to score easily by predicting that substitution of gallium for aluminum in $ZnAl_2O_4$:Mn will shift the emission spectrum to the red. The "rule" suffers another discrediting blow at this point since manganese-activated zinc galliate, $ZnGa_2O_4$:Mn has an even bluer emission than the aluminate, $ZnAl_2O_4$:Mn (compare lines 34 and 35, Fig. 5).

Score at the end of the fifth series of tests:

Expected results — 6
Unexpected results — 7

Activated materials have given such anomalous results that Mr. Q returns to the unactivated sulphide materials and gratifyingly finds his "rule" obeyed by the sequence:

Unactivated Phosphor	*Emission Color*
ZnO	violet[9]
ZnS	blue
Zn(S, Se)	green to red
(Zn, Cd)S	green to red

The emission spectra of pure unactivated α-Zn_2GeO_4 and α-Zn_2SiO_4 phosphors, as shown in Fig. 6, however, defy the "rule" by shifting in the opposite direction to the sequence of their "rule"-obeying, manganese-activated counterparts.

Score at the end of the sixth series of tests:

Expected results — 8
Unexpected results — 9

Most of the unfinished series of tests have been completed with further "expected" and "unexpected" results, some of which may be deduced from the figures.

Figs. 4 and 5 afford a compendium of the properties of some well-known cathodoluminescent materials

[1] *Op. cit.*, pages 490–492.
[8] U. S. Patent 2,129,096.

[9] Previously counted as an expected result in the second series of tests.

measured at room temperature (25 degrees centigrade). Several of the oxygen-containing phosphor systems afford a variety of emission colors and are designated as "variable" in the column headed "color of luminescence." Zinc-sulphide, zinc-cadmium-sulphide, and zinc (cadmium)-seleno-sulphide phosphors systems also produce widely variable emission colors which are represented by several specific examples shown in the figures.[10] Spectral-distribution curves intermediate to the extremes shown may be obtained by varying the initial compositions, degrees of combination, and structural arrangements of the variable color phosphors. Certain phosphors such as the alkaline-earth sulphides, carbonates, sulphates, and phosphates are omitted because they are too inefficient and/or too unstable for use in cathode-ray tubes. Strontium-sulphide phosphor, for example, has only 2 to 3 per cent efficiency of cathodoluminescence as compared with the arbitrarily chosen standard α-Zn_2SiO_4:Mn. The relative efficiencies were measured on the bombarded side of thick phosphor layers excited at 6 kilovolts and a current density of approximately 1 microampere per square centimeter. These values, particularly those of sulphide phosphors as compared with oxygen-containing phosphors, change somewhat with changes in voltage and current density. The arbitrary standard, α-$ZnO \cdot SiO_2$:Mn phosphor has an efficiency of 2 to 2.5 candle power per watt, in the range of 6 to 10 kilovolts at 1 microampere per square centimeter when used in conventional kinescope screens.[11]

It is evident that phosphors largely disobey the regimentation of chemical substituents as expressed in the periodic system of the elements. Actually, phosphors are both impurity- and structure-sensitive, being perhaps more sensitive to their induced and inherent submicroscopic faults than they are to their macroscopic regularities. Advanced synthetic chemistry, although indispensable in phosphor research, is nevertheless secondary in importance to the physics of phosphors. Particular consideration must be given not only to chemical compatibilities, but also to physical entities such as the sizes, valencies, polarizabilities, ionization potentials, and electron configurations of any chemical elements proposed for incorporation in a particular phosphor.

The mechanism of luminescence in a phosphor crystal is on an atomic scale, involving intangible interactions of photons, electrons, ions, atoms, and lattice forces. There are, as yet, no theories which give quantitative agreement with experiment. Because it is only rarely possible to predict the luminescent properties of proposed new phosphors, research in this field must be guided by "scientific intuition" rather than by logic. Scientific intuition derives its discernment from colligating and applying myriad bits of latent knowledge, sometimes from apparently unrelated fields.

[10] Most of the sulphide and seleno-sulphide phosphors listed in Figs. 2, 3, 5, and 6 were synthesized by E. J. Wood. Many of the measurements were made by R. E. Shrader.

[11] H. W. Leverenz, "Problems concerning the production of cathode-ray tube screens," *Jour. Opt. Soc. Amer.*, vol. 27, pp. 25–35; January, 1937.

The Graphical Design of Cathode-Output Amplifiers*

DAVID L. SHAPIRO†, NONMEMBER, I.R.E.

Summary—**This report describes a convenient graphical method for analyzing and designing cathode-followers. It considers the details of operation only so far as they are essential to this description. The familiar equivalent circuit analysis is presented first for convenience. This is followed by a description of the graphical method, a discussion of its application for triode and pentode cathode followers, and instructions for sketching the graphs quickly and conveniently.**

List of Symbols

Instantaneous values of alternating components

i_p = cathode current
e_g = ground-to-grid voltage
e_{kg} = cathode-to-grid voltage

Instantaneous total values

i_b = cathode current
e_c = ground-to-grid voltage
e_d = ground-to-cathode voltage
e_b = ground-to-plate voltage
e_{dc} = cathode-to-grid voltage
e_{db} = cathode-to-plate voltage
e_{cb} = grid-to-plate voltage

Average values

E_c = ground-to-grid voltage
E_b = ground-to-plate voltage

Parameters

R_k = cathode resistance
R_L = load resistance
R_g = grid resistance
r_p = tube plate resistance
μ = tube amplification factor
g_m = tube transconductance

* Decimal classification: R363. Original manuscript received by the Institute, October 19, 1943; revised manuscript received, January 19, 1944.

† Hazeltine Electronics Corporation, Little Neck, L. I., N. Y.

I. Introduction

THE cathode-follower is a vacuum-tube amplifier which differs from more familiar amplifiers in that its load is in the cathode circuit instead of the plate circuit. The voltage gain is always less than unity,

but there are several advantages. The high input impedance and low output impedance associated with the cathode-follower make it useful as a current amplifier.

The cathode-follower has come into widespread use in television and other systems where it is necessary to transmit video signals along low-impedance transmission lines. These uses raise design problems involving the limits of the operating regions of tube characteristics. Graphical analysis is most useful for the solution of problems of this kind where equivalent-circuit analysis is not adequate.

II. Equivalent Circuit

Fig. 1 shows the basic cathode-follower circuit. The signal is fed to the control grid and the load is placed

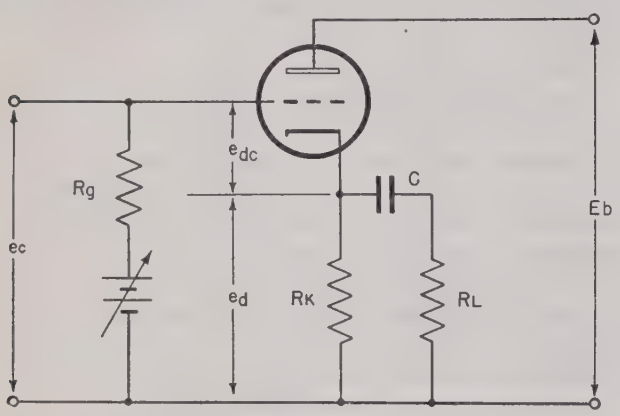

Fig. 1—Cathode-follower circuit.

across a resistor R_k between cathode and ground. The plate and the screen, when there is one, are at fixed potentials relative to ground. If the grid potential is made more positive, the tube draws more current, causing the potential at the cathode to become more positive. Thus the cathode "follows" the grid.

Fig. 2 shows the common equivalent circuit for alternating components. The tube is represented by a source

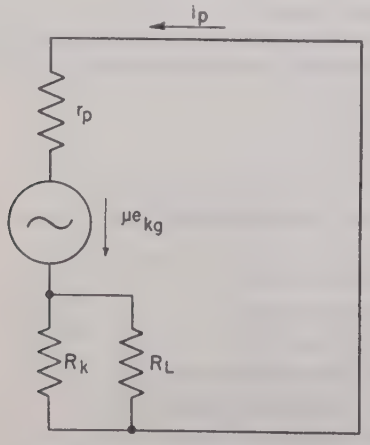

Fig. 2—Equivalent circuit for alternating current.

equal to its amplification factor times the cathode-to-grid voltage in series with a resistor equal to the tube plate resistance. The capacitor between the cathode and load resistors is omitted since its impedance is assumed to be negligible at the signal frequencies used.

From this equivalent circuit it can be shown (see Appendix A) that a cathode-follower can be approximately represented by a source equal to the applied grid voltage e_g and a series impedance equal to $1/g_m$, the reciprocal of the transconductance of the tube employed.

This representation is limited in that it does not consider the effect of reactances anywhere in the circuit, which the rest of this report will not consider either, and in that it does not consider the limitations imposed by cutoff of the tube and by the effect of grid current being drawn. These latter limitations are clearly demonstrated by the graphical analysis which follows.

III. Graphical Analysis

Tube characteristics in handbooks are generally presented as curves of plate current versus plate voltage for different values of grid voltage. The plate and grid voltages are referred to the cathode of the tube. The graphs here to be used for designing cathode-followers will differ from those of the handbooks in that they are plots of cathode current versus cathode voltage for different values of grid voltage. Since the plate is the element whose potential remains fixed, these cathode and grid voltages are considered relative to the plate. Fig. 3 is a sample set of such curves for a 6SN7 tube.

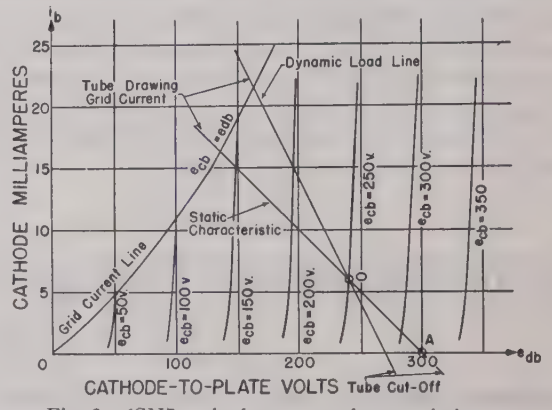

Fig. 3—6SN7 cathode-current characteristics.

The line labeled "Grid Current Line" is the locus of points where the cathode-to-plate voltage equals the grid-to-plate voltage. Above this line the grid is positive with respect to the cathode and the tube draws grid current. The horizontal axis represents the line $i_b = 0$. Below this line the tube is cut off. Hence normal operations is between these two lines, although occasionally a low-impedance driver is used to drive the grid positive with respect to the cathode, in order to increase the power available at the cathode.

A static characteristic can be drawn on this graph for a given cathode resistor. (The capacitor prevents the load resistor from having any effect on a static characteristic.) For convenience, consider the common ends of the grid resistor, the cathode resistor, and the load resistor, and the negative return of the B-supply voltage to be at ground potential. When the cathode current is zero, the cathode is at ground potential, and the cathode-to-plate voltage is equal to the B supply. This

information supplies one point on the static characteristic. Assuming a 300-volt B supply, point A of Fig. 3 is the point referred to. The static cathode-to-plate voltage is equal to the B-supply voltage minus the product of the cathode current and the cathode resistance R_k. A line of slope $-1/R_k$ on the graph of Fig. 3 fills this condition. This line is drawn for $R_k=10{,}000$ ohms. The supply voltage and the cathode resistor thus determine the static characteristic, the direct-current relation between cathode current and cathode voltage.

Selection of a particular grid bias E_c determines an operating point on the static characteristic. Point 0 of Fig. 3 is for a ground-to-grid voltage of 50 volts, or a grid-to-plate voltage of 250 volts since the B supply is 300 volts. The dynamic load line, representing the relation between instantaneous values of cathode current and cathode voltage, must pass through this point. The instantaneous rate of change of cathode voltage with respect to cathode current is equal to the parallel combination of the cathode and load resistors $R_k\ R_L/(R_k+R_L)$. Hence the slope of the dynamic load line, the rate of change of cathode current with respect to cathode-to-plate voltage, is $-(R_k+R_L)/R_k\ R_L$. This line is also drawn on Fig. 3 for $R_L=10{,}000$ ohms. The dynamic line shows where limiting may be expected due to cutoff on negative swings and to grid current on positive swings if the grid driving source has a high impedance.

IV. Construction of Triode Cathode-Follower Characteristic

All the information needed to plot the grid-current line and the constant grid-to-plate-voltage curves for a triode can be taken directly from the plate-current—plate-voltage characteristics in the tube handbooks. The grid-current line is exactly the same as the curve for zero grid bias, and can be copied directly even though the horizontal axis has been relabeled "cathode-to-plate voltage." To construct any constant grid-to-plate-voltage curve, a series of points can be taken: one point from each grid-voltage curve at the plate voltage corresponding to the desired grid-to-plate voltage. Thus for the curve for grid-to-plate voltage equals 150 volts, the point on the curve for -6 grid volts will be taken at $150-6=144$ plate volts (point P in Figs. 4 and 5). Figs. 4 and 5 demonstrate the location of the curve for a grid-to-plate voltage of 150 volts using the characteristics of a 6SN7 tube.

V. Approximate Triode Graph Construction

The grid voltage is the same as the cathode voltage along the grid-current line of Fig. 3, and the slope of this line is the rate of change of cathode current with respect to cathode-to-plate voltage. This is the same as the rate of change of plate current with respect to plate voltage, and is defined to be $1/r_p$.

The slope of the lines of constant grid-to-plate voltage is approximately equal to the transconductance g_m (rate of change of plate current with respect to grid voltage), since the variation along these lines of potential difference between cathode and grid is the main factor in producing cathode-current variations. The variation in cathode-to-plate potential is relatively unimportant.

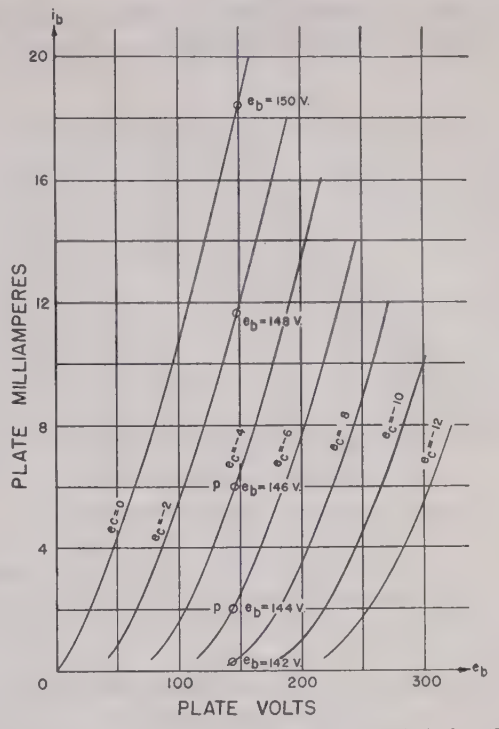

Fig. 4—Plate-current—plate-voltage characteristic for 6SN7.

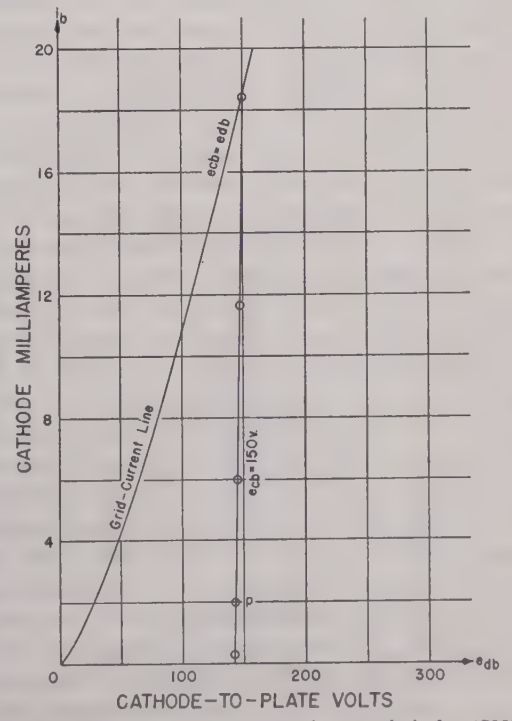

Fig. 5—Partial cathode-follower characteristic for 6SN7.

From the above considerations it becomes apparent that if the plate resistance and transconductance of a triode are known, the cathode-follower characteristics can immediately be approximately constructed. The grid-current line is first drawn from the origin with slope

$1/r_p$ on a graph with cathode-current ordinates and cathode-to-plate-voltage abscissas. Lines with slope g_m are labeled for values of grid-to-plate voltage corresponding to the cathode-to-plate voltage at their intersection with the grid-current line. Fig. 6 shows such a graph constructed from the handbook values of $r_p = 7700$

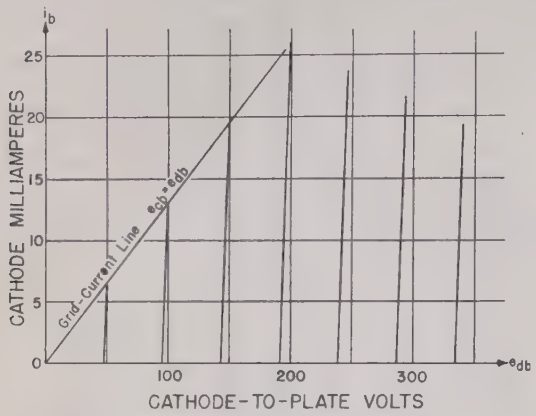

Fig. 6—Approximate graph for 6SN7 triode.

ohms and $g_m = 2600$ micromhos. This can be compared with Fig. 3, demonstrating that the method is rough, but still handy and usable.

VI. Pentode Cathode-Follower Graph Construction

Cathode-follower characteristics for pentodes or tetrodes with their screens by-passed to ground are very much like those for triodes, in contrast with the difference observed in plate-loaded amplifier characteristics. In pentode amplifiers the plate voltage has very little effect on the plate current so long as it exceeds the screen voltage, since the latter is generally held constant in amplifier circuits and maintains the electrostatic field at the control grid. In cathode-followers, however, the difference in potential between cathode and screen varies with the cathode current and the resulting characteristic is, therefore, very much like that of a triode.

If the pentode screen is connected to its plate, the values for μ and g_m for triode connection can usually be taken from the handbook and used in the manner described above to draw the cathode-follower characteristics. If there is a fixed difference in potential between screen and plate, a point can be read from the plate-current—plate-voltage characteristic where this difference in potential obtains, and where the cathode-to-grid voltage is zero. Figs. 7 and 8 demonstrate the above for a 6SJ7 pentode. The fixed screen-to-plate voltage is assumed to be 75 volts. The handbook gives the plate-current—plate-voltage characteristic for a screen potential of 100 volts. Reading the grid-voltage curve $e_{cl} = 0$ at the point for 175 plate volts (point P in Fig. 7) gives one value of plate current fitting the assumed screen-to-plate voltage. This, added to the screen current under the same conditions, is plotted on the cathode-follower characteristic as a point on the grid-current line for the value $e_{db} = 175$ volts (point P on Fig. 8). The cathode current will be very nearly cut off when the cathode potential rises above the screen potential, and therefore the grid-current line passes through the point $i_b = 0$, $e_{db} = 75$ volts. To a first approximation a straight line between these points is the grid-current line.

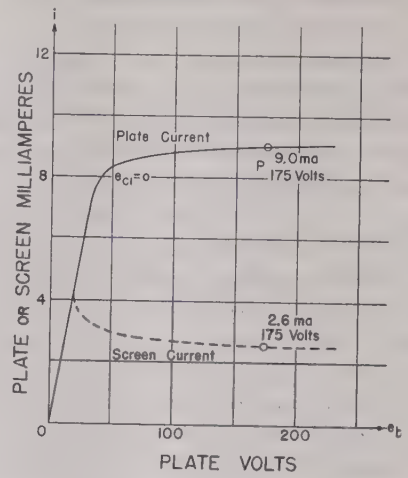

Fig. 7—6SJ7 characteristic from handbook.

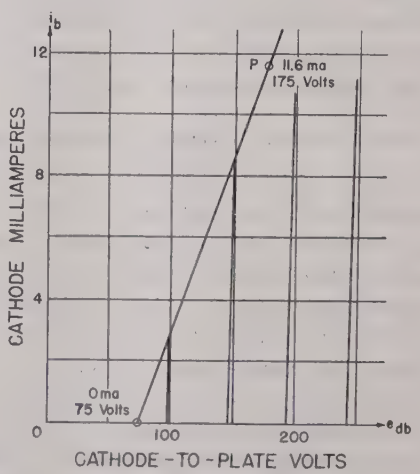

Fig. 8—6SJ7 cathode-follower characteristic.

The transconductance g_m is the rate of change of plate current with respect to grid voltage. Assuming that a constant fraction of the total cathode current goes to the screen as the grid voltage is varied, the rate of change of cathode current with respect to grid voltage (the slope of the constant grid-to-plate-voltage lines) will be the transconductance times the ratio of cathode current to plate current. At point P, the handbook gives g_m as about 1600 micromhos. The plate current is 9 milliamperes and the screen current is 2.6 milliamperes, so the cathode current is 11.6 milliamperes, and the slope of the grid-current lines will be $11.6/9 \times 1600 \times 10^{-6} = 2060 \times 10^{-6}$. These lines are also plotted in Fig. 8, using the same method as was used above for triodes. The effect of suppressor potential on cathode current is usually negligible and is here ignored.

The data given in most handbooks are adequate only

for these rough graphs. If sets of curves were given for different screen potentials, more accurate curves could be constructed.

It is also of interest to consider the pentode connection with screen by-passed to cathode. The above-described effective increase in transconductance does not obtain in this case, and the effective source impedance is therefore somewhat higher. However, the input impedance which is often very important is increased, and the range of operation is that shown in Fig. 9, which may sometimes be more useful than obtains with screen by-passed to ground.

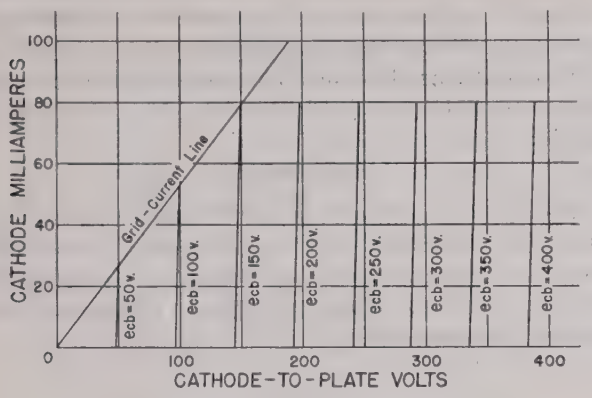

Fig. 9—Cathode-follower characteristic for 6AG7 triode connection.

VII. Conclusions

These graphs are closely similar in their method of application to the plate-current—plate-voltage characteristics published by tube manufacturers. Where triodes are concerned, the information contained in these cathode-follower graphs is the same as that in these published characteristics, and hence can be drawn accurately from them. They can be approximated more quickly from a knowledge of the transconductance and the plate resistance of the tube concerned.

Published pentode characteristics do not generally contain the required information for construction of cathode-follower graphs, and so the approximate characteristics must be resorted to until such time as more appropriate data are published by the tube manufacturers. However, these approximate characteristics are satisfactory for most applications.

The use of these graphs will simplify cathode-follower design considerably as compared with a trial-and-error method. They will supply directly the information in a given design as to where cutoff of the tube or drawing of grid current may be expected, and as to the ratio of output to input voltage levels.

Further investigation of cathode-followers should include the operation of several variations of the basic circuit and should, perhaps, cover more thoroughly than has been done in the past the effect of reactive elements in the circuit, as well as other high-frequency effects.

Appendix A

From the equivalent circuit (Fig. 2):

$$i_p = \frac{\mu e_{kg}}{r_p + R_k R_L/(R_k + R_L)}; \tag{1}$$

$$e_{kg} = e_g - i_p(R_k R_L/(R_k + R_I)). \tag{2}$$

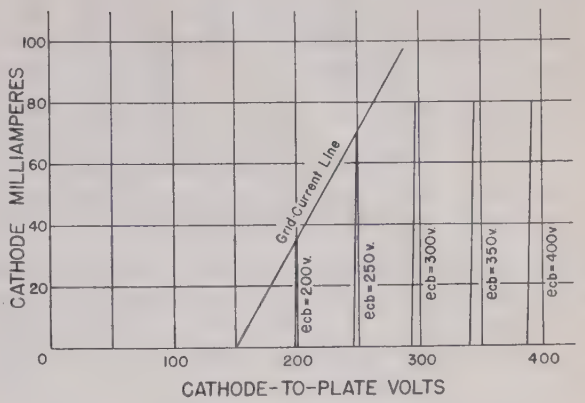

Fig. 10—Cathode-follower characteristic for 6AG7—screen-to-plate volts = 150.

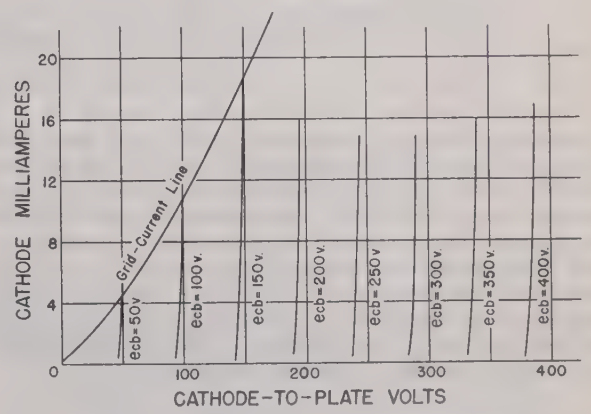

Fig. 11—6SN7 cathode-follower characteristic.

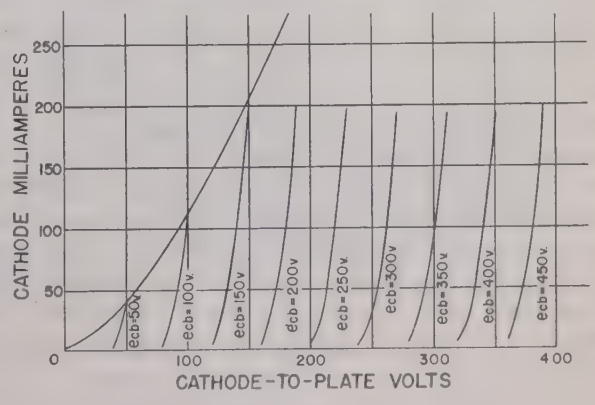

Fig. 12—6A3 cathode-follower characteristic.

From (1) and (2)

$$i_p = \frac{\mu e_g - \mu i_p(R_k R_L/(R_k + R_L))}{r_p + R_k R_L/(R_k + R_L)}. \tag{3}$$

Solving for i_p

$$i_p = \frac{\mu e_g}{r_p + (1 + \mu) R_k R_L/(R_k + R_L)}. \tag{4}$$

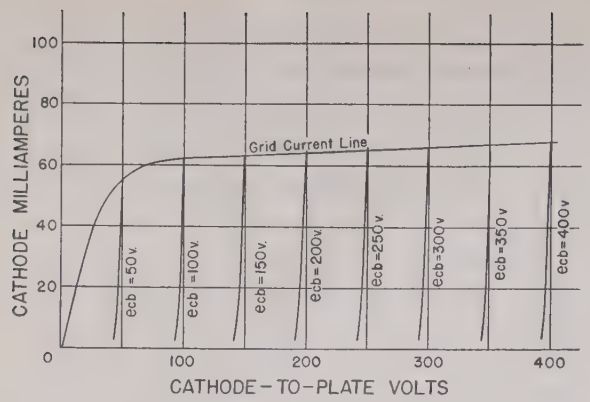

Fig. 13—Cathode-follower characteristic for 6AG7 cathode-to-screen volts = 150. Screen by-passed to cathode.

For purposes of comparison consider a source e in series with a source resistance R_s and a load resistance R_r. The load current i_r is

$$i_r = e/(R_s + R_r). \tag{5}$$

Equation (4) can be rewritten

$$i_p = \frac{(\mu/(1+\mu))e_g}{r_p/(1+\mu) + R_kR_L/(R_k+R_L)} \tag{6}$$

and by comparison with (5) the cathode-follower may be represented by a source $(\mu/(1+\mu))e_g$ with a resistance $r_p/(1+\mu)$.

If μ is large compared to 1, as is usually the case, the source is approximately e_g and the resistance is $r_p/\mu = 1/g_m$. This is based upon the treatment of R_k and R_L in parallel as the load. The source and impedance looking back from a load R_L alone are, of course, a function of R_k.

Appendix B

Figs. 9, 10, 11, 12, and 13 are cathode-follower characteristics constructed for several popular tube types. The graphs for the triodes are accurate. Those for the pentodes are constructed according to the approximate method described above.

Modulated-Beam Cathode-Ray Phase Meter*

ALAN WATTON, JR.†, ASSOCIATE, I.R.E.

Summary—**This paper describes a phase meter developed to measure the phase-shift characteristics of amplifiers used in vibration-measurement work. It employs a cathode-ray tube, in conjunction with a circuit establishing a circular time base on the screen of the tube, and a "clipper" circuit fed in turn by the two voltages, the phase difference of which it is desired to measure. The change in angular position of the semicircle obtained on the screen is the phase difference in the voltages. The method possesses several distinct advantages, including indication of the sense of the phase difference and accurate operation at subaudible frequencies.**

Introduction

AMPLIFIERS used in vibration measurement generally employ negative feedback to stabilize gain and phase shift. An accurate knowledge of the transmission characteristics of the complete feedback loop of such amplifiers, in both gain and phase, is required if an appreciable amount of feedback is applied over more than two stages of amplification. In addition, the phase-shift characteristics of the completed amplifiers are of interest. The band of frequencies involved in vibration waves extends approximately from 8 to 3000 cycles per second; however, due to the properties of negative feedback,[1] it is generally necessary to control loop characteristics over a much wider range.

Methods of Measuring Phase

Because of the importance of phase-angle determination, a great variety of circuits and instruments has been devised. Probably the best known is to apply the two voltages each to a pair of plates of a cathode-ray tube and obtain the angle from a measurement of the geometry of the ellipse. This method, although in common use, is neither particularly accurate nor convenient.

The method which is the basis of the meter described in this paper employs a cathode-ray tube, in conjunction with a circuit establishing a circular time base on the screen of the tube, and a "clipper" circuit fed in turn by the two voltages, the phase difference of which it is desired to measure. The change in angular position of the semicircle obtained on the screen is the phase difference in the voltages.

The method is not new; it is noted by von Ardenne,[2] and an instrument of this type has been described by Nijenhuis.[3] Apparently it has not received attention in American journals. It is readily adapted to use at subaudible frequencies and possesses other advantages in accuracy and convenience.

Outline of Modulated-Beam Method

A block diagram of the modulated-beam cathode-ray phase meter is given in Fig. 1. The four-terminal network, amplifier, etc., under test are fed from a source of sine-wave voltage, e.g., an audio-frequency oscillator. This test voltage is also fed into phase-shifting networks that give two voltages of equal magnitude but 90 degrees apart in phase.

* Decimal classification: R254. Original manuscript received by the Institute, July 12, 1943.

† First Lieutenant, United States Army Air Corps, Materiel Center, Wright Field, Dayton, Ohio.

[1] H. W. Bode, "Relations between attenuation and phase in feedback amplifiers," *Bell Syst. Tech. Journ.*, vol. 19, pp. 421–454; July, 1940.

[2] Manfred von Ardenne, "Cathode-Ray Tubes," Sir Isaac Pitman and Sons, Ltd., London, England, 1939.

[3] W. Nijenhuis, "Measurement of phase angles by the cathode-ray oscillograph," *Elektrotech. Zeit.*, vol. 62, pp. 411–412; April 24, 1942; summary from *Philips Tech. Rundschau*, vol. 5, p. 210 onwards; July, 1940; also in *Philips Tech. Rev.*, vol. 5, pp. 189–216; July, 1940.

These voltages, amplified and put upon the deflecting plates of a cathode-ray tube, produce a circular trace on the screen. At the same time, first the input voltage and then the output voltage of the network under test are passed in turn through a clipper circuit and onto the intensity grid of the cathode-ray tube. When the direct-current potential of the grid is suitably adjusted, the output voltage of the clipper will cause a semicircle to appear on the screen. (Fig. 2.)

The difference in the angular position, measured on a scale at the edge of the screen, of the semicircle when the clipper is fed with one voltage to its position when the clipper is fed with the other, is the phase difference between the voltages. A knowledge of the direction of spot motion will allow determining which voltage lags (or leads) the other.

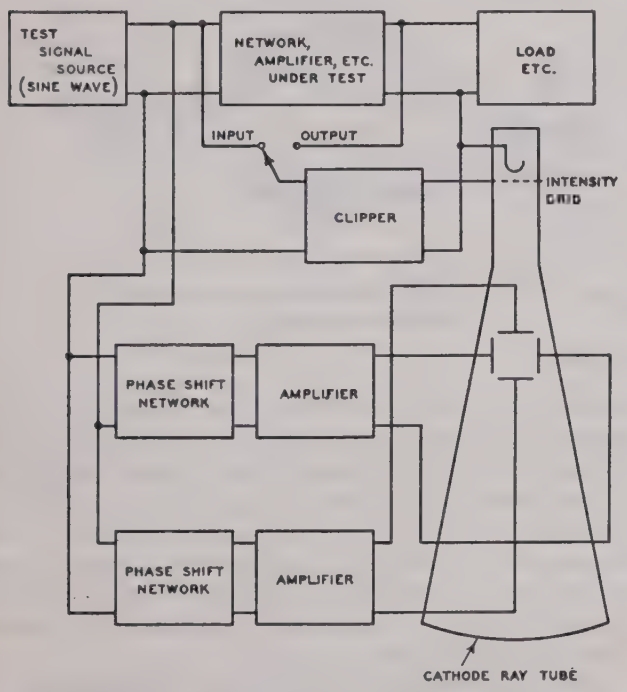

Fig. 1—Schematic block diagram of modulated-beam cathode-ray phase meter.

Typical Instrument

The front view of a phase meter, built in accordance with this outline, is shown in Fig. 3. It is capable of measuring phase differences to an accuracy of ± 1 degrees from 3 to 10,000 cycles per second, and with somewhat less accuracy down to 0.5 cycle per second and up to 20,000 cycles per second. Moderate control voltages of the order of 1 volt are required for its operation. The internal construction is similar to that of commercial oscilloscopes; the cathode-ray tube is shielded magnetically, and the transformers and chokes are well to the rear of the case.

The complete circuit diagram is shown in Fig. 4 and a parts list is given in the Appendix. The production of the circular time base is accomplished by first amplifying the sine-wave signal from the oscillator, etc., through a pair of tubes in a phase-inverter circuit. Then the signal is fed through a phase-shifting network of the resistance-capacitance bridge type.[4] The capacitance is varied in steps to cover the frequency range while the rheostats are used for fine adjustment. Additional fine adjustment, acting on the gains of the two amplifiers, is also provided. At each test frequency these controls are adjusted to obtain the circle on the screen of the tube.

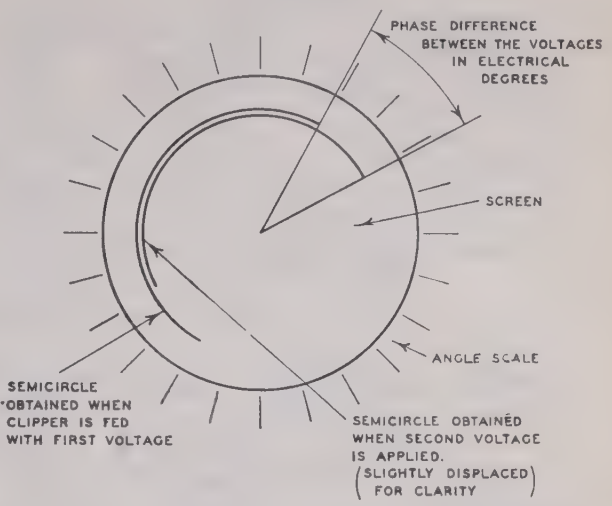

Fig. 2—Method of measuring phase difference from the images formed on the screen of the cathode-ray tube.

Very little distortion is allowable in the circle circuit; the output tubes are triodes in push-pull, and the deflecting plates are balanced to ground.[5]

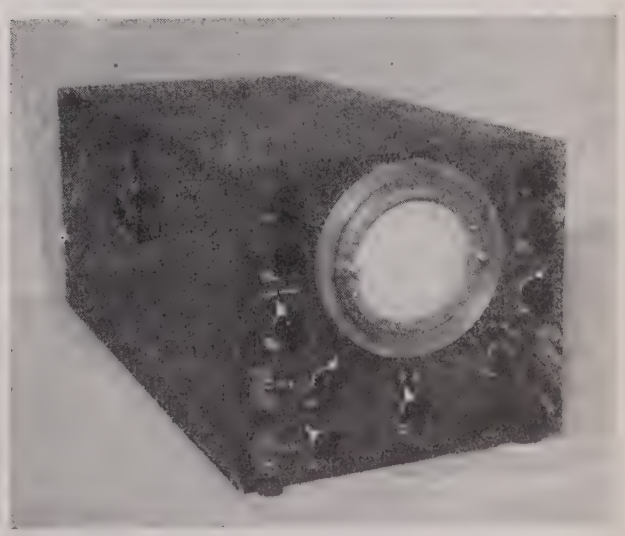

Fig. 3—Photograph of instrument.

The "clipper" circuit is of the biased-diode type.[6] Its operation is illustrated in Fig. 5. Its purpose is to produce a "square" wave whose time of passage through zero potential is the same as that of the voltage whose

[4] F. A. Everest, "Phase shifting up to 360 degrees," *Electronics* vol. 14, pp. 46–49; November, 1941.
[5] G. Robert Mezger, "Oscillograph design considerations," Proc. I.R.E., vol. 27, pp. 192–198; March, 1939.
[6] "Radio Engineering Handbook," edited by Keith Henney, McGraw-Hill Book Co., New York, N. Y. 1941.

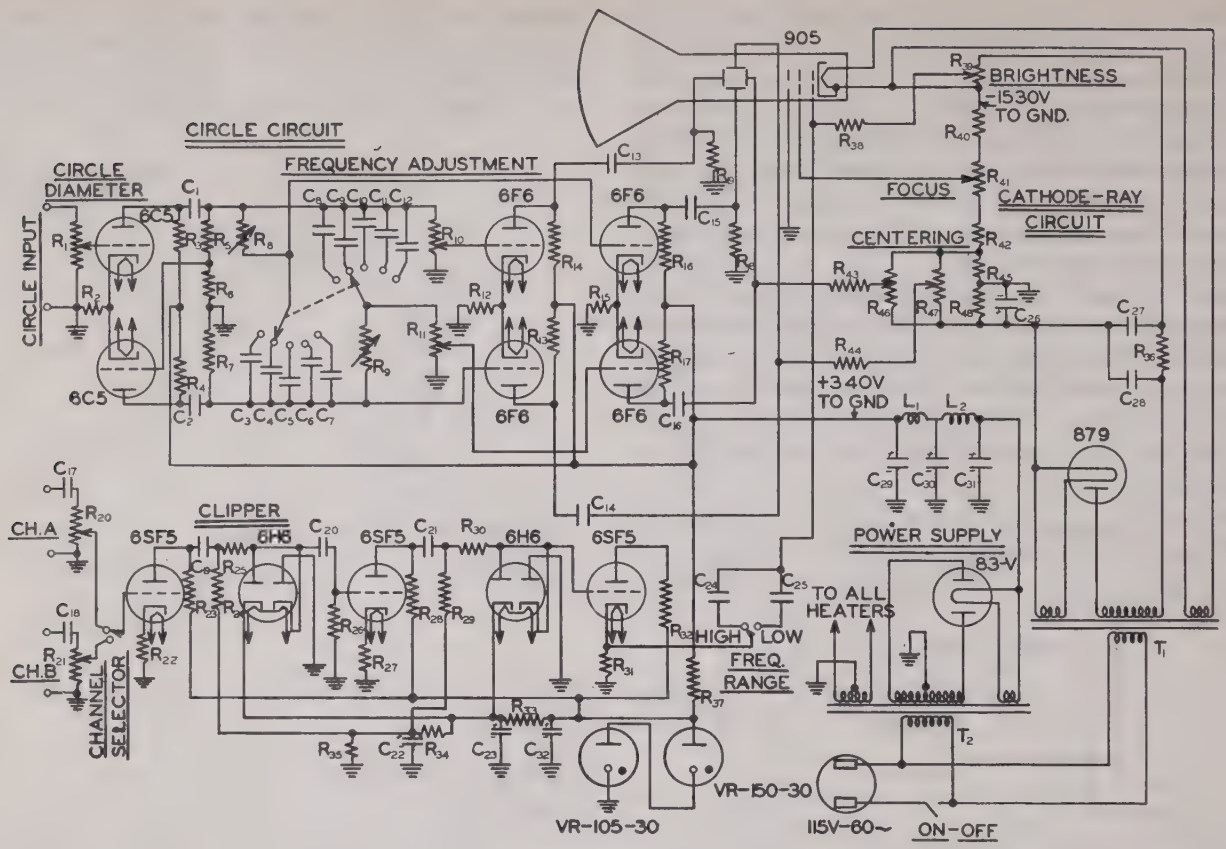

Fig. 4—Circuit diagram.

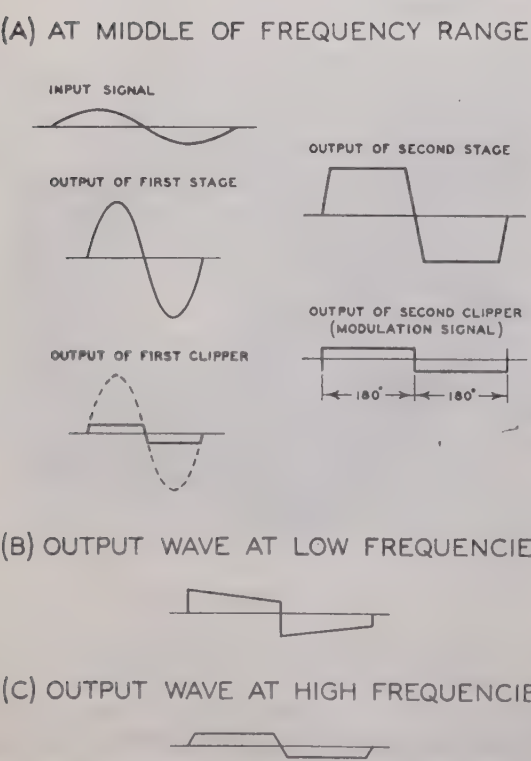

Fig. 5—Operation of clipper circuit.

phase is to be measured. It is important that the change from positive to negative is very fast. For example, if it is desired to measure to 1 degree at 10,000 cycles per second, the time for the change is only 1/3,600,000 second. At high frequencies the clipper will fail, as shown in Fig. 5, due to the effects of stray capacitance in the output circuit of the clipper. Thus the exact position of the zero point becomes somewhat uncertain. At low frequencies the phase shifts in the coupling circuit cause another type of distortion, as shown. This is overcome to some extent by using a very large coupling capacitor when operating at this low range.

The plate supply of the clipper is thoroughly decoupled from the main high-voltage supply by means of the gas-regulator tubes because any crosstalk from the circle circuit is harmful to the accuracy of operation of the clipper.

Angle Scale

The end of the cathode-ray tube is covered with a piece of transparent plastic, marked with a circle to guide in adjusting the circle circuit and with a diametral index line. This piece may be rotated. Around its rim is a scale accurately engraved in half degrees so that the shift in the position of the semicircle thus may be noted readily.

Use of Instrument

The method of use and the versatility of the instrument may be illustrated by the typical problem of measuring the transmission characteristic of a multisection wave filter. The attenuation characteristic may be measured by the usual methods. The circuit used to

obtain the phase-shift characteristic by means of the phase meter is shown in Fig. 6.

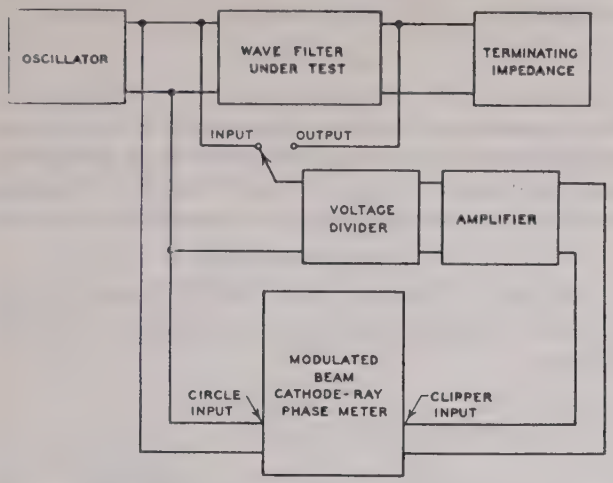

Fig. 6—Circuit used to measure the phase-shift characteristics of multisection wave filter.

Note that any considerable difference between the input and output levels will, in general, necessitate the use of a voltage divider to equalize these levels, and then an amplifier to bring both up to about one volt to operate the "clipper." The phase-shift characteristics of the voltage divider must be accurately known; preferably, it should be zero throughout the frequency range of interest. Note that the effect of phase shift in the amplifier is balanced out and does not affect the accuracy of the readings. Indeed almost any kind of decoupling circuit, wave filter, analyzer, etc., desired, may be added into the circuit along with the amplifier without loss in the accuracy of measurement.

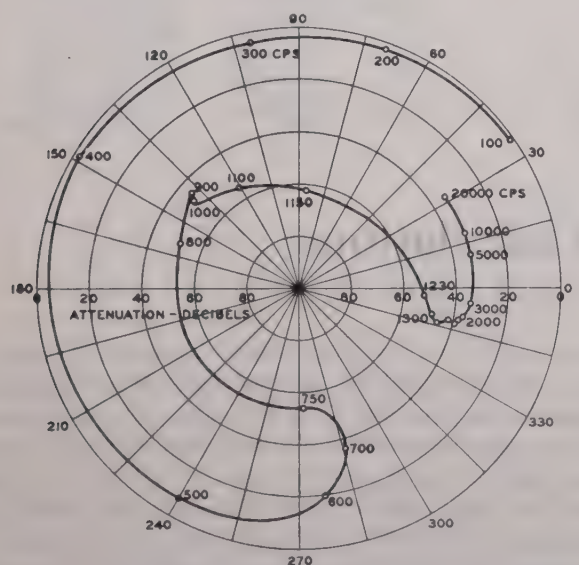

Fig. 7—Transmission characteristics of a multisection wave filter as measured by use of the modulated-beam phase meter, attenuation characteristic being obtained by the usual methods.

The filter characteristics as measured are given in a polar plot in Fig. 7. This problem involved measurement of phase shifts over a frequency range of 100 to 20,000

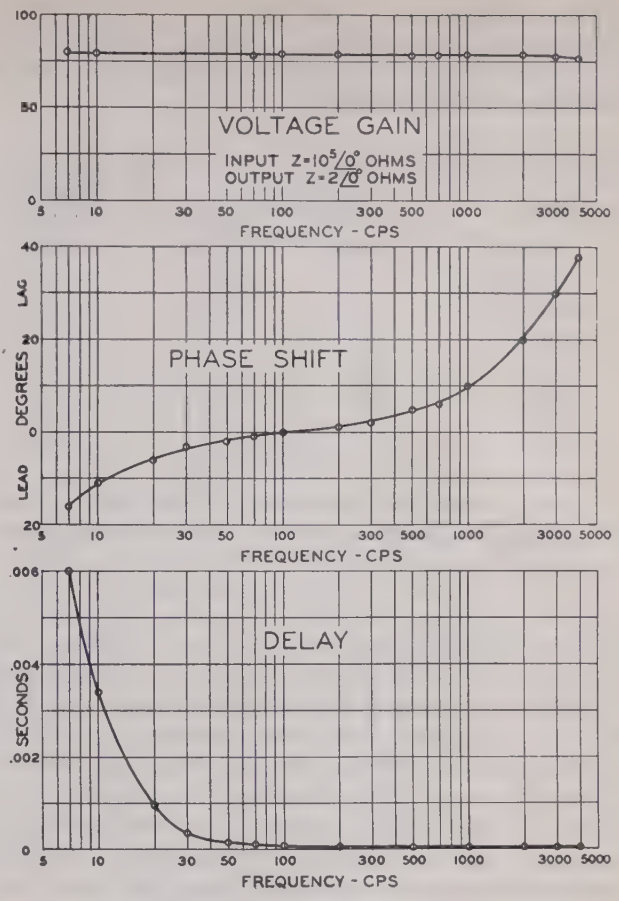

Fig. 8—Typical frequency characteristics of a vibration-measuring amplifier.

cycles per second and between voltages differing as much as 60 decibels in level.

Another application is in the measurement of the characteristics of amplifiers used in vibration measurement work. Typical results are given in Fig. 8.

Finally, as an illustration of the accuracy possible with this phase meter, a simple resistance-capacitance circuit, Fig. 9, was set up and the phase difference between the applied voltage and that across the resistive

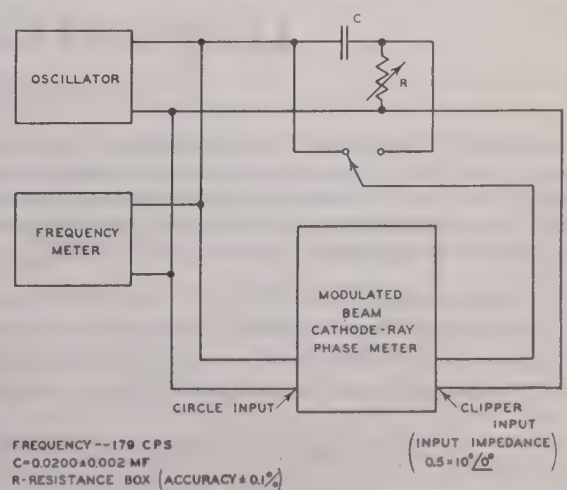

Fig. 9—Circuit used to illustrate accuracy of phase meter. (For results see table in text.)

element measured. A comparison between the measured and calculated values of phase shift for different values of R (input impedance of clipper being 0.5 megacycle resistive) is given in Table I.

TABLE I

Value of R	Phase Shift		Difference (Calculated-Measured)
	Calculated	Measured	
Ohms	Degrees	Degrees	Degrees
10,000	77.5	77.5	±0.0
20,000	66.6	66.0	+0.6
30,000	57.5	57.0	+0.5
40,000	49.5	49.5	±0.0
50,000	44.5	44.0	+0.5
60,000	39.7	39.5	+0.2
70,000	36.0	36.0	±0.0
80,000	32.8	32.5	+0.3
90,000	30.2	30.5	−0.3
100,000	28.4	28.0	+0.4
110,000	26.2	26.0	+0.2

Frequency = 179 cycles per second.

It may be seen that accuracies of better than ±1 degree are possible under favorable circumstances if sufficient care is taken.

Discussion

Examination of the circuit will show that due to its null-reading properties and the many self-checks upon the operation, the first-order effects of many sources of error are eliminated. The circuit possesses definite advantages in the measurement of the phase between voltages at widely different levels. No calibration is required, the dial being accurately engraved directly in degrees of angle. It is capable of operation at the subaudible frequencies of interest in connection with vibration-measuring amplifiers.

In operation, the circle circuit must be adjusted for each change in test frequency. However, the operator will soon obtain skill, so that the operation can be performed with surprising speed. The circle marked on the plastic window is a definite aid.

The sense of the phase differences, i.e., which voltage is leading or lagging the other, is readily obtained from a knowledge of the spot direction. In this meter the spot moves clockwise. Angles up to 360 degrees are measured directly; beyond that, the number of rotations contained in the angle must be obtained from a theoretical consideration of the circuit behavior or elsewhere.

Conclusion

The phase meter described above is well adapted to the measurement of the characteristics of vibration amplifiers employing negative feedback. In addition, it lends itself readily to use in a great variety of problems wherein phase between voltages or currents is of interest.

Acknowledgment

The author is indebted to Mr. R. E. Conover for advice and encouragement in the development of this instrument.

Appendix

List of component parts:

R_1	0.5	megohm	volume control
R_2	630	ohms	½-watt resistor
$R_{3,4}$	50,000	ohms	½-watt resistor
$R_{5,7}$	1	megohm	½-watt resistor
R_6	0.1	megohm	½-watt resistor
$R_{8,9,10,11}$	0.5	megohm	volume control
$R_{12,15}$	1,500	ohms	1-watt resistor
$R_{13,14,16,17}$	15,000	ohms	1-watt resistor
$R_{18,19,43,44}$	2	megohms	½-watt resistor
$R_{20,21}$	0.5	megohm	volume control
R_{22}	4,500	ohms	½-watt resistor
$R_{23,28}$	0.5	megohm	½-watt resistor
$R_{24,26,29}$	1	megohm	½-watt resistor
R_{25}	0.1	megohm	½-watt resistor
R_{27}	2,000	ohms	½-watt resistor
R_{30}	50,000	ohms	½-watt resistor
R_{31}	4,000	ohms	½-watt resistor
R_{32}	20,000	ohms	½-watt resistor
R_{33}	0.25	megohm	½-watt resistor
$R_{34,35}$	2,000	ohms	½-watt resistor
R_{36}	0.8	megohm	4-watt resistor
R_{37}	10,000	ohms	10-watt resistor
R_{38}	1.5	megohms	½-watt resistor
R_{39}	25,000	ohms	volume control
R_{40}	0.25	megohm	1-watt resistor
R_{41}	80,000	ohms	volume control
R_{42}	0.4	megohm	4-watt resistor
$R_{45,46}$	0.5	megohm	½-watt resistor
$R_{46,47}$	0.5	megohm	volume control
$C_{1,2,13,14,15,16,19,20,21}$	1	microfarad	500-volt condenser
$C_{3,8}$	0.3	microfarad	500-volt condenser
$C_{4,9}$	0.04	microfarad	500-volt condenser
$C_{5,10}$	0.005	microfarad	500-volt condenser
$C_{6,11}$	0.0006	microfarad	500-volt condenser
$C_{7,12}$	80	micromicrofarads	500-volt condenser
$C_{17,18}$	0.5	microfarad	500-volt condenser
$C_{22,23,25,32}$	8	microfarads	450-volt condenser
C_{24}	2	microfarads	3000-volt condenser
C_{25}	500	micromicrofarads	3000-volt condenser
$C_{27,28}$	1	microfarad	3000-volt condenser
$C_{29,30,31}$	16	microfarads	450-volt condenser
$L_{1,2}$	20	henries	70-milliampere choke coil

Graphical Gang Calculations*

J. J. ADAMS†, ASSOCIATE, I.R.E.

Summary—**It is possible to calculate graphically the inductance and capacitance relations for cut gangs and padded gangs for superheterodyne receivers. The method for cut gangs is as accurate as the plotting. For the padded gang this is very nearly true. One assumption made in the calculations is found to be very accurate.**

IN a superheterodyne receiver, it is desired to move the oscillator and antenna (and radio-frequency) tuning condensers together so that the resonance of these circuits will have a constant difference over the band equal to the intermediate frequency. Theoretically, this is possible to achieve with properly shaped plates in the two sections of the gang. All constants for the two circuits can be found in terms of the maximum capacitance of each section if the end frequencies of the band are given. This maximum capacitance needed depends on the distributed capacitance of the circuit, including wiring and tube capacitance, coil-distributed capacitance, gang-section minimum capacitance, and trimmer capacitance. It is necessary to guess the value of this distributed capacitance (which can be done accurately with practice) with the trimmer in the middle of its range. Then the maximum capacitances and the

* Decimal classification: R220. Original manuscript received by the Institute, March 22, 1943; revised manuscript received, January 10, 1944.

† Engineering Department, Zenith Radio Corporation, Chicago, Illinois.

other values are determined. If variable condensers are used with the same plate shapes in the two sections, a padding condenser is used. It is possible, in this case, to obtain exact tracking at only three points in the band. To procure the least mistracking at other points in the band, the three tracking points are chosen so that one will be near the middle of the band and the other two near the ends of the band. It is possible to find all the constants of the two circuits in terms of the maximum capacitances if the end frequencies of the band and the three tracking frequencies are given. The rest involves assuming values for the distributed capacitances as above.

Graphical solutions for these two problems are given below, starting with the cut section.

With a properly designed cut section gang it is possible to have the antenna (and radio-frequency) and oscillator sections track at every point on the band. (All calculations are based on the simple diagrams shown in Figs. 1 and 3, and do not take into account any automatic-volume-control condensers that may be in series with the antenna or radio-frequency coils, or the effect of primaries on the secondary inductances.)

For any per cent rotation of the gang, if the antenna capacitance of the gang is given, the oscillator capacitance can be found, or vice versa. Gang manufacturers usually have curves of capacitance against per cent rotation that they like to use. These give a starting point. The maximum capacitances of the sections depend on the distributed capacitance and frequency range.

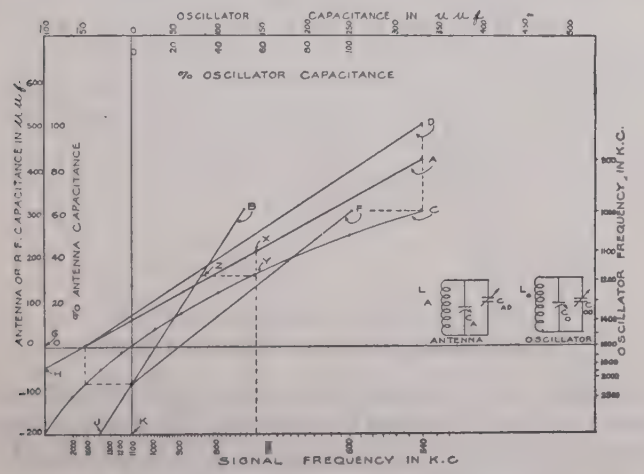

Fig. 1—Graphical method of solving the cut gang.

The curves in Fig. 1 are based on the following theory:

Let

C_a = antenna or radio-frequency capacitance. (This is zero at zero rotation; maximum at 100 per cent.)

C_{ad} = antenna distributed capacitance (including the minimum of the gang, the trimmer capacitance, the distributed capacitance of the coil, and wiring)

C_a max = maximum of section

L_a = antenna inductance

ω_a = $2\pi X$ signal frequency

C_o = oscillator capacitance

C_{od} = oscillator distributed capacitance

C_o max = maximum of section

L_o = oscillator inductance

ω_o = $2\pi X$ oscillator frequency

Then,

$$C_a + C_{ad} = 1/\omega_a^2 L_a, \qquad C_o + C_{od} = 1/\omega_o^2 L_o.$$

Let

$$C_a = x_1, \qquad C_o = x_2$$
$$1/\omega_a^2 = y_1, \qquad 1/\omega_o^2 = y_2$$

we have

$$x_1 + C_{ad} = (1/L_a)y_1$$

and

$$x_2 + C_{od} = (1/L_o)y_2.$$

These are straight lines, having slopes that are reciprocals of the inductances and x intercepts equal to the distributed capacitances. Since $y = 1/\omega^2$, the frequency is plotted as a reciprocal square scale. The antenna-capacitance curve is drawn between the left-hand and bottom co-ordinates and the oscillator capacitance between the upper and right-hand co-ordinates. The line C in Fig. 1 is the intermediate-frequency curve plotted between the two frequency scales, and is defined by $\omega_o = \omega_a + \omega_{I.F.}$, where $\omega_{I.F.} = 2\pi \times$ intermediate frequency.

In Fig. 1 is an example: given

frequency of band

upper	1620 kilocycles
lower	540 kilocycles
intermediate	455 kilocycles

C_a max = 420 micromicrofarads

C_o max = 126 micromicrofarads

Curve A is the antenna-capacitance curve drawn between points (540 kilocycles, 420 micromicrofarads), and (1620 kilocycles, 0). GH on the left scale is the antenna distributed capacitance. Curve B is the oscillator-capacitance curve drawn between points ((540+455) kilocycles, 126 micromicrofarads), and ((1620+455) kilocycles, 0). JK on the upper scale is the oscillator distributed capacitance. (It is not necessary to have a complete oscillator-frequency scale as the oscillator frequency can be found from the signal frequency by using line C.) Given the curve of antenna capacitance against rotation, the oscillator curve against rotation can be obtained as follows: Point X on line A is the antenna capacitance for a certain rotation. The signal frequency at this rotation can be read on the lower scale. From X go vertically to Y on line C, and then horizontally to Z on line B. Z gives the oscillator capacitance for this rotation. Curve A in Fig. 2 is a typical antenna section curve, and B is its tracking curve obtained from Fig. 1. Curve C is the composite of these two curves multiplied by the ratio of the two maxima. It can be shown that this curve C, which is the relation between the plate shapes, is independent of the maximum capacitances.

For example, if the oscillator maximum is doubled, each of the other oscillator values is doubled for the same

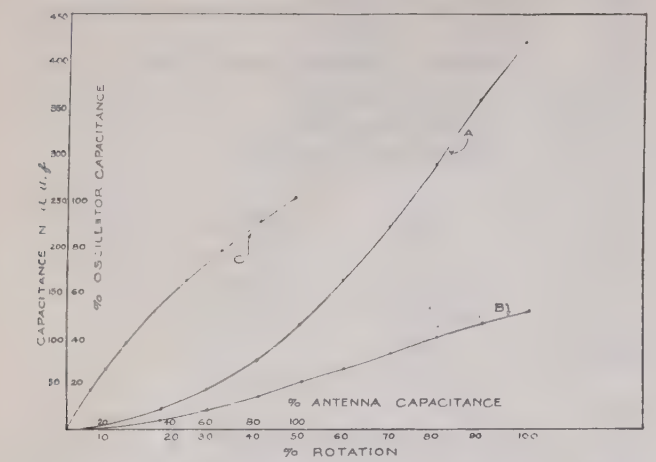

Fig. 2—Cut gang curves.

tracking. This can be expressed as a relation between C_a/C_a max and C_o/C_o max, which becomes

$$\frac{C_o}{C_o\,\max} = \frac{(\omega_2+\omega_o)^2}{(\omega_1+\omega_o)^2-(\omega_2+\omega_o)^2}\left[\frac{(((\omega_1^2-\omega_2^2)/\omega_2^2)(C_a/C_a\,\max)+1)(\omega_1+\omega_o)^2}{(\omega_1+\omega_o\sqrt{((\omega_1^2-\omega_2^2/)\omega_2^2)(C_a/C_a\,\max)+1})^2}-1\right]$$

where ω_1 = top frequency of band
ω_2 = lower frequency of band
ω_o = intermediate frequency

This equation can be solved by lines D and F in Fig. 1, using the per cent capacitance scales. Curve C in Fig. 2 is obtained directly from these lines. This solution for the cut gang is much less laborious than the regular solution.

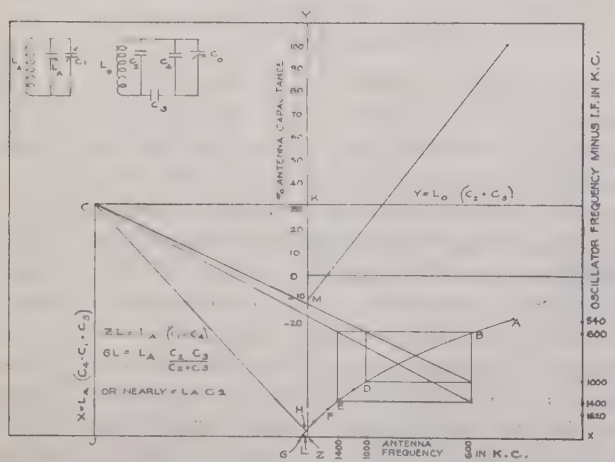

Fig. 3—Graphical method of solving the padded gang.

The padded gang can also be solved graphically. Starting with the circuit of Fig. 3, the following equations can be written:

$$C_a + C_1 = 1/\omega_a^2 L_a \qquad (1)$$

and

$$\frac{1}{1/(C_o+C_4)+1/C_3} + C_2 = \frac{1}{\omega_o^2 L_o}. \qquad (2)$$

Equation (2) can also be written

$$C_3 + C_2 - C_3^2/(C_o+C_4+C_3) = 1/\omega_o^2 L_o. \qquad (3)$$

Assuming similar sections, $C_o = C_a/K$ where K is a constant. We can solve the problem for $C_o = C_a$, then multiply C_a and C_1 by K and divide L_a by K.

If $C_o = C_a$, combining (1) and (3) gives

$$C_3 + C_2 - \frac{C_3^2}{1/\omega_a^2 L_a + C_4 - C_1 + C_3} = \frac{1}{\omega_o^2 L_o} \qquad (4)$$

or

$$(C_3+C_2)L_o - \frac{C_3^2 L_o L_a}{1/\omega_a^2 + L_a(C_4 - C_1 + C_3)} = \frac{1}{\omega_o^2}. \qquad (5)$$

If in this equation we let $X = 1/\omega_a^2$ and $Y = 1/\omega_o^2$, then (5) is an hyperbola of the form $Y - A = -B^2/(X+D)$. This is an equilateral hyperbola with horizontal and vertical asymptotes.

At the three tracking points we know that $\omega_o = \omega_a + \omega_{I.F.}$. We are then given three points on the curve and the direction of the asymptotes. This happens to be a set of necessary and sufficient conditions for the complete determination of an hyperbola.

In Fig. 4 is a sketch of an equilateral hyperbola and some characteristics necessary in the construction. If chord CD is drawn, then $AD = BC$ (OA and OB are the asymptotes). Then, if lines are drawn parallel to the asymptotes through C and D, the line between the intersections (JK) will pass through the intersection of the asymptotes (O). This can be seen from the similar

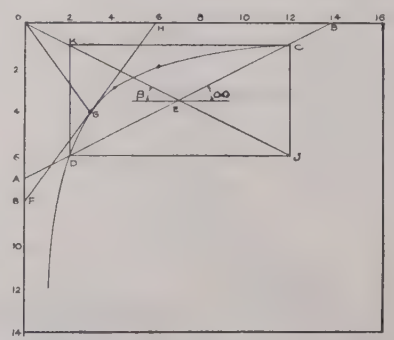

Fig. 4—Characteristics of an equilateral hyperbola.

triangles. Also, E is the center point of CD, so that the point (O) can be found by bisecting CD and drawing EK. If this is done for another set of two points on the curve, we obtain two lines passing through the point (O). This method of finding the intersection of the asymptotes is good for any hyperbola. In an equilateral hyperbola there is also another construction possible, since angle α = angle β.

Another characteristic of the equilateral hyperbola to be used is shown in Fig. 4. For any hyperbola, if FH is tangent to the curve at G, then $FG = GH$. For an equitateral hyperbola, the line joining the point on the curve to the intersection of the asymptotes (OG) has the negative slope of the tangent.

Having the asymptotes and a point on the curve, any other point on the curve can be found by the fact that the product of the perpendicular distances to the asymptotes is a constant. This is most easily done by counting squares on the graph paper.

In Fig. 3 is a plot of (5). After C (the intersection of the asymptotes) has been determined from the given points (B, D, and E) by the above construction, the antenna resonant frequencies corresponding to the oscillator frequencies at the ends of the range can be found (points A and F). Equation (1) can now be plotted between antenna frequency and antenna capacitance as was done for the cut section. This gives L_a (slope of line) and C_1 ($=OM$). Now to secure L_o and C_3. From (5), when X equals $-L_a\ (C_4-C_1)$, dy/dx = slope of tangent $=L_o/L_a$. If C_4 is known (trimmer across coil), we can immediately plot point L at X equals $-L_a\ (C_4-C_1)$, since all these values are known. Point H can now be obtained by $xy=K$ (using C as center of co-ordinates). Then CH has the slope $-L_a/L_o$. This determines L_o. Also, $ZJ=-L_a\ (C_4-C_1+C_3)$, which gives $JL=L_aC_3$, thus determining C_3. If C_2 is known (trimmer across gang), the job is much more difficult. The solution can be obtained by using $xy=C_3^2L_oL_a$, (this x and y being co-ordinates of any point on the hyperbola using C as origin), and $ZK=L_o\ (C_2+C_3)$. (These can be used as check formulas.) This simplification can be used:

When $y=0$, $x=-L_a(C_4-C_1+(C_2C_3/(C_2+C_3))$. This is point G. Then $GL=L_aC_2C_3/(C_2+C_3)$. If we let $GL=L_aC_2$ and go through the construction as before, it is much simpler. When C_2 is known, it (being the coil distributed) is usually very small compared with C_3, and the assumption that $C_2=C_2C_3/(C_2+C_3)$ is very accurate.

When evaluating a $1/\omega^2$ term such as L_aC_3, mark off the distance from Z along ZX to the right of Z and read ω_1 on the lower scale. Then $C_3=1/\omega_1^2L_a$.

The example shown in Fig. 3 is one that often appears. The vertical co-ordinate (oscillator frequency) was made twice the horizontal co-ordinate (antenna frequency) for more accuracy in plotting.

Given

oscillator range 540 to 1620 kilocycles
tracking points 600, 1000, and 1400 kilocycles
C_2 $=10$ micromicrofarads
C_o max $=C_a$ max $=400$ micromicrofarads

The results are

antenna range 534 to 1690 kilocycles
$L_a=200$ microhenries
$L_o=106.5$ microhenries
$C_1=44$ micromicrofarads
$C_4=49$ micromicrofarads
$C_3=470$ micromicrofarads

The tracking error curve can be found from the hyperbola. To do this, a smooth curve must be drawn through the points already obtained. For the determination of the circuit constants, only four points on the hyperbola (A, F, H, and G) need be plotted (excepting the given points B, D, and E.)

These solutions involve considerable work, but probably not as much as the involved formulas and calculations necessary with the regular solution, and they present a picture of the problem that the formulas fail to do.

Bibliography

(1) P. G. Gardiner, "Superheterodyne tracking simplified," *Electronics*, vol. 15, pp. 74–75; November, 1942.
(2) R. deCola, "A superheterodyne tracking solution," *Electronics*, vol. 15, pp. 29–30; February, 1942.
(3) Martin Wald, "Ganging superheterodyne receivers," *Wireless Eng.*, vol. 17, pp. 105–109; March, 1940.
(4) "Design of oscillator circuits for superheterodyne receivers" (covering Philips Setmakers' Bulletin, November, 1938), *Electronics*, January, 1939, review note, page 46.
(5) T. R. W. Bushby, "Thermal-frequency-drift compensation," Proc. I.R.E., vol. 30, pp. 546–554; December, 1942.
(6) F. L. Smith, "Radiotron Designer's Handbook," RCA Manufacturing Company, Harrison, N. J., 1941, p. 110.

Theoretical Gain and Signal-to-Noise Ratio of the Grounded-Grid Amplifier at Ultra-High Frequencies*

MILTON DISHAL†, ASSOCIATE, I.R.E.

Summary—**With the grounded-grid or cathode-input-amplifier circuit the input signal is applied between the grid and cathode of the tube and the output signal is obtained between the grid and plate of the tube.**

It is shown that, to obtain maximum gain, the input circuit should be designed to impedance-match the equivalent generator resistance to R_t/M and the output circuit should be designed to impedance-match the final load resistance to R_pM where R_t is the shunt resistance between cathode and grid due to transit-time loading and Rp is the effective plate resistance of the tube and $M=\sqrt{1+[(u+1)R_t/R_p]}$. Under these conditions the ratio of the voltage across the final load to the generator voltage (i.e., the gain of the complete stage) is $G=[(u+1)\sqrt{R_t/R_1}\ \sqrt{R_1/R_p}]/2(1+M)$. Using the acorn tube 955 the noise factors of a receiver, using the cathode-input circuit and one using the more usual grid-input circuit, are compared showing that for this specific case the noise factor of the cathode-input circuit is almost 3.5 decibels smaller than that for the grid-input circuit, at 100 megacycles. At higher frequencies however the two noise factors approach the same values.

I. Introduction

IT HAS been shown that a triode is always less noisy than a pentode of comparable transconductance.[1] In fact, it has been shown[2] that, with the usual pentodes available, the use of a pentode radio-frequency stage in front of a triode mixer may lower the signal-to-noise ratio of a receiver instead of bettering it. It can be stated that to obtain the best possible signal-to-noise ratio a triode radio-frequency amplifier input stage should be used which should give enough gain to overide the mixer or first-detector noise as much as possible; the input resistance should be high enough so that noise from the input circuit will overide, as much as possible, the triode-tube noise.

The usual method of using a triode as an amplifier has been to apply the input signal between the cathode and grid and to obtain the output between the cathode and plate. This will be spoken of as the grounded-cathode or grid-input circuit. Much use has also been made of the circuit wherein the input signal is applied between the plate and the grid and the output signal is obtained between the plate and the cathode. This will be called the grounded-plate on cathode-follower circuit. For certain applications this circuit has a number of advantages, one of which is its high input impedance and low output impedance. Thus, if one desires to feed an equivalent high-impedance generator into a low-impedance line for example, and the use of impedance-matching circuit elements is impracticable, the cathode-follower circuit can be used with advantage.

Where radio frequencies are concerned, one runs into trouble with the above two circuits because of undesired feedback between the output and input circuits, which necessitates neutralization. In the grounded-cathode circuit, the undesired feedback is due to the grid-to-plate capacitance plus transit-time effects. In the grounded-plate circuit the undesired feedback is due to the grid-to-cathode capacitance plus transit-time effects.

A third method of using a triode as an amplifier is to apply the input signal between the grid and the cathode and to obtain the output between the grid and the plate.[3] This is the grounded-grid or cathode-input circuit. One of the characteristics obtained by using the tube in this way is a low input impedance and a high output impedance. Thus the grounded-grid circuit can be used to advantage when a low-impedance line, for example, feeds a high-impedance load and the use of impedance-matching circuit elements is impracticable. With this circuit, undesired feedback is due to the plate-to-cathode capacitance. With the usual tube in which the grid is between the plate and cathode, the tube can be so constructed that, due to the shielding action of the grid, the plate-to-cathode capacitance is very low in comparison with the other capacitances in the circuit. Under this condition, a triode can be used without neutralization at very high frequency and ultra-high frequency without fear of a large amount of regeneration or oscillation. At frequencies where coaxial lines have to be built around tubes, the lack of need for neutralizing elements is of course a great advantage. In the case of a receiver which is to cover a range of frequencies, freedom from neutralization worries greatly simplifies the design problem. In practice, radio-frequency chokes should be used in the filament leads to remove effectively the cathode-to-filament capacitance from its position across the input circuit.

Since there are tubes available in which the inductance of the leads is negligible, even at ultra-high frequency, these inductances will not be considered in this paper. If present they can cause regeneration and oscillation unless the circuit is neutralized.[3]

It is assumed that an impedance-transforming circuit will be used between the antenna or equivalent generator and the input terminals of the tube, and that an

* Decimal classification: R132×R363.1. Original manuscript received by the Institute, May 11, 1943; revised manuscript received, October 25, 1943.

† Federal Telephone and Radio Corporation, New York, N. Y.

[1] B. J. Thompson, D. O. North, and W. A. Harris, "Fluctuations in space-charge-limited currents at moderately high frequencies," *RCA Rev.*, vol. 4, pp. 269–286; January, 1940; vol. 4, pp. 441–473; April, 1940; vol. 5, pp. 106–125; July, 1940; vol. 5, pp. 244–261; October, 1940; vol. 5, pp. 371–389; January 1941; vol. 5, pp. 505–525; April, 1941; and vol. 6, pp. 114–125; July, 1941.

[2] E. W. Herold, "An analysis of the signal-to-noise ratio of ultra-high-frequency receivers," *RCA Rev.*, vol. 6, pp. 302–332; January, 1942.

[3] C. E. Strong, "The inverted amplifier," *Elec. Comm.*, vol. 19, no. 3, pp. 32–36, 1941; *Electronics*, vol. 13, pp. 14–16; July, 1940.

impedance-transforming circuit will be used between the output terminals of the tube and the final load, which is usually the input impedance of the mixer stage or of a second radio-frequency stage.

This paper will deal only with that frequency band in which transit-time loading is so great compared to the loading caused by circuit losses that the losses in the above circuits can be considered to be negligible, i.e., the circuit elements may be considered to be pure reactances. To see what the magnitude of the transit-time loading would have to be so that the losses in good coaxial line circuits may be considered negligible, let us examine the parallel input resistance of a short-circuited quarter wavelength coaxial line of characteristic impedance Z_0. For a copper line, (b is the inside radius of the outer conductor, and a is the outside radius of the inner conductor) this is[4]

$$R_{sc(\lambda/4)} = 122.2\sqrt{f_0}\, b\, \frac{(\log b/a)^2}{(1 + b/a)}. \qquad (1)$$

Using $b/a = 9.2$ for maximum impedance, $b = 3$ centimeters, and $f_0 = 200$ megacycles we find an input impedance of 475,000 ohms. The above assumes a very good short circuit at the end of the line; for even if the line were loss-free the input impedance to a quarter-wave line terminated in an impedance Z_R is $Z_{in(\lambda/4)} = Z_0^2/Z_R$. To overcome the bad effects of oxidation of the copper, the lines should be silver-plated and polished.

Capacitance across the front of the lines causes the length of line required for resonance to be less than $\lambda/4$. The electrical length $\theta(\theta = 2\pi(l/\lambda))$ required is $\theta = \tan^{-1}(X_c/Z_0)$ and the resonant impedance of the capacitor and line is[5]

$$R_{sc\theta} = R_{sc(\lambda/4)}\{\pi/2 \times [(1 - \cos 2\theta)/(2\theta + \sin 2\theta)]\}. \qquad (2)$$

Thus, assuming that tube and wiring capacitance across the line is such as to make the length of the above line required for resonance be, for example, 60 degrees, we find $R_{sc\theta} = 0.8R_{sc(\lambda/4)} = 380{,}000$ ohms.

We can thus make the rough qualitative statement that so long as the actual and transformed impedances entering in the circuit are very much less than 350,000 ohms (say) at 200 megacycles, we may consider the losses in the above type of circuit elements to be zero with negligible error resulting from this assumption. Since $R_{sc(\lambda/4)}$ is proportional to the square root of the frequency the above values would have to be scaled down if the frequency being considered is lower than 200 megacycles.

II. Equivalent Tube Circuit

The equivalent circuit of a triode which holds from very low frequencies up to those frequencies at which the transit angle is about 30 degrees is given by Llewellyn,[6–8] in Fig. 1.

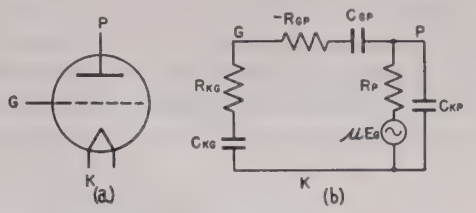

Fig. 1—Equivalent circuit of a triode.

Within the above frequency limits, the values of the elements in the above equivalent circuit are independent of frequency and the grid-to-plate resistance is negative and much smaller than R_{KG}, and μ and Rp are the familiar low-frequency constants.

For $(X_c/R)^2 \gg 1$, a series combination of resistance and capacitance has the same frequency characteristics as has a resistance inversely proportional to the square of the frequency which is in parallel with a capacitance. As Llewellyn points out, this gives a beautifully simple explanation of the fact that the shunt resistance between the grid and cathode due to transit time is inversely proportional to the square of the frequency. Because of the simplification in the equations the equivalent shunt resistance will be used.

In all that follows the negative resistance in series with the grid-to-plate capacitance will be assumed to be so small in comparison with the reactance of the grid-to-plate capacitance that it may be neglected. If this is not true, it is possible to obtain, with the grounded-grid circuit, an input impedance which increases with frequency due to the effect of this negative resistance.

As already mentioned, the plate-to-cathode capacitance will be considered negligible.

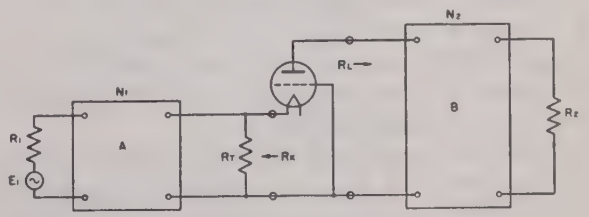

Fig. 2—Circuit to be analyzed to obtain the gain equation.

III. Alternating-Current Circuit

Disregarding direct voltages, the amplifier circuit is given in Fig. 2.

A is any type of impedance-transforming circuit. This must include the dynamic-grid-to-cathode capacitance of the tube.

B is any type of impedance-transforming circuit. This must include the dynamic-grid-to-plate capacitance of the tube.

[4] F. E. Terman, "Resonant lines in radio circuits," *Elec. Eng.*, vol. 53, pp. 1046–1053; July, 1934.

[5] L. S. Nergaard, and B. Salzberg, "Resonant impedance of transmission lines," Proc. I.R.E., vol. 27, pp. 579–584; September, 1939.

[6] F. B. Llewellyn, "Operation of ultra-high-frequency vacuum tubes," *Bell Sys. Tech. Jour.*, vol. 14, pp. 632–665; October, 1935.

[7] F. B. Llewellyn, "Equivalent networks of negative grid vacuum tubes at ultra-high-frequencies," *Bell Sys. Tech. Jour.*, vol. 15, pp. 575–586; October, 1936.

[8] F. B. Llewellyn, "Electron Inertia Effects," Cambridge University Press, New York, N. Y., 1941.

E_1 = equivalent generator voltage

R_1 = generator resistance

N_1 = effective step-up of the input circuit A. That is, at the resonant frequency of the input circuit $N_1 = \sqrt{R_b/R_a}$ where R_b is the shunt resistance one would see between the output terminals of the circuit if a resistance R_a is placed across the input terminals.

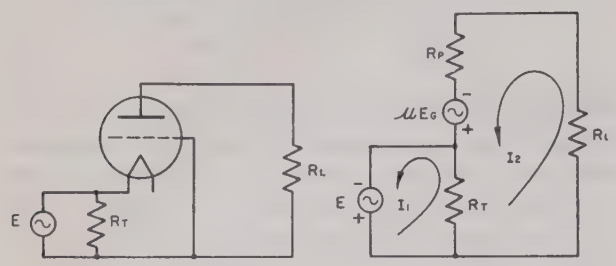

Fig. 3—Circuit analyzed to obtain input impedance.

R_t = shunt resistance between grid and cathode due to transit-time loading.

It should be realized that the transit-time resistance and the transconductance of a tube are interdependent, the relationship being given by $R_t = 1/KG_m f^2\tau^2$ where K is a constant dependent upon electrode spacing and voltages, G_m is the transconductance, f is the frequency, and τ is the cathode-to-plate transit time.[9,10]

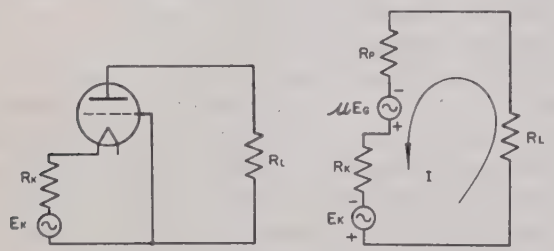

Fig. 4—Circuit analyzed to obtain output impedance.

R_k = resistance seen when looking back from input terminals of the tube = R_t in parallel with $N_1^2R_1$.

R_L = resistance seen looking forward from the output terminals of the tube = R_2/N_2^2.

N_2 = effective step-up of the output circuit B. That is, at the resonant frequency of the output circuit $N_2 = \sqrt{R_d/R_c}$ where R_d is the shunt resistance one would see at the output terminals of the circuit if a resistance R_c is placed across the input terminals.

R_2 = final load. In this analysis this load will be taken to be the shunt transit-time input resistance between grid and cathode of a grid-input triode mixer.

R_p = effective plate resistance of the tube.

[9] W. R. Ferris, "Input resistance of vacuum tubes as ultra-high-frequency amplifiers," PROC. I.R.E., vol. 24, pp. 82–105; January, 1936.

[10] D. O. North, "Analysis of the effect of space charge on grid impedance," PROC. I.R.E., vol. 24, pp. 108–136; January, 1936.

IV. Input and Output Inpedance of Tube

To find the input impedance of the tube we consider the circuit shown in Fig. 3.

$$Z_{in} = \frac{E}{I_1} = \frac{[(R_p + R_L)/(\mu + 1)]R_t}{[(R_p + R_L)/(\mu + 1)] + R_t}. \tag{3}$$

We recognize the input impedance to be the parallel combination of R_t and $[(R_p+R_L)/(\mu+1)]$. If R_t is very large, e.g., at low frequencies, then the input impedance to the tube is merely $[(R_p+R_L)/(\mu+1)]$. Later a constant $M=\sqrt{1+(\mu+1)R_t/R_p}$ will be introduced and in terms of M,

$$Z_{in} = [(R_p + R_L)/(M^2R_p + R_L)]R_t. \tag{3a}$$

To obtain the equivalent output circuit of the tube we consider the circuit shown in Fig. 4.

In the complete circuit of Fig. 2 the E_k of Fig. 4 is $E_k = [R_t/(R_t+N_1^2R_1)]N_1E_1$ and as previously defined $R_k = R_tN_1^2R_1/(R_t+N_1^2R_1)$ and $R_L = R_2/N_2^2$.

Solution for I gives

$$I = \frac{(\mu + 1)E_k}{R_p + (\mu + 1)R_k + R_L}.$$

We recognize this expression as being that which would be obtained from the below equivalent output circuit, shown in Fig. 5

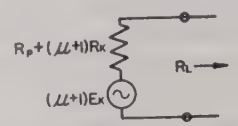

Fig. 5—Equivalent output circuit.

The output impedance of the tube thus is,

$$Z_{out} = R_p + (\mu + 1)R_k. \tag{4}$$

Substituting the general expression for R_k from above and again introducing $M=\sqrt{1+(\mu+1)R_t/R_p}$ we obtain

$$Z_{out} = [(R_t + MN_1^2R_1)/(R_t + N_1^2R_1)]R_p. \tag{4a}$$

V. Gain Equation

The gain of the circuit is defined as the ratio of the voltage V_2 across the final load (R_2) to the generator voltage E_1. This is

$$G_k = \frac{V_2}{E_1} = \frac{(\mu + 1)N_1N_2}{1 + \frac{R_1}{R_t}N_1^2 + \frac{R_p}{R_2}N_2^2 + \frac{R_1\sqrt{1 + (\mu + 1)R_t/R_p}}{R_t}N_1^2\frac{R_p\sqrt{1 + (\mu + 1)R_t/R_p}}{R_2}N_2^2}. \tag{5}$$

Throughout the analysis the quantity $\sqrt{1+(\mu+1)R_t/R_p}$ will occur many times and since it is a constant fixed by the tube used, we shall represent it by

$$M = \sqrt{1 + (\mu + 1)R_t/R_p} \doteq \sqrt{1 + G_mR_t}. \tag{6}$$

The choice of this constant M demonstrates again that this analysis applies only to the very high and ultra-high frequencies, for at the very low frequencies R_t would approach infinity allowing an infinite step-up in the input circuit with M also becoming infinite. It is of course the circuit-element losses which we have

neglected which makes the attainment of infinite step-ups impossible at the low frequencies. Actually, in so far as the gain equations are concerned, they can be applied to low frequencies if R_t is taken as the resultant of the resonant or dynamic resistance of the input circuit in parallel with the transit-time loading. Thus, we have

$$G_k = \frac{(\mu+1)N_1N_2}{1+(R_1/R_t)N_1^2+(R_p/R_2)N_2^2+(R_1M/R_t)N_1^2(R_pM/R_2)N_2^2}. \quad (5a)$$

Voltage gain, rather than power gain, is used because one of the very convenient methods of measuring stage gains make use of the cathode-ray oscilloscope wherein voltages are worked with directly.

The value of N_1 which gives maximum gain is found by setting $\partial G_k/\partial N_1=0$. This results in

$$N_1^2 = \frac{[(R_p+R_2/N_2^2)/(M^2R_p+R_2/N_2^2)]R_t}{R_1}. \quad (7)$$

Since $[(R_p+R_L)/(M^2R_p+R_L)]R_t$ is the input impedance to the cathode for a given $R_2/N_2^2=R_L$ we see that for maximum gain with a given R_L we should use the input circuit to impedance-match the generator impedance to the resultant cathode input impedance.

The value of N_2 which gives maximum gain is found by setting $\partial G_k/\partial N_2=0$. This results in

$$N_2^2 = \frac{R_2}{[(R_t+MN_1^2R_1)/(R_t+N_1^2R_1)]R_p}. \quad (8)$$

Since $[(R_t+MN_1^2R_1)/(R_t+N_1^2R_1)]R_p$ is the output impedance of the tube with given $N_1^2R_1$ we see that for a given $N_1^2R_1$ the output circuit should be used to impedance-match the load impedance to the resultant tube output impedance.

For the case where we can make both N_1 and N_2 optimum (which is the case we wish to consider) substituting (8) in (7) and vice versa gives

$$\left.\begin{aligned} N_1^2 &= [(R_t/M)]/R_1 \\ N_2^2 &= R_2/R_pM \end{aligned}\right\} \text{ for maximum gain} \quad (9)$$

and for this condition we see that the input impedance to the cathode is R_t/M and the output impedance of the tube is (R_pM).

Substituting (9) in the gain equation (5a) the maximum obtainable gain becomes

$$G_{k\max} = \frac{(\mu+1)\sqrt{R_t/R_1}\sqrt{R_2/R_p}}{2(1+M)}. \quad (5b)$$

Comparing this with the maximum gain obtainable with neutralized grid feed, viz.,

$$G_{G\max} = \frac{\mu\sqrt{R_t/R_1}\sqrt{R_2/R_p}}{4} \quad (10)$$

we see that the ratio of maximum gain obtainable by cathode feed to that obtainable by grid feed is

$$G_{k\max}/G_{G\max} = [2/(1+M)](\mu+1)/\mu \doteq 2/(1+M). \quad (11)$$

Thus we see that at the ultra-high frequencies where R_t becomes so small that M approaches unity the maximum gain obtained with cathode feed is the same as that obtained with grid feed and in the limit both gains approach zero.

In many cases, for the sake of mechanical simplicity, it is desirable to connect the generator directly to the input terminals of the tube and the final load directly to the output terminals of the tube. In this case $N_1=N_2=1$ and the gain equation becomes

$$G_1 = \frac{(\mu+1)}{1+R_p/R_2+(\mu+1)R_1/R_2+R_1/R_t+R_1R_p/R_tR_2}. \quad (5c)$$

Finally, if the generator is connected to the final load by an impedance-matching transformer without using a tube the gain would be

$$G_2 = 1/2[\sqrt{R_2/R_1}]. \quad (12)$$

As a specific numerical example let us consider the case of a 250-ohm antenna, a 955 acorn tube as the input radio-frequency stage using cathode feed, and a 955 grid-fed mixer at a frequency of 400 megacycles. Here R_t is approximately 1000 ohms, R_2 is approximately 1500 ohms, $\mu=25$, and R_p is 12,000 ohms. Therefore, $M=\sqrt{1+(\mu+1)R_t/R_p}=1.78$. The input impedance to the cathode, for maximum gain will be $R_{in}=R_t/M=560$ ohms. The output resistance of the tube will be $R_{out}=R_pM=21{,}400$ ohms. The input circuit step-up should be $N_1=\sqrt{(R_t/M)/R_1}=1.56$ and the output circuit step-up should be $N_2=\sqrt{R_2/R_pM}=0.265$. The gain then will be

$$G_{k\max} = \frac{(\mu+1)\sqrt{R_t/R_1}\sqrt{R_2/R_p}}{2(1+M)} = 3.25$$

while with grid feed the maximum gain obtained would be

$$G_{G\max} = \frac{\mu\sqrt{R_t/R_1}\sqrt{R_2/R_p}}{4} = 4.42.$$

If the 250-ohm generator is connected directly to the input and the load directly to the output the gain obtained would be (using (5c)) $G_1=1.67$.

It should be noted that with the grounded-grid circuit it is important to use an impedance-matching transformer (B) between the output terminals of the tube and the final load. This is because of the large impedance ratio between the output resistance and the load resistance (i.e., due to its feedback the grounded-grid circuit produces a relatively high output impedance, while due to transit-time effects and dielectric losses, we have forced upon us low input or load impedances).

In the above specific example the change in gain from 3.25 with impedance matching, to 1.67 without impedance matching, is due, almost entirely, to the lack of the output-matching circuit.

Of course, if the generator resistance was of such a

value as to produce a large impedance ratio between the generator resistance and the input resistance of the circuit, the input-matching circuit (A) would become equally important.

If an impedance-matching transformer only is used the gain will be (using (12)) $G_2 = 1.24$.

VI. Bandwidth of the Circuits at Critical Coupling

It is usually necessary to know what band of frequencies will be passed by the circuits for the maximum gain condition.

If, unfortunately, the distributed capacitances and those due to the tube are too large, the band pass of the circuits when critically coupled for maximum gain may be too narrow to be used for a particular application. If this should be the case, greater than critical coupling must be used in the circuit which is too narrow. If the circuit is an equivalent single-tuned, impedance-matching circuit as in Fig. 6, for example, increasing the

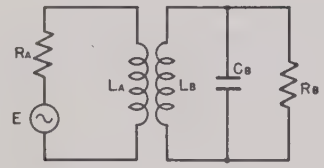

Fig. 6—One type of impedance-matching circuit.

coupling is all that is required satisfactorily to widen the pass band. If an equivalent double-tuned, impedance-matching circuit, as in Fig. 7, is used then, besides increasing the coupling, additional damping is required to remove the resultant valley in the center of the pass band. Due to the much higher resistance involved on

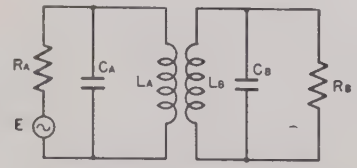

Fig. 7—Another type of impedance-matching circuit.

the plate side, we will find that for the usual capacitances met with, the output-circuit band pass is much narrower than that of the input circuit. This, also, means that in tuning the circuits the output circuit will be much more critical to adjust then the input circuit.

An approximate expression (true for small percentage bandwidths) for the bandwidth between the 0.707 voltage-ratio points of any equivalent, double-tuned circuit, such as Fig. 7, when it critically couples two resistances is

$$(\Delta f_{0.707}/f_0) = -(n_A - n_B)^2/2 + \sqrt{[(n_A - n_B)^2/2]^2 + 4n_A^2 n_B^2}. \quad (13)$$

$n_A = 1/Q_A$ for primary circuit

$n_B = 1/Q_B$ for secondary circuit

If parallel resonance is used as in Fig. 7 $n = X_p/R_p$ where R_p is the resistance in parallel with the tuned circuit and X_p is the reactance of the capacitance (or inductance). If series resonance is used $n = R_s/X_s$ where X_s is the reactance of the capacitance (or inductance) and R_s is the resistance in series with the tuned circuit. (This equation is obtained from (7) on page 989 of Purington's paper.[11] If the critical coupling condition $K = \sqrt{n_A n_B}$ (K is the coefficient of coupling) is inserted in this equation we can obtain (13) of this paper.) This expression assumes that the Q's of the two circuits remain constant, which is not strictly true. The answer obtained from its use, however, is a very close approximation to the actual bandwidth obtained.

Let us consider the output circuit in our former example using the 955's, and assume it consists of a double-tuned circuit of the type of Fig. 7. We shall allow 1 micromicrofarad on each side for the wiring capacitance, We thus have $C_A = Cpg + 1$ micromicrofarad $= 2.4$ micromicrofarads. Since the second tube is a grid-fed mixer we have $C_B = Cgk + Cgp + 1$ micromicrofarad $= 3.4$ micromicrofarads. We found previously that $R_A = R_p M = 21{,}400$ ohms, and $R_B = R_2 = 1500$ ohms.

Therefore, at 400 megacycles $n_A = X_A/R_A = 0.0078$ and $n_B = X_B/R_B = 0.078$.

With these Q's, the coefficient of coupling which will give the required step-up, i.e., which will impedance-match R_2 and $R_p M$ is $K = \sqrt{n_A n_B} = 0.025$. By substituting in (9) we have $\Delta f_{0.707} = 6.9$ megacycles.

The same steps would be carried out for the input circuit if it is a double-tuned circuit. If it is an equivalent single-tuned circuit as in Fig. 6, simple approximation formula for the bandwidth between the 0.707 voltage ratio points is

$$\Delta f_{0.707}/f_0 = 1/\omega C_B R_T \quad (14)$$

where $R_T = R_B N^2 R_A/(R_B + N^2 R_A)$ where N is the effective step-up (as defined before) of the circuit.

VII. Signal-to-Noise Ratio

The circuit which must be analyzed to obtain the output noise is given in Fig. 8.

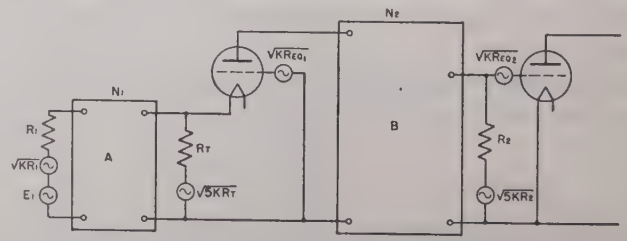

Fig. 8—Circuit to be analyzed to obtain the signal-to-noise ratio.

The sources of noise in this circuit are:

1. The antenna or generator resistance which is considered to be at room temperature.

2. The transit-time-loading resistance which is considered to be a temperature of $5t$. North and Ferris have

[11] E. S. Purington, "Single- and coupled-circuit systems," Proc. I.R.E., vol. 18, pp. 983–1017; June, 1930.

shown[12] that with grid-controlled tubes with control grid next to the cathode, the induced grid noise is equivalent to the thermal noise due to a resistance of the same value as the shunt transit-time loading resistance whose temperature is about 5 times room temperature. They have also shown that, to a first approximation, induced grid noise may be considered to be independent of the plate noise of the tube.

3. The tube, whose noise is represented by a noise voltage generator at the grid.[1] It will be assumed that the noise due to the tube can be represented by a voltage generator at the grid for the case where there is feedback as well as for the case where there is no feedback. It will also be assumed that the value of the noise-equivalent resistor for the tube is the same when the tube is used with and without feedback.

The noise-equivalent resistor $R_{eq\cdot 1}$ for the tube is considered to be at room temperature t.

4. The load resistance which, in our case, is the transit-time resistance of the next tube and so is considered to be at a temperature $5t$.

5. The next tube and all noise sources after it. This noise voltage is given in terms of an equivalent-noise resistance, $R_{eq\cdot 2}$.

The open-circuit root-mean-square noise voltage due to these resistors is[13,14]

$$E_n = \sqrt{4KT\Delta f R} \tag{15}$$

thus $$E_{n27^\circ C} = \sqrt{1.65 \times 10^{-20}\,\Delta f R} = \sqrt{kR}$$

where T = absolute temperature of resistors.

Δf = the resultant band pass of the receiver which is assumed to be rectangular and to be narrower than the band pass of the radio-frequency circuits.

K = Boltzman's constant, 1.37×10^{-23} joule per degree absolute

Considering each noise generator separately (superposition theorem) and using the equivalent output circuit of the tube, we obtain the noise voltage across R_2 due to R_1

$$V_{R_1} = G_k\sqrt{kR_1} \tag{16}$$

where G_k is given by (5).

The noise voltage across R_2 due to R_t is

$$V_{R_t} = G_k N_1\sqrt{R_1/R_t}\sqrt{5kR_1}. \tag{17}$$

The noise voltage across R_2 due to $R_{eq\cdot 1}$ is

$$V_{Req\cdot 1} = G_k\frac{(1 + N_1^2R_1/R_t)}{N_1}\sqrt{kR_{eq\cdot 1}}. \tag{18}$$

To obtain (18), the approximation that $(\mu+1) = \mu$ is made.

The noise voltage across R_2 due to R_2 is

$$V_{R_2} = G_k\frac{[(R_pN_2^2/R_2) + (R_1MN_1^2/R_t)(R_pMN_2^2/R_2)]}{(\mu + 1)N_1N_2}\sqrt{5kR_2} \tag{19}$$

and the noise voltage across R_2 due to $R_{eq\cdot 2}$ is

$$V_{Req\cdot 2} = G_k\sqrt{kR_{eq\cdot 2}}/G_k. \tag{20}$$

The total noise voltage across R_2 is

$$V_n^2 = V_{R_1}^2 + V_{R_2}^2 + V_{Req\cdot 1}^2 + V_{R_2}^2 + V_{Req\cdot 2}^2.$$

The signal voltage across R_2 is

$$V_s = G_kE_1. \tag{21}$$

The signal-to-noise ratio is, therefore,

$$\left(\frac{V_s}{V_n}\right)_k^2 = \frac{E_1^2}{kR_1\left[1 + 5\frac{R_1N_1^2}{R_t} + \frac{(1 + R_1N_1^2/R_t)^2}{R_1N_1^2}\left\{R_{eq\cdot 1} + \frac{(H)^2 5R_2 + (J)^2R_{eq\cdot 2}}{[(\mu + 1)N_2/2]^2}\right\}\right]} \tag{22}$$

where

$$H = \frac{R_pN_2^2/R_2 + (R_1MN_1^2/R_t)(R_pMN_2^2/R_2)}{2(1 + R_1N_1^2/R_t)} \tag{23}$$

$$J = \frac{1 + R_1N_1^2/R_t + R_pN_2^2/R_2 + (R_1MN_1^2/R_t)(R_pMN_2^2/R_2)}{2(1 + R_1N_1^2/R_t)}. \tag{24}$$

It is of interest to compare the above general equation for the signal-to-noise ratio for the grounded-grid circuit with that obtained for the usual grid-fed amplifier circuit which is[2]

$$\left(\frac{V_s}{V_n}\right)_G^2 = \frac{E_1^2}{kR_1\left[1 + 5\frac{R_1N_1^2}{R_t} + \frac{(1 + R_1N_1^2/R_t)^2}{R_1N_1^2}\left\{R_{eq\cdot 1} + \frac{[R_p/(R_p + R_2N_2^2)]^2 5R_2 + R_{eq\cdot 2}}{\left[\frac{\mu N_2}{1 + R_pN_2^2/R_2}\right]^2}\right\}\right]}. \tag{25}$$

Comparing (22) and (25) we see that if there were no noise due to the load resistance R_2 and any noise sources

[12] D. O. North, and W. R. Ferris, "Fluctuations induced in vacuum-tube grids at high frequencies," PROC. I.R.E., vol. 29, pp. 49–50; February, 1941.

[13] J. B. Johnson, "Thermal agitation of electricity in conductors," *Phys. Rev.*, vol. 32, pp. 97–109; July, 1928.

[14] H. Nyquist, "Thermal agitation of electric charge in conductors," *Phys. Rev.*, vol. 32, pp. 110–113; July, 1928.

$R_{eq\cdot 2}$ beyond R_2 the signal-to-noise ratio for the two cases would be identical, i.e., the effect of noise due to the generator resistance, the induced grid noise and the plate noise is the same in both cases; the negative feedback involved in the cathode input circuit does not change the effect of these noises in so far as the signal-to-noise ratio is concerned. However, for the same N_1 and N_2 in both cases it will be seen that since M is always greater than unity, the factors multiplying R_2 and $R_{eq\cdot 2}$ will always be larger for the cathode-feed case and so the effect of the noise due to R_2 and $R_{eq\cdot 2}$ will be greater with cathode feed than with grid feed. This result may be said to be due to the lower gain obtainable with cathode feed.

It is also of interest to note that for the grid-feed circuit the effect of the noise due to R_2 and $R_{eq\cdot 2}$ is a function of the step-up N_2 in the output circuit only. For the cathode-feed circuit however, the effect of R_2 and $R_{eq\cdot 2}$ on the signal-to-noise ratio is a function of both the step-up N_1 of the input circuit and the step-up N_2 of the output circuit.

Since the signal voltage V_S and the noise voltage V_n are across the same resistance, the square of the signal-to-noise voltage ratio is the ratio of signal power to noise power. It is common practice to consider the signal-to-noise power ratio rather than the signal-to-noise voltage ratio.

We see that the denominator of the signal-to-noise ratio (power) consists of the square of the noise voltage kR_1 due to the antenna or generator resistance, multiplied by a factor. This factor is called the noise factor of the receiver. A receiver with a noise factor of unity would be a noise-free receiver, the signal-to-noise ratio being affected only by the generator resistance. Another way of defining the noise factor, which of course leads to the same result, is to state that it is the ratio of the signal-to-noise ratio obtained with the actual receiver to the signal-to-noise ratio which would be obtained if the generator resistance were the only noise source, the receiver being noise-free.

VIII. Signal-to-Noise Ratio for Maximum Gain

Because it was felt that there is a real advantage, in so far as circuit adjustments are concerned, in working with circuits designed for maximum gain, no attempt has been made to find the values of N_1 and N_2 which make the signal-to-noise ratio a maximum. Rather the maximum-gain condition will be used and the signal-to-noise ratio for this condition will be found. It is also probable that, just as with the grid-feed circuit, the improvement in signal-to-noise ratio that can be obtained with any N_1 or N_2, other than those for maximum gain, will be quite small for values of the circuit components which are encountered in practice.[2]

When the maximum-gain conditions (9) are fulfilled (22) becomes,

$$\left(\frac{V_s}{V_n}\right)_k^2 = \frac{E_1^2}{kR_1\{1 + 5/M + [(1 + M)^2/M](R_{eq\cdot k}/R_t)\}} \quad (22a)$$

where

$$R_{eq\cdot k} = R_{eq\cdot 1} + \frac{5/4R_2 + R_{eq\cdot 2}}{\{[(\mu + 1)/2]\sqrt{R_2/R_pM}\}^2}. \quad (26)$$

The receiver noise factor for this case is thus

$$F_k = \{1 + 5/M + [(1 + M)^2/M](R_{eq\cdot k}/R_t)\}. \quad (27)$$

The generator signal which will give a 1-to-1 signal-to-noise ratio is from (22a)

$$E_{k_{1:1}} = \sqrt{kR_1}\sqrt{F_k}. \quad (28)$$

It is of interest to compare the above noise factor with the noise factor obtained when a grid-fed amplifier circuit is coupled for maximum gain. The signal-to-noise ratio for this case is obtained by substituting the maximum-gain conditions, $N_1 = \sqrt{R_t/R_1}$ and $N_2 = \sqrt{R_2/R_p}$ in (25). We then have

$$\left(\frac{V_s}{V_n}\right)_G^2 = \frac{E_1^2}{kR_1[1 + 5 + 4(R_{eq\cdot G}/R_t)]} \quad (25a)$$

where

$$R_{eq\cdot G} = R_{eq\cdot 1} + \frac{(5/4)R_2 + R_{eq\cdot 2}}{[(\mu/2)\sqrt{R_2/R_p}]^2}. \quad (29)$$

The noise factor is, therefore,

$$F_G = [1 + 5 + 4(R_{eq\cdot G}/R_t)] \quad (30)$$

and the generator voltage required for 1:1 signal-to-noise ratio is, from (25a),

$$E_{G_{1:1}} = \sqrt{kR_1}\sqrt{F_G}. \quad (31)$$

Comparing (27), (26), (30) and (29), we can say the following with reference to the advantages and disadvantages of cathode feed as compared to grid feed in so far as signal-to-noise ratio is concerned when maximum gain is obtained in both cases. Of the three terms in (27) and (30), the first term may be said to represent the effect of the noise due to the generator impedance, the second term the effect of the noise due to the transit-time loading resistance considered to be at a temperature of $5t$, i.e., the induced grid noise, and the third term may be said to represent the effect of all the noise on the plate side of the tube. We see that the effect of the generator impedance noise is the same in both cases. The effect of the induced grid noise is less in the case of cathode feed by the factor M; we may say this is so because the transit-time noise is loaded down more by the lower input impedance of the cathode-input circuit. The effect of the noise due to all the sources on the plate side of the tube is greater in the case of cathode feed. This is due to two effects; both of which are connected with the fact that the maximum gain obtained with cathode feed is always less than the maximum gain obtained with grid feed; first and most important the factor $(1+M)^2/M$ is always larger than 4 since M is always larger than unity and second; the grid-to-grid gain with grid feed, i.e., $\mu/2\sqrt{R_2/R_p}$ is always larger than the factor $(\mu+1)/2\sqrt{R_2/R_pM}$ for cathode feed.

A plot of the square root of the noise factors given by (27) and (30) is shown in Fig. 9 for the previous specific example using the acorn tube 955 over the range from 100 megacycles to 1000 megacycles. We are assuming

that $R_t = 1000$ ohms and $R_2 = 1500$ ohms at 400 megacycles and that they both vary inversely as the square of the frequency. For the 955 amplifier $R_{eq\cdot 1} = 1250$ ohms and for the 955 mixer $R_{eq\cdot 2} = 8000$ ohms. R_p is 12,000 ohms and as before $M = \sqrt{1+(\mu+1)R_t/R_p}$. The ratio of the maximum gain obtained with cathode feed to that obtained with grid feed is also plotted on the same graph.

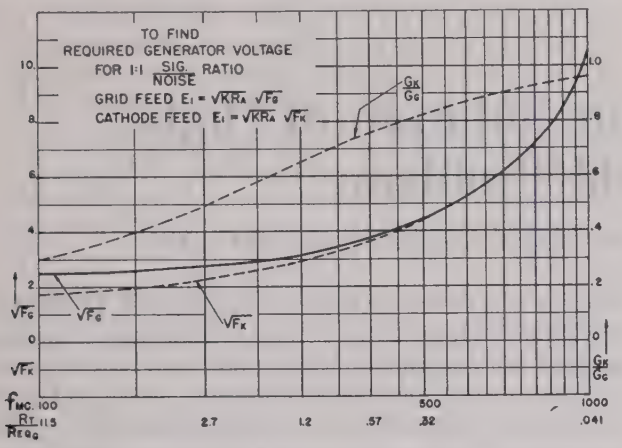

Fig. 9—Square root of noise factors for the impedance-matched case.

For this specific example we see that at 100 megacycles, the cathode-feed noise factor is a small amount (almost 3.5 decibels) smaller than the grid-feed noise factor. We also see that this improvement becomes smaller and smaller as the frequency increases or as $R_t/R_{eq\cdot G}$ decreases. This is the same as saying that the improvement becomes smaller and smaller as the effect of the plate side noise becomes larger and larger. At about 400 megacycles, there is practically no advantage in using cathode feed in so far as signal-to-noise ratio is concerned. Herold[2] shows that just about the same signal-to-noise improvement can be obtained with a grid-fed amplifier by using a smaller value of step-up N_1 in the input circuit than that required for maximum gain.

We see also that for this specific example at 100 megacycles cathode-feed gain is only 30 per cent of grid-feed gain. However, for this example we see that, at 100 megacycles, the gain obtainable with cathode feed is still great enough so that the third term in the cathode-feed noise factor is still small compared to the other terms, just as it is with grid feed. Since the second term in the cathode-feed noise factor is definitely smaller than that in the grid-feed noise factor we conclude with a better signal-to-noise ratio, as above. Another way of stating this is; even though the gain obtained with cathode feed was only 30 per cent of that obtained with grid feed it was still large enough practically to override the tube noise on the plate side and that due to succeeding stages. The lower input noise obtained with cathode feed then gives a better signal-to-noise ratio. Since, in most applications, a radio-frequency stage is used to obtain an improved signal-to-noise ratio, not additional gain, the lower gain obtained in this case with cathode feed is no drawback.

IX. Improvement in Noise Factor Due to Radio-frequency Stage

It is of interest to see just what improvement in noise factor is obtained by the use of a stage of radio-frequency amplification before the mixer, as compared to using a simple impedance-matching circuit to connect the mixer and generator.

For the case of a transformer connecting the generator to the mixer grid, we would obtain for the signal-to-noise ratio an equation of the exact form of (25) in which R_t would become the input resistance of the mixer (i.e., our former R_2); $R_{eq\cdot 1}$ would become our former $R_{eq\cdot 2}$; μ and R_p would become the conversion μ and R_p for the mixer; and $R_{eq\cdot 2}$ would become the noise-equivalent resistor of the first intermediate-frequency tube.

We shall assume, as was done in the former examples, that enough mixer gain can be obtained effectively to make the noise due to the first intermediate-frequency circuit resistance and tube negligible. With this assumption, and substituting the proper subscripts, we have for the mixer

$$\left(\frac{V_s}{V_n}\right)^2_M = \frac{E_1^2}{kR_1\left[1+5\frac{R_1N_1^2}{R_2}+\frac{(1+R_1N_1^2/R_2)^2}{R_1N_1^2}R_{eq\cdot 2}\right]} \quad (32)$$

Considering the impedance-matched or maximum-gain condition which is $N_1^2 = R_2/R_1$, we have

$$\left(\frac{V_s}{V_n}\right)^2_M = \frac{E_1^2}{kR_1[1+5+4(R_{eq\cdot 2}/R_2)]} \quad (32a)$$

and so the noise factor for this case is

$$F_M = 6 + 4(R_{eq\cdot 2}/R_2). \quad (33)$$

A plot of the square root of the noise factors given by (27), for the grounded-grid amplifier preceding the mixer, and (33) for the simple impedance-matching circuit preceding the mixer, is given in Fig. 10. From this

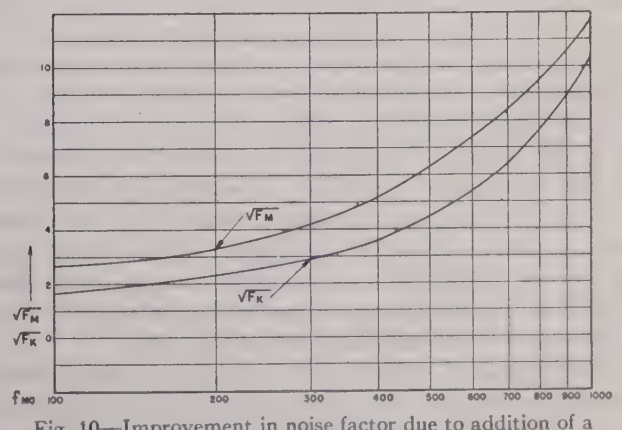

Fig. 10—Improvement in noise factor due to addition of a radio-frequency amplifier stage.

graph we note that at 100 megacycles a 4-decibel improvement in noise factor is obtained by the use of a radio-frequency stage, a 3-decibel improvement is obtained at about 500 megacycles, and a 1-decibel improvement at about 1000 megacycles. In no case is the improvement in the noise factor of the receiver due to the addition of a radio-frequency stage very startling.

X. Conclusion

It may be said that with reference to a triode the cathode-feed circuit is a more stable circuit than grid-feed due to small plate-to-cathode capacitance; that with maximum-gain conditions fulfilled a small gain in signal-to-noise ratio can be obtained by its use at 100 megacycles or where $R_t/R_{eq.G}$ is in neighborhood of 10, that at higher frequencies for the case where $R_t/R_{eq.G}$ is much smaller than 10 there is only a small advantage in using cathode feed in so far as signal-to-noise ratio is concerned.

Acknowledgment

I wish to acknowledge and express appreciation for the helpful discussions I have had on this subject with Messrs A. D. Smith, Jr., and J. S. LeGrand of the Federal Telephone and Radio Laboratories.

A New Approach to the Solution of High-Frequency Field Problems*

J. R. WHINNERY†, ASSOCIATE, I.R.E., AND SIMON RAMO†, ASSOCIATE, I.R.E.

Summary—**A discussion is presented of the possible application of an equivalent circuit suggested by Kron to the solution of high-frequency field problems.**

Introduction

KRON recently has called attention[1,2] to certain distributed constant networks which give approximate representations of Maxwell's equations. This report is concerned with one of those networks that has to do with waves with no variation along one co-ordinate. Specifically, if the derivatives are replaced by finite differences in the field equations, then the equations which result will be found identical with Kirchhoff's laws for certain interconnections of impedance elements. The currents or voltages in the circuits of the network are regarded as representing the E or H of the actual field. Thus, in many field problems, it may be possible to obtain useful approximate solutions by measuring voltages and currents in a proper electrical network whose boundaries correspond to those of the field problem. In addition, appreciation of the relation between some field problems and circuits appears to be extended by consideration of these equivalent circuits, and new analytical approaches may suggest themselves. It is the purpose of this paper to discuss the equivalent-circuit technique for solving high-frequency field problems in a preliminary way so as to speed its evaluation, and to point out that certain classes of problems may be solved with sufficient accuracy on analyzers now available. It may be that some important problems which the readers now have are of this type.

The feeling of the writers that the equivalent-circuit approach may have important and immediate usefulness comes in a large part from the results of a preliminary experimental investigation. What was first thought to be an inadequate board, enough impedance elements to yield the equivalent of only 60 units of space, was connected into a network representing wave guides and transmission lines which were two-dimensional or axially symmetric. Uniform cases and some containing large discontinuities were tried. The results were compared against calculated values and differences of only a few per cent were noted in many cases. These experimental results are discussed in detail in a companion paper.[3]

In these tests, only around ten units were available per wavelength. It had been previously feared that because of the large discontinuities and the known sensitivity of wave-guide characteristics to the ratio of wavelength to dimensions, only the remotest similarity might be observed between theoretical results and measured values. It was more or less assumed that thousands of units would be needed in the network analyzer to be of practical value. Now it appears that a board with hundreds of units might easily prove valuable.

The Equivalent-Circuit Approach

For static fields, where Laplace's equation applies, it is known that a network of like impedance elements can be made to solve the distribution problem if suitably distributed voltages are applied and the resulting current or voltage distribution noted. Also, one-dimensional networks of distributed circuit constants have long been used to represent the principal waves on a transmission line, and recently use has been made of equivalent lumped circuit elements to replace end effects and discontinuities on various wave-guiding systems or antennas. Other than the static case, these equivalent circuits deal with over-all characteristics of a particular wave (as in the principal wave of a transmission line) or a sum of waves (as in the discontinuity impedance). The distributed-constant representation of the common transmission-line problem does not deal, in other words,

* Decimal classification: R140. Original manuscript received by the Institute, December 22, 1943. Presented, Winter Technical Meeting, New York, N. Y., January 28, 1944.

† Electronics Laboratory, General Electric Co., Schenectady, N. Y.

[1] Gabriel Kron, "Equivalent circuits to represent the electromagnetic field equations," *Phys. Rev.*, vol. 64, pp. 126–128; August 1 and 15, 1943.

[2] Gabriel Kron, "Equivalent circuit of the field equations of Maxwell," PROC. I.R.E., this issue, pp. 289–299.

[3] J. R. Whinnery, C. Concordia, W. Ridgway, and Gabriel Kron, "Alternating-current network analyzer studies of electromagnetic cavity resonators," PROC. I.R.E., to be published.

with the distribution of electric or magnetic field between conductors; as a matter of fact, these in general have to be known before the constants of the network can be calculated. Nor does this network represent the action of any local or propagating higher-order waves that can exist along the transmission line.

Kron, on the other hand, starts with Maxwell's equations, replaces the derivatives by finite differences, and recognizes that the series of linear algebraic equations are the circuit equations for certain networks. The network constants are functions only of the space (and also, of course, of the volume of the space element being represented by the block of impedances). That is, if the dielectric constant, the permeability, and the conductivity of the medium are known, then the two-dimensional circuit, for example, is completely fixed and it represents that portion of the medium for all electromagnetic effects that have no variations with the one co-ordinate selected. The only approximations involved are those which vanish in importance as the number of units in a given space approaches infinity. The circuit configuration and distributed constants L, C, and R, once chosen to represent a medium, are the same for all frequencies and all boundary conditions consistent of course with the "two-dimensional" aspect of the original assumption.

As to the newness of this work, it appears that in recent years the usefulness of the distributed-constant approach for universal field problem work has been both denied and defended. It has seemed reasonable to many that complex wave modes precluded the existence of an equivalent circuit with distributed constants, which, perhaps accidentally, serve the electrical engineer so well for ordinary line analysis. Others, notably Schelkunoff,[4] have insistently called attention to the fact that the engineer's use of distributed constants has always been done on a sound basis in electromagnetic theory and implied that the approach, properly handled, has universal application. The present equivalent circuits appear to be in support of the correctness of this latter feeling.

Two-Dimensional Networks: Derivation of an Example

The two-dimensional equivalent circuit lies in one plane, the two significant remaining co-ordinates being used to specify position on that plane. Problems of this class include those of axial symmetry, such as coaxial-line discontinuities, tapered lines, most resonant-cavity structures, and certain antennas. Also included are changes of cross section in two-dimensional guides, corner-turning, and diaphragm problems in certain rectangular wave guides, and problems of finding the ideal propagation characteristics for uniform guides of arbitrary cross section.

The derivation of the equivalent circuits will now be illustrated by carrying through a special case of axial symmetry. In cylindrical co-ordinates, with $\partial/\partial\phi = 0$, the field equations divide into two independent groups, one of which contains only E_r, E_z, and H_ϕ. We concern ourselves for the moment with problems in which only these components are present. The equations in rational mks units are

$$p\mu H_\phi = \partial E_z/\partial r - \partial E_r/\partial z \tag{1}$$

$$(\sigma + p\epsilon)E_r = -\partial H_\phi/\partial z \tag{2}$$

$$(\sigma + p\epsilon)E_z = (1/r)(\partial/\partial r)(rH_\phi) \tag{3}$$

where $p = \partial/\partial t$ and σ, ϵ, and μ are conductivity, dielectric constant, and permeability, respectively. We first transform these equations slightly by multiplying (2) and (3) by r and substituting $rH_\phi = H_\phi'$ to obtain

$$(p\mu/r)H_\phi' = \partial E_z/\partial r - \partial E_r/\partial z \tag{4}$$

$$r(\sigma + p\epsilon)E_r = -\partial H_\phi'/\partial z \tag{5}$$

$$r(\sigma + p\epsilon)E_z = \partial H_\phi'/\partial r. \tag{6}$$

Next, the partial differentials are replaced by finite differences.

$$\left.\frac{\partial E_z}{\partial r}\right|_{r,z} \simeq \frac{E_z\big|_{r+\Delta r/2,z} - E_z\big|_{r-\Delta r/2,z}}{\Delta r}$$

$$\left.\frac{\partial E_r}{\partial z}\right|_{r,z} \simeq \frac{E_r\big|_{r,z+\Delta z/2} - E_r\big|_{r,z-\Delta z/2}}{\Delta z}$$

$$\left.\frac{\partial H_\phi'}{\partial z}\right|_{r,z} \simeq \frac{H_\phi'\big|_{r,z+\Delta z/2} - H_\phi'\big|_{r,z-\Delta z/2}}{\Delta z}$$

$$\left.\frac{\partial H_\phi'}{\partial r}\right|_{r,z} \simeq \frac{H_\phi'\big|_{r+\phi r/2,z} - H_\phi'\big|_{r-\Delta r/2,z}}{\Delta r}.$$

If we further take the special case of $\Delta r = \Delta z$ (this simplification will not interfere with a demonstration of principles), then the field equations finally become

$$\frac{\Delta r p\mu}{r} H_\phi'\big|_{r,z} = E_z\big|_{r+\Delta r/2,z} - E_z\big|_{r-\Delta r/2,z} - E_r\big|_{r,z+\Delta z/2} + E_r\big|_{r,z-\Delta z/2} \tag{7}$$

$$\Delta r\, r(\sigma + p\epsilon)E_r\big|_{r,z+\Delta z/2} = -H_\phi'\big|_{r,z+\Delta z} + H_\phi'\big|_{r,z} \tag{8}$$

$$\Delta r\, r(\sigma + p\epsilon)E_z\big|_{r+\Delta r/2,z} = H_\phi'\big|_{r+\Delta r,z} - H_\phi'\big|_{r,z}. \tag{9}$$

(The points at which H_ϕ', E_r, and E_z are evaluated in (7) to (9) are made different by a half unit so that then comparison with circuit quantities below may be seen more easily).

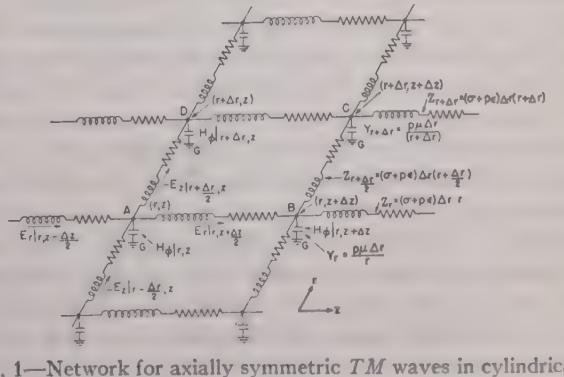

Fig. 1—Network for axially symmetric TM waves in cylindrical co-ordinates.

We now are able to identify these equations with the relations between voltages and currents in a network.

[4] S. A. Schelkunoff, "Guided propagation," *Elec. Eng.*, vol. 62, pp. 235–246; June, 1943.

This network may be thought of as consisting of series impedances along the (r=constant) lines and along the (z=constant) lines (Fig. 1). The junctions are tied together and in addition connected to a common ground through an admittance. The series impedances have the value $r(\sigma+p\epsilon)\Delta r$; the admittances the value $(p\mu/r)\Delta r$. The current flowing in the z direction is E_r, that flowing in the r direction is $-E_z$. The voltage from the junction points to ground, i.e., across the admittances, is H_ϕ'. The equation (7) then corresponds to the Kirchhoff current equation at the junction A and (8) and (9) correspond to the voltage equations around the meshes G-A-B-G and G-A-D-G, respectively. The remaining voltage equation, that about the mesh A-B-C-D, corresponds to the divergence equation which is implied by (1) to (3).

Dual Use of the Network

Had the network been derived for a two-co-ordinate problem in any co-ordinate system other than the cylindrical, the form of the network (the geometrical arrangement of impedances) would still have been the same, although the manner in which the impedances and admittances vary with the co-ordinates would depend upon the metrical coefficients of that system.

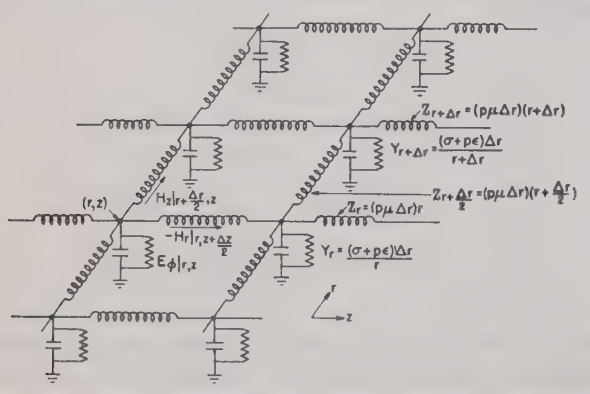

Fig. 2—Network for axially symmetric TE waves in cylindrical co-ordinates.

We can also recognize at once that the same network configuration (impedances at right angles on a plane, admittance to ground at each junction) can be used for waves having two H components, one axial and one transverse, and a single transverse E component. This may be seen in two ways. The derivation we have just gone through for the TM wave can be repeated with the TE wave components. Or, it can be recalled that the two curl equations $\nabla\times\overline{H}=(\sigma+p\epsilon)\overline{E}$ and $\nabla\times\overline{E}=-p\mu\overline{H}$ remain unchanged in form, if for $\overline{E}$, $\overline{H}$, μ, $(\epsilon+\sigma/p)$ are substituted $\overline{H}_1$, $-\overline{E}_1$, $(\epsilon_1+\sigma_1/p)$, μ_1, respectively: $\nabla\times\overline{E}_1=-p\mu_1\overline{H}_1$ and $\nabla\times\overline{H}_1=(\sigma_1+p\epsilon_1)\overline{E}_1$. This says, of course, that the distribution of E and H in one problem may, if the boundary conditions are proper, be exactly the same as the distribution of H_1 and $-E_1$ in another problem. A network configuration capable of reproducing the distribution of TE waves is thus also capable of reproducing TM waves. Of course, the impedances will be different in the two networks because of the interchange of μ and $(\epsilon+\sigma/p)$ though the connection diagram remains the same. The resulting circuit for the TE wave is shown in Fig. 2 also for an axially symmetric case for comparison with Fig. 1. Here, currents in the planar impedances represent magnetic-field intensity, and the voltages across the junction admittances represent the electric field.

Physical Pictures from the Two-Dimensional Circuits

As a first example, let us consider the equivalent circuit that would be used for a rectangular wave guide to study the class of waves for which there are no variations in one direction—say the y direction of Fig. (3a). The practically important TE_{10} wave is of course the lowest order of these. Since there are no variations in the y direction, this is a two-dimensional problem, and moreover only TE waves can exist inside the guide without variations in all three co-ordinates. A suitable equivalent circuit obtainable from a derivation similar to that given for the circularly symmetric case in this report, is similar to that of Fig. 2 except that impedances do not vary with a co-ordinate. The boundary condition of $E_y=0$ at $x=0$ and $x=A$ is applied to the network by short-circuiting the admittances to ground along these planes. The resulting equivalent circuit, assuming no losses in the dielectric, is as shown in Fig. 3(b). This is similar to the equivalent circuit used to represent an ordinary transmission line, except that it is two-dimensional rather than one-dimensional.

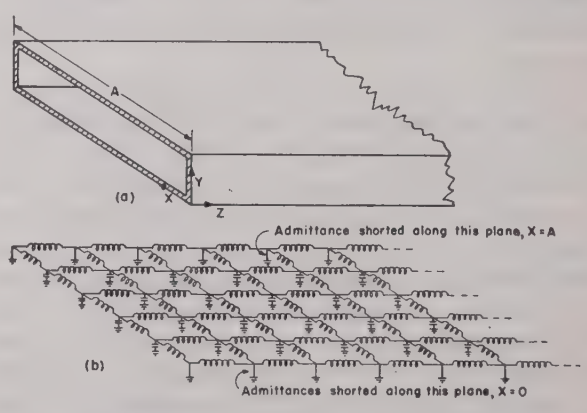

Fig. 3—Rectangular wave guide and equivalent circuit for TE waves without y variations.

The above type of equivalent circuit may be used not only with the uniform guide of Fig. 3 but also with a guide with any type of discontinuities that excite waves with E_y, H_x, and H_z only and with no variations in the y direction. The corner bend of Fig. 4(a) and the change in section of Fig. 4(b) are two examples of this type of "inductive" discontinuity. The new boundary conditions must of course be applied to obtain the complete equivalent circuits for these problems.

The major difference between these circuits and that of an ordinary transmission line is apparent in these examples. While the transmission-line equivalent circuit applies only to the single wave, the principal wave, the

equivalent circuits for the examples of Figs. 3 or 4 may reveal many waves. Thus that of Fig. 3(b) would reveal any of the TE_{mo} waves in the guide of Fig. 3(a), whether these were above or below cutoff. The circuits that would be drawn for the guides of Fig. 4(a) or 4(b)

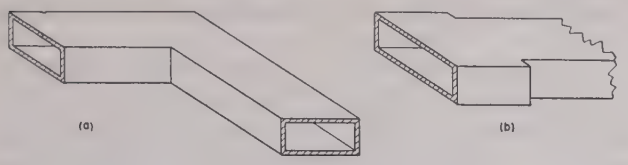

Fig. 4—Examples of wave guides with discontinuities for which two-dimensional equivalent circuits may apply.

would be capable of properly representing the local waves excited at the discontinuities, in addition to the propagating wave.

As a final example, it is interesting to look at an equivalent circuit for representation of waves of the TE_{om} type in a circular wave guide. The circuit suitable for waves with E_ϕ, H_r, and H_z only in problems of axial symmetry was shown in Fig. 2. Thus, assuming that the dielectric of the guide has no losses, the circuit for the circular guide is as shown in Fig. 5(b). Here the values of inductance increase proportionally to radius, and the values of capacitance are inversely proportional to radius. This circuit then looks like the two-dimensional transmission-line representation for a wedge formed by two planes intersecting along a line through the axis.

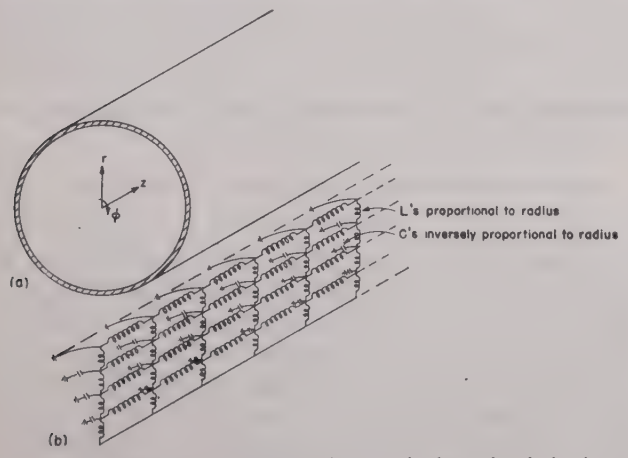

Fig. 5—Circular wave guide and an equivalent circuit for its TE_{om} waves.

From the foregoing examples, it is apparent that certain physical ideas long used in conventional transmission-line analysis may be extended to some wave-guide problems. For example, in ordinary lines the actual current through a section of a conductor is identified with the current in the inductance of the equivalent circuit. The integral of electric field between conductors is identified with the voltage across the condenser of the equivalent circuit. In the network of Fig. 3, the values of L and C could be chosen so that, with the LC product remaining constant to satisfy the field equations, the L/C ratio makes the voltage across the condensers identical with the integral of electric field across the guide, while the currents in the inductances will be identical with the corresponding components of the current flow in the conductors of the guide.

Number of Units Required for a Practical Analyzer

Some ideas on the degree of fineness to which a region should be divided in order that the difference equations of the network should approximate the differential equations of the field with engineering accuracy may be obtained from the studies reported in the companion paper.[3] In representative problems set up on the General Electric Company's alternating-current network analyzer, the number of units varied in the range of about 7 to 14 per wavelength and many results read from the network were within 5 per cent agreement with the theoretical results. There was, however, an appreciable difference in some cases which could accumulate to a serious error if a region several wavelengths long were to be studied. Difference equation analyses reported in the Appendix of the companion paper[3] also point to about 10 to 15 units per wavelength for accuracy within a few per cent for a particular example studied there. From these two clues, it appears that about 20 units per wavelength should be sufficient for engineering accuracy in many problems, although of course more might be required in the neighborhood of sharp boundary discontinuities.

For problems with a considerable degree of complexity, there are several lines of thought that may lead to a decrease in the over-all number of units required. For one thing, fine subdivisions may be made only near sharp discontinuities, and larger ones in the more uniform regions, following similar technique in graphical field mapping. It is also possible that techniques may be worked out for solving only portions of a given region at a time, and combining results from these individual parts by calculation or on the analyzer. Convergence might be obtained, for example, by using overlapping regions in such a procedure.

Effect of Losses in Analyzer Elements

A second important question in considering the construction of an analyzer for the study of field problems has to do with the Q required. The Q of the inductance elements in the General Electric Company's analyzer, used in the studies of the accompanying paper, was around 25. The effects of the losses were definitely noticeable. Particularly, the phase shifts were affected so much that magnitudes only were used in studying results. This would constitute a definite limitation if unknown phase shifts or if the effects of actual losses in the dielectric or the boundaries were required. A somewhat higher Q, say of the order of 100, could be obtained still using lumped circuit elements, but even this is low compared to the Q of many field problems (in the thousands).

The use of low-Q circuits to represent high-Q field

problems is much the same as the use of a model with a much lossier dielectric than that of the problem to be studied. There are several ways in which information can still be made useful.

1. In many problems the quantities desired are not affected greatly by reasonable losses. For example, such quantities are the characteristic impedance of a transmission line and the phase constants in a wave guide.
2. The characteristics arising from true losses in the field problem may in many cases be calculated by taking current and field distributions from the analyzer results and finding what power losses these would give rise to in the actual conductors and dielectric of the problem.
3. Values read from the analyzer may actually be corrected by calculation to decrease the errors caused by dissipation in the analyzer elements.
4. Certain quantities have corrections linearly related to losses if these are small. A possibility then exists of taking readings with loss components actually increased, then extrapolating into the region of smaller losses.

Application of Boundary Conditions

Some of the boundary conditions arising in field problems are:

1. Portion of region bounded by a conductor.
2. Electric field applied over some portion of the region.
3. Magnetic field applied over some portion of the region.
4. Region extending to infinity.

For the study of a wave in which electric field is represented in the network by the voltage across the condensers to ground, these should be short-circuited along the boundary to simulate a perfectly conducting boundary. For the wave in which electric field in a given direction is represented by currents in the network in inductances at right angles to that direction, the inductances entering normally to the boundaries should be open-circuited to insure zero component of electric field tangential to the boundary. If the conducting boundary has a known and finite conductivity, this can be taken into account by using corresponding resistances and conductances in place of the perfect short and open circuits.

For certain wave types, application of voltages across the condensers of the network represents application of electric fields, and applied currents correspond to applied magnetic fields. For other wave types the reverse is true. It will most often be necessary to apply several values of field. Since it is usually much easier to adjust the several voltages than the several currents, the problem should be set up with applied voltages if possible. If applied currents are to be used, the current generators should have high series impedance for ease in adjustment.

For radiation problems (and some others) a region at infinity constitutes one of the boundaries. Such a boundary condition is probably the hardest to handle on the analyzer, but it is at least evident that if one may go far enough from the radiator so that the local fields have died out, the small regions may be approximated by plane-wave regions, and it is possible to terminate the network in the intrinsic impedance of space (377 ohms). It is also conceivable that "lossy-line" technique now in use in microwave measurements might suggest some means of taking advantage of losses in the elements for elimination of reflected waves without ruining the answers to be obtained. The best technique may well come after several attempts are made to solve such problems by means of the network.

Representative Values of Elements

The size of the elements of a simple analyzer may be determined from the relation $\sqrt{LC}=\Delta l/\lambda \cdot 1/f$ where f is the frequency chosen for the board, λ is the wavelength corresponding to excitation in the field problem, and Δl is the size of elemental square chosen for the field problem. For a board to operate with 1.3 megacycles per second, inductances of 15 microhenries and capacitances of 100 micromicrofarads would correspond to about 20 elements per wavelength.

Contributions to Analytical Approaches to Field Problems

In addition to the straightforward application of an analyzer to solution of field problems, the circuits may also contribute to analytical methods, or combined analytical and analyzer methods. For example, it may conceivably be efficient to obtain only certain parts of the information from an analyzer study, using that information in analytical methods from thereon. It is also possible to solve the difference equations of the network, sometimes in closed form and always numerically. There are also many techniques and theorems long worked out for handling networks that may well find wide application to field problems after a study of the ties between the two.

Equivalent Circuit of the Field Equations of Maxwell—I*

GABRIEL KRON†, NONMEMBER, I.R.E.

Summary—An equivalent circuit is developed representing the field equations of Maxwell for an electromagnetic field containing conductors and bound charges. Both transient and sinusoidal field phenomena may now be studied by the network analyzer or by numerical and analytical circuit methods. Examples are radiation from antennas, propagation through wave guides and cavity resonators of arbitrary shapes, eddy currents in conductors, stresses in current-carrying structures, and other general problems in which moving charges either do not enter, or if they do, they may be replaced by equivalent dielectric constants, as in small signal waves on stationary or moving space charge.

The circuits are developed for all curvilinear orthogonal reference frames to allow the solution, to any desired degree of accuracy, of special three-dimensional problems with axial and other symmetry by the use of only a two-dimensional network. The electromagnetic field may be nonhomogeneous, nonisotropic (of a special form), and may be divided into blocks of uneven length in different directions. The transient character of the circuit allows the variation of the frequency of the impressed quantities on the alternating-current network analyzer without varying the magnitude of the circuit impedances.

One set of two-dimensional networks, the transmission-line type, requires only resistances, inductances, and capacitors, while its dual set requires also ideal transformers in series with the inductive coils. (In the transmission-line type of networks the dual ideal transformers consist of impedanceless conductors.) The three-dimensional network, being its own dual, requires both ideal transformers and impedanceless conductors. The appearance of the two types of ideal transformers plays a basic part in the identification of the scalar, vector, and Hertzian potentials and their duals on the equivalent circuit. The latter definitions will be treated in a subsequent part.

A Principle to Establish Models for Physical Systems

IN attempting to set up stationary networks to simulate the performance of rotating electrical machinery under transient or steady-state conditions, it was discovered that the equations, to be reproduced by an electrical model, could not be stated and their terms could not be grouped in any haphazard manner. It has been found that it is not sufficient that a set of equations be written in a form that satisfies the rules of calculus; in addition, the whole set of equations, every term in the equations, and every letter in the terms must correspond to some definite physical entity or its components. By ignoring the very alive phenomena underlying the lifeless symbols it is still possible to get correct numerical answers, but it is not possible to form a correct physical picture, much less to build a physical model that corresponds term by term to the equations.

The following principle was formulated to serve as a guide in visualizing the behavior of and in establishing models for physical systems:[1]

"A set of equations, representing the performance of any physical system (be it mechanical, thermal, or any other system) may be represented by a physical model (equivalent circuit) only if the set of equations is a tensor equation. The invariance of the set of equations is a necessary, but not a sufficient condition."

Manners of Application of the Principle

This principle proved to be an indispensable guide in finding equivalent circuits for the steady-state performance and small oscillation of combined electromagnetic and mechanical systems. Considering for instance the case of their small oscillations,[1] the conventional equations $e=z\cdot i$ may be expressed also as $A+B=O$ where none of the sets of expressions A or B, nor the combination $A+B$ (or O) are tensors. The tensorial equations for small oscillations (not used by engineers) may be written as $e'=z'\cdot i'$, or $A+B+C-C=O$ where C represents a set of expressions that otherwise would cancel.

Now while neither A nor C is a tensor, the combination $A+C$ is a tensor, so is the combination $B-C$. Hence each expression in the equation $(A+C)+(B-C)=O$ is a tensor (including now O as it had acquired a different law of transformation by the appearance of C). Therefore $A+C$ must be and was found to be a visualizable, measurable, and physically reproducible quantity, and so was $B-C$. That is, this last equation $e'=z'\cdot i'$ was a tensor equation (while the conventional equation $e=z\cdot i$ was not) and it satisfied the primary characteristic of all stationary networks that their equation of performance $e=z\cdot i$ or $I=Y\cdot E$ (or any other form) is always a tensor equation.

As a result of reorganizing a mathematically correct, but physically deficient, set of equations, a stationary network could be constructed in which a combination of voltages, currents, and impedances represented such an advanced tensorial concept as the Riemann-Christoffel curvature tensor. However, it proved to be impossible to construct a stationary network to satisfy a set of linear equations that had a much simpler form, gave the correct answer, but was not a tensor equation.

In constructing a model that represents the field equations of Maxwell, a slightly different situation arises. The conventional sets of curl and divergence equations along orthogonal curvilinear co-ordinates may be written as $A\cdot B=O$ where neither A, nor B, nor the combination $A\cdot B$ are tensors. (Of course even in the absence of bound charges, hence in the absence of the divergence equations the conventional curl equations, when expressed along curvilinear axes, are not tensor equations either.) The tensorial equations $(D\cdot A\cdot C)$

* Decimal classification: R140. Original manuscript received by the Institute, December 22, 1943; revised manuscript received, February 29, 1944. Presented, Winter Technical Meeting, New York, N. Y., January 28, 1944.

† Consulting Engineer, General Electric Company, Schenectady, N. Y.

[1] Gabriel Kron, "Equivalent circuits for oscillating systems and the Riemann-Christoffel curvature tensor," *A.I.E.E. Trans.* (*Elec. Eng.*, vol. 62, January, 1943), pp. 27–34; January, 1943.

$\cdot(\boldsymbol{C}^{-1}\cdot\boldsymbol{B})=\boldsymbol{O}$ will be found to supply certain additional sets of expressions $\boldsymbol{C}$ and $\boldsymbol{D}$ that may be canceled out to re-establish the conventional equations. Thereby the combination $\boldsymbol{D}\cdot\boldsymbol{A}\cdot\boldsymbol{C}$ becomes a tensor, so does $\boldsymbol{C}^{-1}\cdot\boldsymbol{B}$. Hence by virtue of the above principle of physical models, *if the field equations do admit an equivalent circuit, the network must correspond to this form of the equations and not to the simplified form.*

That's just what happens. When Ohm's law $\boldsymbol{e}=\boldsymbol{z}\cdot\boldsymbol{i}$ and $\boldsymbol{I}=\boldsymbol{Y}\cdot\boldsymbol{E}$ are written for the various meshes and junction pairs of the equivalent circuit, they correspond not to the conventional, but to the tensorial form of Maxwell's equations.

Since in the present problem the reference frames and the material media characterized by μ, ϵ, and σ are all stationary in space, the set of expressions $\boldsymbol{C}$ and $\boldsymbol{D}$ are of a simpler form than in the previously treated case of rotating electrical machinery, where the reference frames and the material media had relative motions. However, even in a simple case such as where $\boldsymbol{C}$ or $\boldsymbol{D}$ contain only a scalar factor $\frac{1}{2}$ or j, the nonrecognition of the situation may signal the difference between success or failure in discovering a model.

The Conventional Form of Maxwell's Equations

Stratton[2] gives the following field equations for any orthogonal curvilinear co-ordinate system

$$\begin{aligned}
&\frac{1}{h_2h_3}\left[\frac{\partial}{\partial u^2}(h_3E_{(3)})-\frac{\partial}{\partial u^3}(h_2E_{(2)})\right]+\frac{\partial B_{(1)}}{\partial t}=0\\
&\frac{1}{h_1h_3}\left[\frac{\partial}{\partial u^3}(h_1E_{(1)})-\frac{\partial}{\partial u^1}(h_3E_{(3)})\right]+\frac{\partial B_{(2)}}{\partial t}=0\\
&\frac{1}{h_1h_2}\left[\frac{\partial}{\partial u^1}(h_2E_{(2)})-\frac{\partial}{\partial u^2}(h_1E_{(1)})\right]+\frac{\partial B_{(3)}}{\partial t}=0\\
&\frac{1}{h_2h_3}\left[\frac{\partial}{\partial u^2}(h_3H_{(3)})-\frac{\partial}{\partial u^2}(h_2H_{(2)})\right]-\frac{\partial D_{(1)}}{\partial t}-I_{(1)}=0\\
&\frac{1}{h_1h_3}\left[\frac{\partial}{\partial u^3}(h_1H_{(1)})-\frac{\partial}{\partial u^1}(h_3H_{(3)})\right]-\frac{\partial D_{(2)}}{\partial t}-I_{(2)}=0 \qquad (1)\\
&\frac{1}{h_1h_2}\left[\frac{\partial}{\partial u^1}(h_2H_{(2)})-\frac{\partial}{\partial u^2}(h_1H_{(1)})\right]-\frac{\partial D_{(3)}}{\partial t}-I_{(3)}=0\\
&\frac{\partial}{\partial u^1}(h_2h_3B_{(1)})+\frac{\partial}{\partial u^2}(h_1h_3B_{(2)})+\frac{\partial}{\partial u^3}(h_1h_2B_{(3)})=0\\
&\frac{\partial}{\partial u^1}(h_2h_3D_{(1)})+\frac{\partial}{\partial u^2}(h_1h_3D_{(2)})+\frac{\partial}{\partial u^3}(h_1h_2D_{(3)})=h_1h_2h_3\rho.
\end{aligned}$$

The relations between field intensities and flux densities are

$$B_{(1)}=(\mu/c)H_{(1)},\ D_{(1)}=(\epsilon/c)E_{(1)},\ I_{(1)}=(\sigma/c)E_{(1)},\ \text{etc.} \qquad (2)$$

The values of the variables u^α and the metrical coefficients h are given in Table I for the three most common orthogonal reference frames. Their values in other orthogonal frames (such as elliptical, spheroidal, etc., frames) may be found in Stratton's work.

[2] J. A. Stratton, "The Electromagnetic Field," McGraw-Hill Book Co., New York, N. Y., 1940.

TABLE I
Values of u^α and h

	u^1	u^2	u^3	h_1	h_2	h_3
Cartesian	x	y	z	1	1	1
Cylindrical	r	θ	z	1	r	1
Spherical	r	θ	ψ	1	r	$r\sin\theta$

The following properties of these conventional equations should be noted:

1. The variables $E_{(1)}$, $H_{(1)}$, etc., are not tensors.
2. The set of equations themselves are not tensor equations; that is, they cannot be transformed, as they stand, to say nonorthogonal reference frames, nor can they be represented by a physical model.

Only in the special case of a Cartesian frame when the metrical coefficients h_1, h_2, and h_3 are unity, do the above equations reduce to a tensor equation.

The Tensor-Density Form of Maxwell's Equations

The tensor-density form of the equations, that the equivalent circuit satisfies, is derived in the Appendix in two different manners:

1. In Appendix I the integral equations of an infinitesimal block are derived by physical reasoning, leading to the desired equations.
2. In Appendix II the well-known tensorial equations given in books on electrodynamics are merely stated, then changed into the needed tensor-density form.

Performing the operations indicated in (38) and multiplying by $\sqrt{g}$, the conventional nontensorial field equations (1) can be brought to the needed tensor-density form by the following steps:

1. The nontensor variables $E_{(r)}$ and $H_{(r)}$ are replaced with the aid of (7) by the tensor variables E_r and H_r, similarly $B_{(r)}$, $D_{(r)}$, $I_{(r)}$, and ρ are replaced with the aid of (8) by the tensor densities $B^{r'}$, $D^{r'}$, $I^{r'}$, and ρ', respectively.
2. The first and fourth equations are divided by h_1, the second and fifth by h_2, the third and sixth by h_3, and the seventh and eighth by $h_1h_2h_3$.
3. All equations are multiplied by $h_1h_2h_3$.

Also the conventional nontensorial relations (2) between the field intensities and flux densities are brought to the tensor-density form (4) by the previous first step and by a fourth step:

4. The quantities μ/c, ϵ/c, and σ/c are replaced with the aid of (9) by the tensor densities $\mu^{rs'}$, $\epsilon^{rs'}$, and $\sigma^{rs'}$, respectively.

The resultant tensor-density field equations, to be used in establishing equivalent circuits, are as follows:

$$\begin{aligned}
\partial E_3/\partial u^2-\partial E_2/\partial u^3+\partial B^{1'}/\partial t&=0\\
\partial E_1/\partial u^3-\partial E_3/\partial u^1+\partial B^{2'}/\partial t&=0 \qquad (3a)\\
\partial E_2/\partial u^1-\partial E_1/\partial u^2+\partial B^{3'}/\partial t&=0\\
\partial B^{1'}/\partial u^1+\partial B^{2'}/\partial u^2+\partial B^{3'}/\partial u^3&=0
\end{aligned}$$

$$\begin{aligned}
\partial H_3/\partial u^2-\partial H_2/\partial u^3-\partial D^{1'}/\partial t-I^{1'}&=0\\
\partial H_1/\partial u^3-\partial H_3/\partial u^1-\partial D^{2'}/\partial t-I^{2'}&=0 \qquad (3b)\\
\partial H_2/\partial u\ -\partial H_1/\partial u^2-\partial D^{3'}/\partial t-I^{3'}&=0\\
\partial D^{1'}/\partial u^1+\partial D^{2'}/\partial u^2+\partial D^{3'}/\partial u^3&=\rho'
\end{aligned}$$

where the relation between the field intensities and flux densities are

$$B^{r'} = \mu^{rs'}H_s \mid D^{r'} = \epsilon^{rs'}E_s \mid I^{r'} = \sigma^{rs'}E_s$$

or explicitly

$$\begin{array}{l|l|l} B^{1'} = \mu^{11'}H_1 & D^{1'} = \epsilon^{11'}E_1 & I^{1'} = \sigma^{11'}E_1 \\ B^{2'} = \mu^{22'}H_2 & D^{2'} = \epsilon^{22'}E_2 & I^{2'} = \sigma^{22'}E_2 \\ B^{3'} = \mu^{33'}H_3 & D^{3'} = \epsilon^{33'}E_3 & I^{3'} = \sigma^{33'}E_3 \end{array} \qquad (4)$$

The primed quantities represent tensor densities. In particular the vector densities are defined by

$$A^{r'} = \sqrt{g}\,A^r = \sqrt{g}\,g^{rs}A_s = \sqrt{g}\,g^{rs}\epsilon_{st}{}^{(t)}A_{(t)} \qquad (5)$$

and the material tensor densities by

$$\alpha^{rs'} = \sqrt{g}\,\alpha^{rs} = \sqrt{g}\,g^{ts}\alpha_t{}^r + \sqrt{g}\,g^{ts}\delta_t{}^r\alpha/c \qquad (6)$$

where $\delta_t{}^r$ is the unit tensor.

Comparing the two types of field equations, the relations between the tensor and the conventional quantities are by (47), (5), and (6)

$$\begin{array}{l|l} E_1 = h_1E_{(1)} & H_1 = h_1H_{(1)} \\ E_2 = h_2E_{(2)} & H_2 = h_2H_{(2)} \\ E_3 = h_3E_{(3)} & H_3 = h_3H_{(3)} \end{array} \qquad (7)$$

$$\begin{array}{l|l|l|l} B^{1'} = B_{(1)}h_2h_3 & D^{1'} = D_{(1)}h_2h_3 & I^{1'} = I_{(1)}h_2h_3 & \rho' = \rho h_1h_2h_3 \\ B^{2'} = B_{(2)}h_1h_3 & D^{2'} = D_{(2)}h_1h_3 & I^{2'} = I_{(2)}h_1h_3 & \\ B^{3'} = B_{(3)}h_1h_2 & D^{3'} = D_{(3)}h_1h_2 & I^{3'} = I_{(3)}h_1h_2 & \end{array} \qquad (8)$$

$$\begin{array}{l|l|l} \epsilon^{11'} = \dfrac{\epsilon}{c}\dfrac{h_2h_3}{h_1} & \mu^{11'} = \dfrac{\mu}{c}\dfrac{h_2h_3}{h_1} & \sigma^{11'} = \dfrac{\sigma}{c}\dfrac{h_2h_3}{h_1} \\ \epsilon^{22'} = \dfrac{\epsilon}{c}\dfrac{h_1h_3}{h_2} & \mu^{22'} = \dfrac{\mu}{c}\dfrac{h_1h_3}{h_2} & \sigma^{22'} = \dfrac{\sigma}{c}\dfrac{h_1h_3}{h_2} \\ \epsilon^{33'} = \dfrac{\epsilon}{c}\dfrac{h_1h_2}{h_3} & \mu^{33'} = \dfrac{\mu}{c}\dfrac{h_1h_2}{h_3} & \sigma^{33'} = \dfrac{\sigma}{c}\dfrac{h_1h_2}{h_3} \end{array} \qquad (9)$$

From (3) and (4) it may be seen that *along curvilinear orthogonal axes the field equations of Maxwell are of the same form as along Cartesian axes except that the conventional variables change to tensor variables and the isotropic homogeneous space changes to a nonisotropic nonhomogeneous one.*

The Network Form of Maxwell's Equation

The general stationary network of the electrical-power engineer consists of at least three different types of networks interlinked and interconnected in various manners, each network defining the path of a particular physical quantity. In particular:

1. The "electrical network" defines the path of electric charges in conductors.

2. The "magnetic network" defines the path of magnetic flux lines.

3. The "dielectric network" defines the path of electrostatic flux lines.

(In a general engineering network there are numerous other types of paths, such as the paths of free charges, of moving mechanical links, of quantities of heat, etc. Each path may occupy various dimensions, may be interlinked and interconnected with each other, and may also have relative motions with respect to the rest.)

It has been shown[3] that each of the various types of networks may be looked upon from three different points of view (the first two a special case of the third) depending on the nature of the known and unknown quantities:

1. As a "mesh" network, a collection of closed meshes (of various dimensions),

2. as a "junction" network, a collection of open meshes or "junction pairs,"

3. as an "orthogonal" (or normalized) network, a collection of both closed and open meshes.

Now the above field equations of Maxwell define just such a multiple stationary network, a combination of electric, magnetic, and dielectric networks, in which

1. The electrical network is an orthogonal network, where one set of Maxwell's equation (the curl ***E*** equations) defines its meshes, and a second set (the curl ***H*** equations) defines its junction pairs,

2. the magnetic network is a mesh network defined by a third (the div ***B***) equation,

3. the dielectric network is a junction network defined by a fourth (the div ***D***) equation.

If then the H's are assumed to represent currents (or rather magnetomotive forces) in a network, the E's voltages and the material constants impedances as

$$z^{rr} = \mu^{rr'}p \quad \text{and} \quad y^{rr} = \epsilon^{rr'}p + \sigma^{rr'} \qquad (10)$$

the two sets of equations (3) may be written in Ohm's-law form as follows:

1. The first set of four equations (3a) appear as those of mesh networks; in particular the curl ***E*** equations as *electrical* mesh equations

$$\begin{aligned} \partial e_3/\partial u^2 - \partial e_2/\partial u^3 + z^{11}i_1 &= 0 \\ \partial e_1/\partial u^3 - \partial e_3/\partial u^1 + z^{22}i_2 &= 0 \\ \partial e_2/\partial u^1 - \partial e_1/\partial u^2 + z^{33}i_3 &= 0 \end{aligned} \qquad (11)$$

and the div ***B*** equation as a *magnetic* mesh equation

$$\partial(\mu^{11'}i_1)/\partial u^1 + \partial(\mu^{22'}i_2)/\partial u^2 + \partial(\mu^{33'}i_3)/\partial u^3 = 0. \qquad (12)$$

If so desired, the right-hand side may include the hypothetical bound magnetic poles m'.

2. The second set of four equations (3b) appear as those of junction networks; in particular the curl ***B*** equations as *electrical* junction-pair equations (dual Ohm's law)

$$\begin{aligned} \partial i_3/\partial u^2 - \partial i_2/\partial u^3 - y^{11}e_1 &= 0 \\ \partial i_1/\partial u^3 - \partial i_3/\partial u^1 - y^{22}e_2 &= 0 \\ \partial i_2/\partial u^1 - \partial i_1/\partial u^2 - y^{33}e_3 &= 0 \end{aligned} \qquad (13)$$

and the div ***D*** equation as a *dielectric* junction-pair equation

$$\partial(\epsilon^{11'}e_1)/\partial u^1 + \partial(\epsilon^{22'}e_2)/\partial u^2 + \partial(\epsilon^{33'}e_3)/\partial u^3 = \rho'. \qquad (14)$$

It is interesting that the *four-dimensional* tensorial form does not differentiate between electric and magnetic meshes, nor between electric and dielectric junction pairs, as is to be expected. That is, the four-dimensional network equation defines the equivalent

[3] Gabriel Kron, "Tensor Analysis of Networks," John Wiley and Sons, Inc., New York, N. Y., 1939.

circuit as an electromagnetic orthogonal network, in which

1. The covariant form, equation (38a) represents the equations of all possible meshes;

2. The contravariant form, equation (38b) represents the equations of all possible junction pairs.

It is only the *three-dimensional* tensorial form that represents an electrical mesh by $e_r = z_{rs} i^s$, a magnetic mesh by $H^r = \rho^{rs} B_s$, and a dielectric mesh by $e_r = s_{rs} D^s$. From a four-dimensional point of view these distinctions disappear, and only the concepts of mesh and junction pair (covariance and contravariance) are retained.

In a charge-free space the two sets of curl equations alone are sufficient to establish the network, while the divergence equations only serve as checks on the correctness of the network. As a matter of fact, if the two divergence equations are replaced by two other equations found by taking the divergence of the two sets of curl equations, then the two new divergence equations

$$\begin{aligned} \text{div } \partial B^{r'}/\partial t &= 0 \\ \text{div } (\partial D^{r'}/\partial t + I^{r'}) &= 0 \end{aligned} \tag{15}$$

can be expressed in an *electrical* circuit form instead of a magnetic and dielectric one. In particular, the mesh form is

$$\partial(z^{11} i_1)/\partial u^1 + \partial(z^{22} i_2)/\partial u^2 + \partial(z^{33} i_3)/\partial u^3 = 0 \tag{16}$$

where $z^{11} = \mu^{11'} p$ and the junction form is

$$\partial(y^{11} e_1)/\partial u^1 + \partial(y^{22} e_2)/\partial u^2 + \partial(y^{33} e_3)\partial u^3 = 0 \tag{17}$$

where $y^{11} = \epsilon^{11'} p + \sigma^{11'}$.

It will be shown that these two divergence equations represent Ohm's law for all those *electrical* meshes and junction pairs that are *not* covered by the two curl equations. Thereby it is assured that every electric, magnetic, and dielectric mesh and junction pair in the equivalent network satisfies some one of Maxwell's equations and none of the circuit elements are left unaccounted for.

The Equivalent Circuit

The equivalent circuit is shown in Fig. 1. Considering first the currents (or rather the magnetomotive forces) in the network:

1. The currents in the spherical inductances are H_r,

2. the currents in the capacitors are the "displacement currents" $pD^{r'}$,

3. the currents in the resistances are the "conduction currents" $I^{r'}$.

Considering next the differences of potentials in the network:

4. The voltages across the capacitors are E_r,

5. the voltages across the inductive coils are the "magnetic displacement currents" $pB^{r'}$,

6. had there existed "magnetic conduction currents" $\tau^{rs'} H_s = J^r$ they would be represented by voltages across resistances placed in *series* with the inductive coils.

In addition to these currents and voltages of the electrical network, three quantites on the underlying magnetic and dielectric networks may be correlated with the electromagnetic field. In particular:

7. The magnetic flux lines represent $B^{r'}$,

8. the electrostatic flux lines represent $D^{r'}$,

9. the charges on the capacitors represent ρ'.

It is also possible to identify on the equivalent network auxiliary quantities such as the scalar potential ψ, the vector potential $\boldsymbol{A}$, the Hertzian vector π, etc., and their duals. Their study will be undertaken in the next part.

If it is assumed that the blocks into which space is divided are bounded by the co-ordinate surfaces, and if all equations are multiplied by $\Delta u^1 \Delta u^2 \Delta u^3$, a physical interpretation of the quantities measured on the network may be given as follows:

1. E_r and H_r (multiplied by Δu^r) represent *line integrals* of the conventional $E_{(r)}$ and $H_{(r)}$ along the edges of unit cubes.

2. $I^{r'}$, $B^{r'}$, and $D^{r'}$ (multiplied by $\Delta u^s \Delta u^t$) represent *surface integrals* of the conventional $I_{(r)}$, $B_{(r)}$, and $D_{(r)}$ on the faces of unit cubes.

3. ρ' (multiplied by $\Delta u^r \Delta u^s \Delta u^t$) represent *volume integrals* of the conventional ρ inside of unit cubes.

4. $\mu^{rr'}$, $\epsilon^{rr'}$, and $\sigma^{rr'}$ (multiplied by $\Delta u^s \Delta u^t / \Delta u^r$) represent the respective admittances of unit cubes of material in the direction indicated by the indexes.

Hence the network does not identify $E_{(r)}$ or $H_{(r)}$ at any particular point of space. It does identify the line integral of their components along the edges of various overlapping cubes, each component of the same vector being integrated along different lines in space.

If so desired, it is possible to throw away every other sphere of inductive coils (multiplying the inductances by two) and to connect the six capacitor leads into a junction. The network still satisfies Maxwell's equations; on the other hand fewer points of space are identified.

It is emphasized that it is not necessary to assume that the blocks into which space is divided are of unit length. Since Δu^1, Δu^2, and Δu^3 each may be any arbitrary constant a, b, and c in any type of orthogonal frame, *each side of these blocks may be of any arbitrary length.*

Summarizing the results of the last two sections, if Ohm's laws are written for the electric, magnetic, and dielectric meshes and junction pairs of the equivalent circuit, the resulting equations are not the conventional equations of Maxwell, but rather the tensorial equations, plus others derivable from them (such as (16) and (17)). Only after all the Ohm's (tensorial) equations of the network have been written down, will it be found that some of the equations are mathematically superfluous, and that some of the factors ($\boldsymbol{C}$ and $\boldsymbol{D}$) cancel. But the *physical* network itself is not aware of these *mathematical* simplifications.

As the field equations of Maxwell have now been represented by a stationary network (within any desired degree of accuracy) it may be stated that:

Any theorem, formula, concept, or law that is valid for

stationary networks (such as reciprocity theorems, Thèvenin's theorem, concepts of dualism, reduction formulas, generalization postulates, etc.) *can be translated into a corresponding theorem, formula, concept, or law relating to the electromagnetic field.*

by the characteristic impedance of free space $Z_0 = \sqrt{\mu/\epsilon} = 377$ ohms resistance.[4]

Known *E-s* or *H-s* are impressed with the aid of voltage or current generators.

It should be emphasized that the network blocks

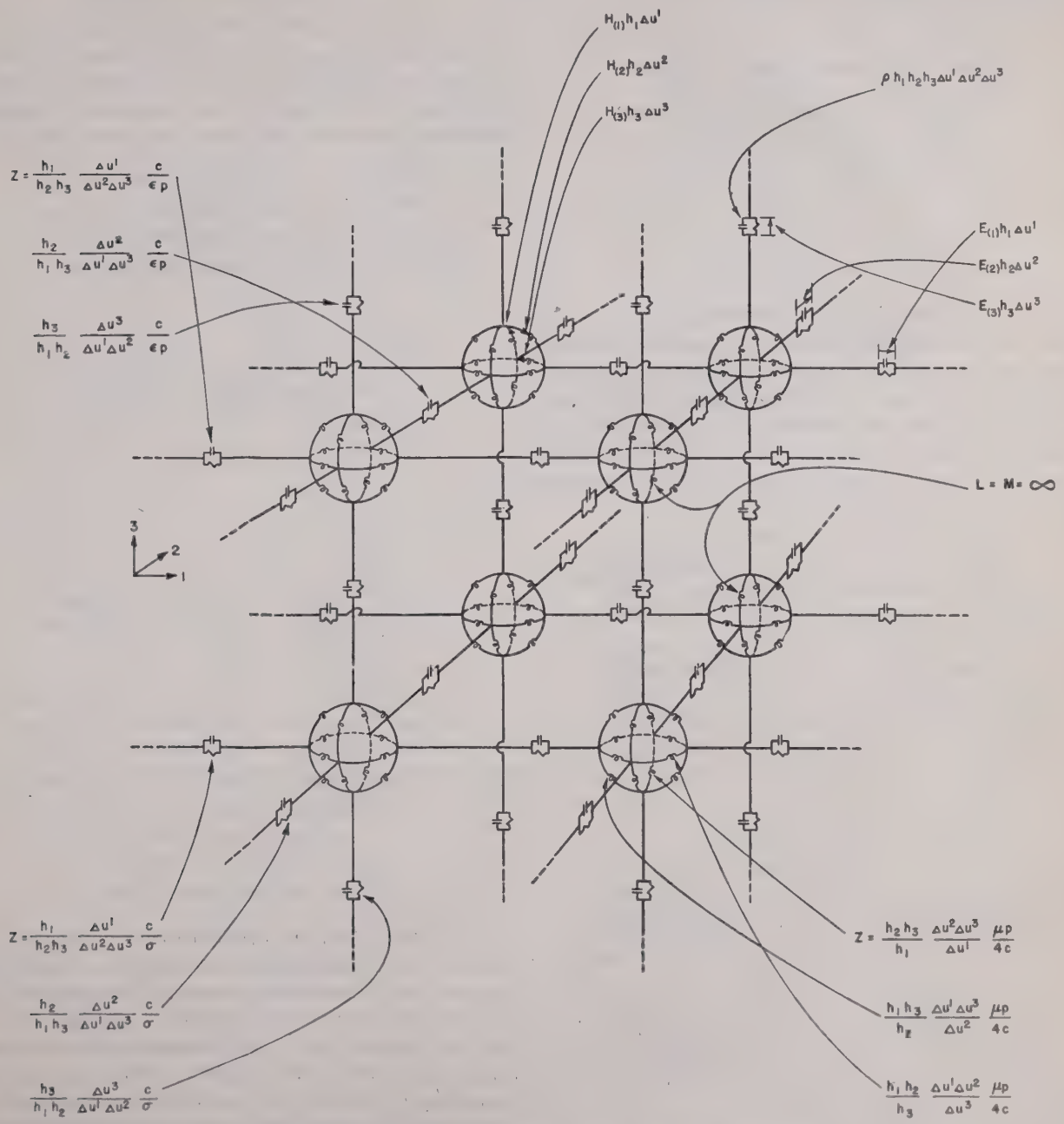

Fig. 1—Transient equivalent circuit of the field equations of Maxwell.

Boundary Conditions

If the boundary, say on the u^1-u^2 plane (Fig. 2) consists of a perfect conductor ($\sigma = \infty$) the capacitors on the boundaries become short-circuited and the tangential component of E_r(E_1 and E_2) and the normal component of H_r (namely H_3) are zero.

If a boundary is the free space, distant from reflecting surfaces, the network at these points may be terminated

representing μ, ϵ, and σ are not coincident but overlap by half a block. Hence there is an uncertainty of half a block in how much actual space the network really represents or rather there is an uncertainty of half a block in deciding where the boundaries of the network lie. The boundaries for the voltages (say *E-s*) do not

[4] S. A. Schelkunoff, "Electromagnetic Waves," D. Van Nostrand Co., New York, N. Y., 1943.

coincide with the boundaries for the currents (*H-s*). It is well known that there is a similar uncertainty of boundaries or position in representing a transmission line by several π or T sections, or for that matter in representing any continuous phenomenon with two or more dependent variables by discrete steps.

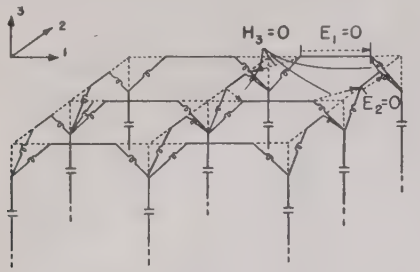

Fig. 2—Conducting boundary.

Other Possible Networks

There are at least three other possible analogous networks that would also satisfy Maxwell's equations, depending on whether E_r (or H_r) is identified by a voltage or by a current, and whether in connection with a condenser or with an inductance. One cube of each of the four networks is shown in Fig. 3. The last two cases

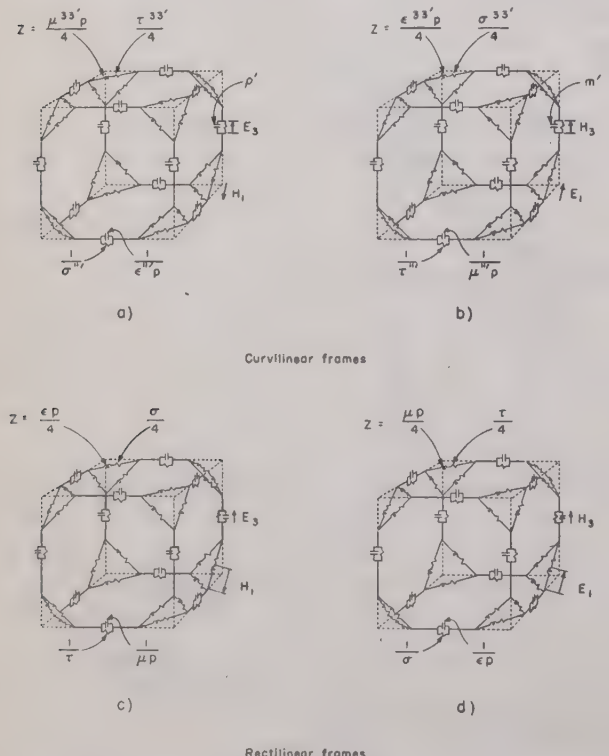

Fig. 3—Four possible equivalent three-dimensional networks.

satisfy only the rectilinear equations, since the field must be isotropic. On Fig. 3(b) the charges on the condensers represent the hypothetical magnetic poles m', while ρ' would have to be represented by magnetic poles placed in the underlying magnetic circuit.

It is interesting that in all four cases the network connection of Fig. 1 remains unchanged (if the hypothetical "magnetic conduction currents" $J^{r'}$ are retained) and only the magnitude of the impedances and the physical interpretations change. These properties follow from the self-dualism of the field equations.

Two-Dimensional Networks

Let it be assumed that all field quantities $E_{(r)}$ and $H_{(r)}$ are constant along one axis (say along u^2) so that $\partial E_r/\partial u^2 = \partial H_r/\partial u^2 = 0$. The field equations (3) then can be grouped into two sets of three independent equations with three unknowns. The first group contains only E_2, H_1, and H_3

$$\begin{aligned} -\partial E_2/\partial u^3 + \partial B^{1'}/\partial t &= 0 \\ \partial E^2/\partial u^1 + \partial B^{3'}/\partial t &= 0 \\ \partial H^1/\partial u^3 - \partial H_3/\partial u^1 - \partial D^{2'}/\partial t - I^{2'} &= 0 \\ \partial B^{1'}/\partial u^1 + \partial B^{3'}/\partial u^3 &= 0 \end{aligned} \tag{18}$$

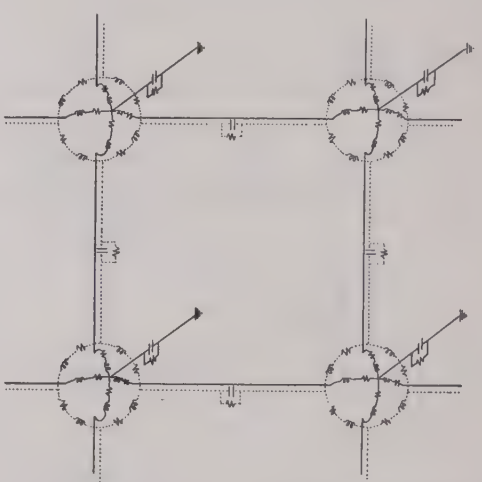

Fig. 4—The split-up into two independent networks.

while the second group contains only H_2, E_1, and E_3

$$\begin{aligned} -\partial H_2/\partial u^3 - \partial D^{1'}/\partial t - I^{1'} &= 0 \\ \partial H_2/\partial u^1 - \partial D^{3'}/\partial t - I^{3'} &= 0 \\ \partial E_1/\partial u^3 - \partial E_3/\partial u^1 + \partial B^{2'}/\partial t &= 0 \\ \partial D^{1'}/\partial u^1 + \partial D^{3'}/\partial u^3 &= \rho'. \end{aligned} \tag{19}$$

Fig. 4 shows how the original three-dimensional network of Fig. 1 now splits into two electrically independent two-dimensional networks. The resultant four networks of the two dual networks of Figs. 3(a) and 3(b) are shown in Fig. 5. They enable us to solve special three-dimensional field problems with axial or other symmetry by means of a two-dimensional network.

It should be noted that the network analogous to a two-dimensional transmission line may be looked upon as representing either transverse magnetic or transverse electric waves simply by changing the impedance values and the terminology.

One-Dimensional Networks

Let it be assumed that all field quantities are constant along two of the axes (say along u^2 and u^3) so that $\partial/\partial u^2 = \partial/\partial u^3 = 0$. Such a case may occur, for instance, in spherical co-ordinates when variation only along the

radius $u^1 = r$ is considered. The first group of independent equations contains now only E_2 and H_3,

$$\partial E_2/\partial u^1 + \partial B^{3'}/\partial t = 0 \qquad (20)$$
$$-\partial H_3/\partial u^1 - \partial D^{2'}/\partial t - I^{2'} = 0$$

while the second group contains now only H_2 and E_3

$$\partial H_2/\partial u^1 - \partial D^{3'}/\partial t - I^{3'} = 0 \qquad (21)$$
$$-\partial E_3/\partial u^1 + \partial B^{2'}/\partial t = 0.$$

The four one-dimensional transmission lines corresponding to the four two-dimensional cases of Fig. 5 are shown in Fig. 6. The impedanceless connections between the capacitors of the first and third figures are the duals of the ideal transformers appearing in the other two figures.

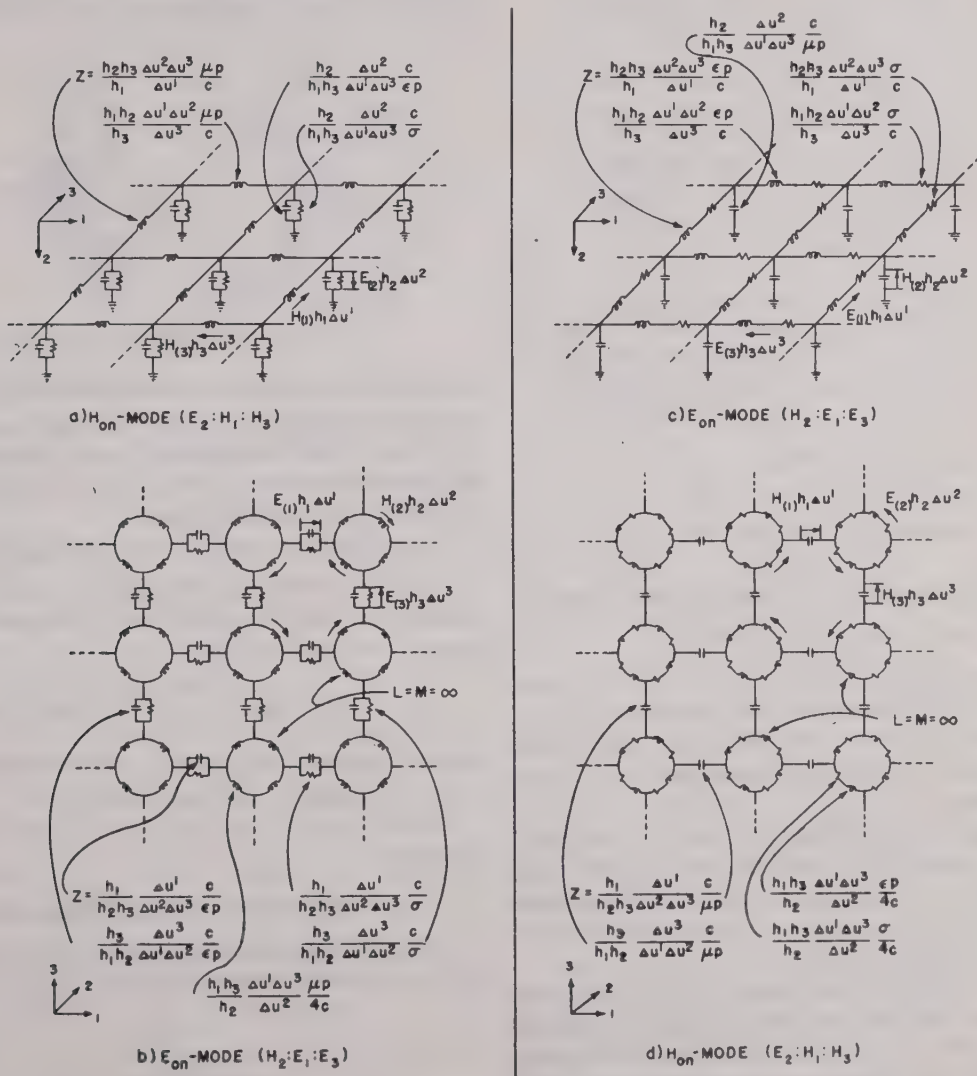

Fig. 5—Two sets of two-dimensional networks.

The Role of the Ideal Transformers

It may be mentioned in passing that in the dual one-dimensional transmission lines, Figs. 6(b) and (d), (but not in the two- and three-dimensional ones) the ideal transformers can be removed without changing the values of E and H. The superfluity of the ideal transformers is however only apparent. Maxwell's equations allow the arbitrary change of the *absolute* (scalar) *potential* at any point of the electromagnetic field without the disturbance of E or H. Hence if the given equivalent circuits are true representations of the electromagnetic field, an analogous change of absolute potentials in the dual networks must act in a similar fashion.

The networks do follow these requirements and it is permissible in any one of the dual one-, two-, and three-dimensional networks to inject across the diameters of the circular inductances generators with arbitrary voltages. The differences of potentials across and the fluxes in the ideal transformers automatically adjust themselves to these arbitrary changes of potentials and leave thereby the conditions in the rest of the network undisturbed.

A detailed study of the representation of the various types of potentials will be undertaken in a following part.

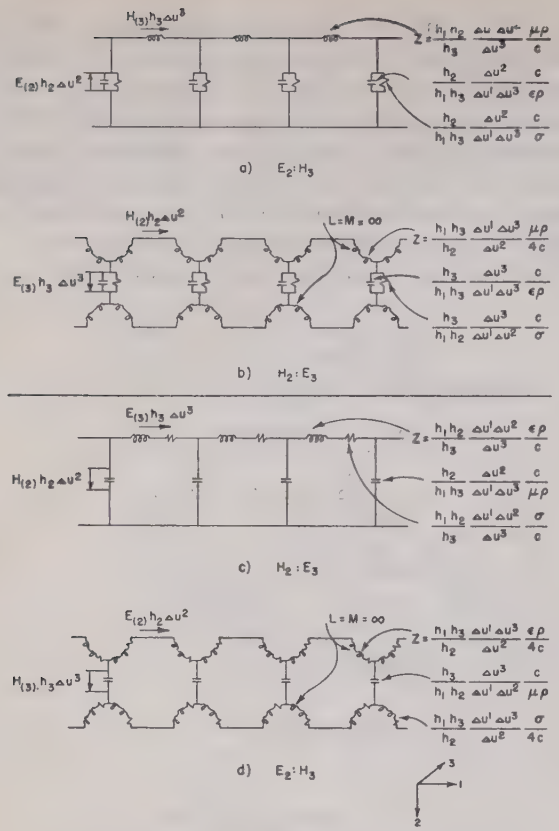

Fig. 6—Two sets of one-dimensional networks.

Appendix I. Proofs of the Equivalent Circuit

The Integral Equations

The equivalent circuit must satisfy any and all of the particular forms in which Maxwell's equations may be expressed. Three of these forms are 1. the differential equations, 2. the finite-difference equations, and 3. the integral equations.

The proofs presently to follow are based on the integral form of the equations as the latter are thought to be in the most easily visualizable form. In the companion paper by Ramo and Whinnery the proofs are based on the finite-difference equations.

The proofs will refer to the network of Fig. 1. Similar proofs can be derived for the other three networks of Fig. 3. In the proofs it will be assumed that the blocks, into which space is divided, are bounded by the coordinate surfaces, so that a surface element is represented by $dS^{23}=\Delta u^2\Delta u^3$, etc.

Proof of the Curl *E* Equations

On Fig. 7 the voltage across a vertical capacitor $E_3\Delta u^3=E_{(3)}h_3\Delta u^3$ represents the line integral of $E_{(3)}$ from A to B. The line integral of E_r around the closed circuit $ABCD$ is then $(E_3'-E_3'')-(E_2'-E_2'')$. By Stokes' theorem this must be equal to the surface integral of the curl of $E_{(r)}$. Since the component of the curl of $E_{(r)}$ along u^1 is

$$[\text{curl } E_{(r)}]_{(1)}=1/h_2h_3\{(\partial E_{(3)}h_3/\partial u^2)-(\partial E_{(2)}h_2/\partial u^3)\} \quad (22)$$

the surface integral of the curl of $E_{(r)}$ along u^1 is

$$\{(\partial E_3/\partial u^2)-(\partial E_2/\partial u^3)\}\Delta u^2\Delta u^3 = (E_3'-E_3'')-(E_2'-E_2''). \quad (23)$$

The average of the four currents in the four inductive coils is $H_1\Delta u^1$ and the sum of fluxes produced by the four currents is

$$(H_1\mu^{11'})\Delta u^2\Delta u^3 = B^{1'}\Delta u^2\Delta u^3 = B_{(1)}h_2h_3\Delta u^2\Delta u^3 \quad (24)$$

(the inductance of each coil is $\mu^{11'}/4$) which itself is the surface integral of the magnetic fluxes $B_{(1)}$ on the surface $ABCD$. (The flux linkages in the ideal transformers

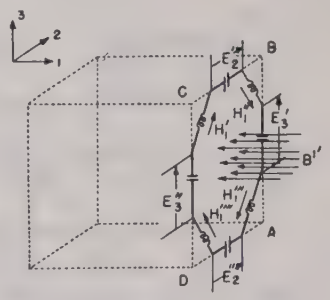

Fig. 7—Proof of Faraday's law.

cancel in defining $B_{(1)}$.) Hence the voltages induced in the four inductive coils $pB^{1'}\Delta u^2\Delta u^3$ (opposite to the direction of the current flow) plus the voltage drops in the capacitors must be zero (as the voltages across the ideal transformers also cancel)

$$[\{(\partial E_3/\partial u^2)-(\partial E_2/\partial u^3)\}+pB^{1'}]\Delta u^2\Delta u^3=0. \quad (25)$$

This physical interpretation of mesh $ABCD$ corresponds to the integral form of Maxwell's equation, namely, to Faraday's law

$$\int_l E_r\Delta u^r+\frac{\partial}{\partial t}\int\int_S B^{r'}n_r dS=0 \quad (26)$$

where (because the blocks are bounded by the coordinate surfaces) $n_1dS=\Delta u^2\Delta u^3$.

Similar derivations apply to the other two curl ***E*** equations.

Proof of the Curl *H* Equations

The previous equation defined $H_1\Delta u^1$ as the average of four currents measured on the face of a unit cube.

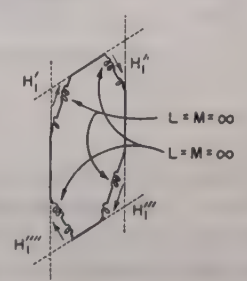

Fig. 8—Two ideal transformers.

Since the currents in the two coils of an ideal transformer are equal (Fig. 8)

$$H_1\Delta u^1 = 1/4(H_1'+H_1''+H_1'''+H_1'''') = 1/2(H_1'+H_1'')=1/2(H_1''+H_1'''). \quad (27)$$

That is, H_1 is defined either as the average of four

currents in the mesh or as *the average of two adjacent currents.* (When every other sphere of inductances is left out, then *one* current defines H_1.)

Considering a junction point on Fig. 9(a) this junction may be considered to be represented also by a plate of the capacitor having an area equal to a face of a unit cube (Fig. 9(b)) whose center lies at a capacitor, and the H currents flow into the junction along the edges of a face.

Again $H_3\Delta u^3 = H_{(3)}h_3\Delta u^3$ represents the line integral of $H_{(3)}$, namely of $(H_3' + H_3'''')/2$, flowing into the two junctions from A to B and from A' to B'. The line inte-

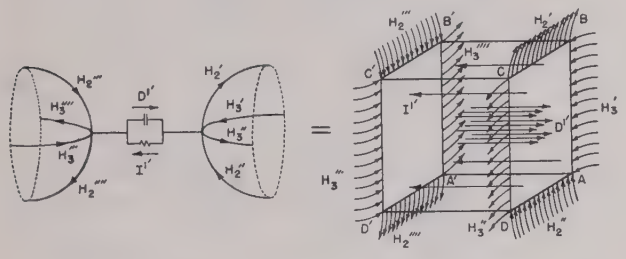

Fig. 9—Proof of Ampere's law.

gral of $H_{(r)}$ around the two closed circuits $ABCD$ and $A'B'C'D'$ is then

$$\begin{aligned}&[1/2(H_3' + H_3'''') - 1/2(H_3'' + H_3''')]\\ &\quad - [1/2(H_2' + H_2''') - 1/2(H_2'' + H_2'''')]\\ &= 1/2(H_3' - H_3'' + H_2'' - H_2')\\ &\quad - 1/2(H_3''' - H_3'''' + H_2''' - H_2'''') \qquad (28)\\ &= (H_3' - H_3'' + H_2'' - H_2')\\ &= (H_3'''' - H_3''' + H_2'''' - H_2''').\end{aligned}$$

This must be equal to the surface integral of the curl of $H_{(r)}$ in the direction u^1:

$$\{(\partial H_3/\partial u^2) - (\partial H_2/\partial u^3)\}\Delta u^2\Delta u^3.$$

The other currents flowing into the plate are the surface integrals of $-I_{(1)}$ and $-pD_{(1)}$ (the currents flow in opposite direction to the voltages) that is, $-I^{1'}\Delta u^2\Delta u^3$ and $-pD^{1'}\Delta u^2\Delta u^3$. Hence the sum of the currents flowing into the junction must be zero

$$[\{\partial H_3/\partial u^2) - (\partial H_2/\partial u^3)\} - pD^{1'} - I^{1'}]\Delta u^2\Delta u^3 = 0. \qquad (29)$$

This physical intepretation corresponds to the integral form, namely, to Ampere's law

$$\int_l H_r\Delta u^r - \frac{\partial}{\partial t}\int\int_s D^{r'}n_r dS - \int\int_s I^{r'}n_r dS = 0. \qquad (30)$$

Similar derivations apply to the other two curl H equations.

It should be noted that these equations define the currents flowing not into a junction, but into a junction pair.

As the *wave equations* are found from the two sets of curl equations by straightforward substitution, the given networks also satisfy the wave equations. By starting with the definition of either E or H the proofs repeat the steps of the last two sections.

Proof of the Div D Equation

If attention is focused on a unit cube with its center in the middle of a sphere of inductances (Fig. 10), the

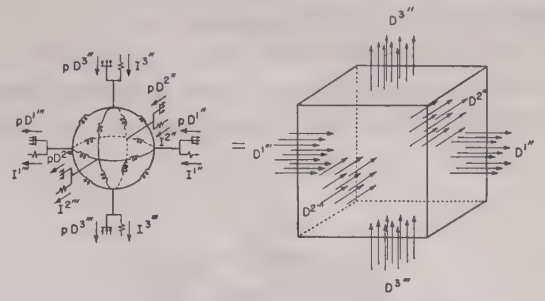

Fig. 10—Proof of div D equation.

electrostatic flux line entering a face is

$$D^{1''} = D^{1'}\Delta u^2\Delta u^3 = D_{(1)}h_2h_3\Delta u^2\Delta u^3, \qquad (31)$$

the surface integral of $D_{(1)}$. (This flux, forming a junction pair, enters on one side of the face and departs through the other side.) The surface integral of $D_{(r)}$ around the six faces of the cube is

$$(D^{1''} - D^{1'''}) + (D^{2''} - D^{2'''}) + (D^{3''} - D^{3'''}).$$

By Green's theorem this must be equal to the volume integral of divergence of $D_{(r)}$. Since the divergence of $D_{(r)}$ is

$$\begin{aligned}\text{div } D_{(r)} = 1/h_1h_2h_3[&\partial/\partial u^1(D_{(1)}h_2h_3) + \partial/\partial u^2(D_{(2)}h_1h_3)\\ &+ \partial/\partial u^3(D_{(3)}h_1h_2)] \qquad (32)\end{aligned}$$

where

$$\begin{aligned}D_{(1)}h_2h_3 &= (D_{(1)}/h_1)(h_1h_2h_3)\\ &= \sqrt{g}\,D_1/(h_1)^2 = \sqrt{g}\,D^1 = D^{1'} \qquad (33)\end{aligned}$$

its volume integral is

$$\begin{aligned}&(\partial D^{1'}/\partial u^1 + \partial D^{2'}/\partial u^2 + \partial D^{3'}/\partial u^3)\Delta u^1\Delta u^2\Delta u^3\\ &= (D^{1''} - D^{1'''}) + (D^{2''} - D^{2'''}) + (D^{3''} - D^{3'''}). \qquad (34)\end{aligned}$$

This sum of the *electrostatic fluxes* entering the unit cube is zero if there are no bound charges present on the capacitors. (The fluxes enter on three faces and depart through the other three.) In the presence of bound charges the above sum of the electrostatic flux lines entering the unit cube is $\rho'\Delta u^1\Delta u^2\Delta u^3$.

This physical interpretation corresponds to the integral form

$$\int\int_s D^{r'}n_r dS = \int\int\int_v \rho' dV. \qquad (35)$$

A similar derivation in connection with $pD^{r'} + I^{r'}$ and (17) (instead of $D^{r'}$) proves that the sum of the *currents* entering the sphere of Fig. 10(a) through its six junctions is zero.

Proof of the Div B Equation

Considering a unit cube bounded by twelve capacitors (Fig. 11) the total magnetic flux produced by the sum of four currents H_1 on one face of the cube represents a surface integral $B^{1''} = B_{(1)}\Delta u^2\Delta u^3$ of $B_{(1)}$. (This flux, forming a closed mesh, enters the face in its center and

departs at its corners on the same side. The flux due to the ideal transformers cancels in defining B.) The surface integral of $B_{(r)}$ around the six faces is again equal to the volume integral of the divergence of $B_{(r)}$. Hence

$$(\partial B^{1'}/\partial u^1+\partial B^{2'}/\partial u^2+\partial B^{3'}/\partial u^3)\Delta u^1\Delta u^2\Delta u^3$$
$$=(B^{1''}-B^{1'''})+(B^{2''}-B^{2'''})+(B^{3''}-B^{3'''})=0 \quad (36)$$

the sum of the *magnetic fluxes* entering the unit cube is zero. (The fluxes enter in the center part of the six faces

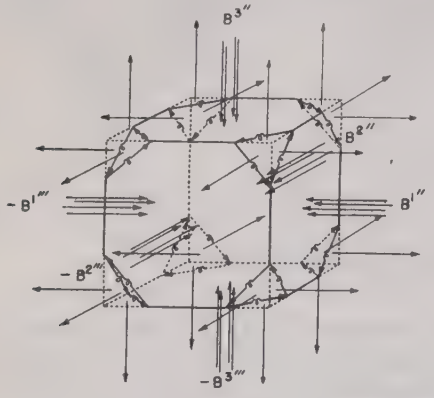

Fig. 11—Proof of div B equation.

and depart through the eight corners.) If bound magnetic poles had existed, the above sum of the magnetic flux lines would be $m'\Delta u^1\Delta u^2\Delta u^3$.

A similar derivation in connection with $pB^{r'}$ (and (16)) proves that the sum of the voltages induced in the eight corner meshes bounded by the inductive coils is zero, as shown by the arrows on Fig. 11.

Appendix II. The Field Equations of Maxwell

The Tensor Form of Maxwell's Equation

The tensor-density form of the field equations of Maxwell has been derived in Appendix I by developing the integral equations of a finite block. Their correctness will be checked against the tensorial equations given in books on electrodynamics.

The tensorial form of Maxwell's field equations in an n-dimensional abstract (curved affine) space is[5]

$$\delta F_{\alpha\beta}/\partial x^\gamma + \delta F_{\beta\gamma}/\partial x^\alpha + \delta F_{\gamma\alpha}/\partial x^\beta = 0 \quad (37a)$$
$$\delta H^{\alpha\beta}/\partial x^\beta = s^\alpha \quad (37b)$$

where the operation $\delta/\partial x^\alpha$ represents covariant (or absolute) differentiation. Since in the special cases to be considered the space is Riemannian and holonomic (in rotating electrical machinery the space is non-Riemannian and nonholonomic) the above equations simplify to[6]

$$\partial F_{\alpha\beta}/\partial x^\gamma + \partial F_{\beta\gamma}/\partial x^\alpha + \partial F_{\gamma\alpha}/\partial x^\beta = 0 \quad (38a)$$
$$(1/\sqrt{-a})(\partial\sqrt{-a}\,H^{\alpha\beta}/\partial x^\beta) = s^\alpha. \quad (38b)$$

Assuming the four-dimensional physical space in orthogonal curvilinear co-ordinates (and allowing Greek indexes to run from 1 to 4 and Roman indexes from 1 to 3), the definitions of the various tensors that occur in Maxwell's equations are as follows:

$x^\alpha =$

α	1	2	3	4
	u^1	u^2	u^3	t

(39)

$F_{\alpha\beta} =$

α \ β	1	2	3	4
1		$\frac{B_3}{(h_3)^2}$	$-\frac{B_2}{(h_2)^2}$	$\frac{E_1}{\sqrt{g}}$
2	$-\frac{B_3}{(h_3)^2}$		$\frac{B_1}{(h_1)^2}$	$\frac{E_2}{\sqrt{g}}$
3	$\frac{B_2}{(h_2)^2}$	$-\frac{B_1}{(h_1)^2}$		$\frac{E_3}{\sqrt{g}}$
4	$-\frac{E_1}{\sqrt{g}}$	$-\frac{E_2}{\sqrt{g}}$	$-\frac{E_3}{\sqrt{g}}$	

(40)

$s^\alpha =$

α	1	2	3	4
	$\frac{I_1}{(h_1)^2}$	$\frac{I_2}{(h_2)^2}$	$\frac{I_3}{(h_3)^2}$	ρ

(41)

$H^{\alpha\beta} =$

α \ β	1	2	3	4
1		$\frac{H_3}{\sqrt{g}}$	$-\frac{H_2}{\sqrt{g}}$	$-\frac{D_1}{(h_1)^2}$
2	$-\frac{H_3}{\sqrt{g}}$		$\frac{H_1}{\sqrt{g}}$	$-\frac{D_2}{(h_2)^2}$
3	$\frac{H_2}{\sqrt{g}}$	$-\frac{H_1}{\sqrt{g}}$		$-\frac{D_3}{(h_3)^2}$
4	$\frac{D_1}{(h_1)^2}$	$\frac{D_2}{(h_2)^2}$	$\frac{D_3}{(h_3)^2}$	

(42)

$a_{\alpha\beta} =$

α \ β	1	2	3	4
1	$-(h_1)^2$			
2		$-(h_2)^2$		
3			$-(h_3)^2$	
4				c^2

(43)

$g_{rs} =$

r \ s	1	2	3
1	$(h_1)^2$		
2		$(h_2)^2$	
3			$(h_3)^2$

(44)

$$\sqrt{-a} = ch_1h_2h_3, \qquad \sqrt{g} = h_1h_2h_3. \quad (45)$$

[5] Gabriel Kron, "Invariant form of the Maxwell-Lorentz field equations for accelerated systems," *Jour. Appl. Phys.*, vol. 9, pp. 196–208; March, 1938.

[6] A. S. Eddington, "The Mathematical Theory of Relativity," Cambridge University Press, New York, N. Y., 1929.

In the above definitions the relations between the field intensities and flux densities are

$$B_r = (\mu/c)H_r, \quad D_r = (\epsilon/c)E_r, \quad I_r = (\sigma/c)E_r. \tag{46}$$

The relations between the tensor quantities (open indexes) used here and the conventional quantities (closed indexes) used in the previous section, are of the form

$$A_r = \epsilon_r^{(s)} A_{(s)} \tag{47}$$

where the set of vectors $\epsilon_r^{(s)}$ are defined as

$\epsilon_r^{(s)}$	(1)	(2)	(3)
1	h_1		
2		h_2	
3			h_3

(48)

The tensorial form of Maxwell's equations are found by substituting the above tensors into (38).

The Tensor-Density Form of Maxwell's Equation

The tensorial equations of Maxwell are defined in (38). They represent the condition of the field at a *point* of the four-dimensional space. Since the meshes of the equivalent circuit represent infinitesimal *blocks* of the three-dimensional space whose volumes are

$$\Delta V = \sqrt{g}\,\Delta u^1 \Delta u^2 \Delta u^3 = h_1 h_2 h_3 \Delta u^1 \Delta u^2 \Delta u^3 \tag{49}$$

it will be necessary to change the tensor equations to tensor-density equations by multiplying all equations through by $\sqrt{g} = h_1 h_2 h_3$ (or by $\sqrt{g}\Delta u^1 \Delta u^2 \Delta u^3$). The resultant expressions are given in (3).

Acknowledgment

The writer wishes to acknowledge his indebtedness to Dr. Simon Ramo who suggested the problem of representing electromagnetic-field phenomena by equivalent circuits, also to G. K. Carter, C. Concordia, and H. A. Peterson of the Central Station Engineering Division, and to J. R. Whinnery and J. F. McAllister of the Electronics Laboratory for numerous discussions.

A companion paper by Simon Ramo and J. R. Whinnery discusses the circuits from the electronic engineer's point of view and another by C. Concordia, G. Kron, W. Ridgway, and J. R. Whinnery gives test results made on the alternating-current network analyzer of various rectangular, cylindrical, and L-shaped cavity resonators. Numerical methods of solving the equivalent circuits will be given in another publication.

Additional Reference

(1) Gabriel Kron, "Equivalent circuits to represent the electromagnetic field equations," *Phys. Rev.*, vol. 69, pp. 126–128; August 1 and 15, 1943.

The Institute desires under present conditions to supply to its membership timely material believed helpful in current educational and experimental work. Through the courtesy of Dean M. L. Enger and Professor E. B. Paine, head of the electrical engineering department, of the University of Illinois, and of the authors, J. Tykocinski Tykociner and Louis R. Bloom, the following paper on "Magnetron Oscillator for Instruction and Research in Microwave Techniques" is reprinted by permission in the PROCEEDINGS.

The Editor

Magnetron Oscillator for Instruction and Research in Microwave Techniques*

J. TYKOCINSKI TYKOCINER†, SENIOR MEMBER, I.R.E., AND LOUIS R. BLOOM‡, NONMEMBER, I.R.E.

***Summary*—A magnetron oscillator for wavelengths from 6 to 17 centimeters (5000 down to 1700 megacycles) has been designed and developed for use either in the research laboratory or for instruction. It consists of a split-anode magnetron inserted between the pole pieces of a magnet whose housing serves to couple the magnetron oscillating circuit to transmission systems of various types. Two methods for producing and controlling the magnetic field have been applied, a permanent-magnet system for the longer wavelengths, and a more powerful electromagnet for the shorter waves. A turntable supported on a stand allows either type of oscillator with its magnet to swing in a horizontal plane. By mounting the oscillator in two distinct positions, either upright, or on its side, the radiating beam may be swept either in the plane of polarization or perpendicular to it.**

* Decimal classification: R355.9. Original manuscript received by the Institute, February 25, 1944. Reprinted by permission from the University of Illinois Engineering Experiment Station Bulletin, series number 48, for January 18, 1944.

† Research Professor of Electrical Engineering, University of Illinois, Urbana, Ill.

‡ Research Assistant in Electrical Engineering, University of Illinois, Urbana, Ill.

I. Introduction

THE purpose of the present investigation was to develop a reliable microwave oscillator for the range of frequencies from 1700 to 5000 megacycles, corresponding to wavelengths 17 to 6 centimeters, which would be convenient in laboratory work for instruction as well as research. It would have to be easily

adaptable for a great range of experimental work such as demonstrating the properties of short electromagnetic waves, methods of measuring wavelengths, mapping radiation-field patterns, and propagation of waves in free space, along wires, concentric lines, or through guides.

Sufficient details are included in the description to enable teachers and investigators to build their own microwave oscillator.

II. Magnetron Tubes

Construction of Magnetron Tube with External Loop (Type I)

In the attempt to construct a magnetron tube suitable for the purpose of experimentation with microwaves it was clear that it would not be necessary to develop a high-power tube. The conditions in a medium-sized laboratory are hardly applicable for utilizing radiation of intensities beyond those measurable with the usual detectors and bolometers. The task was therefore reduced to the design of a compact tube of about 10 watts input so constructed that its power could be controlled easily. This simplified the preparation of the tube and made unnecessary the use of facilities usually absent in a college laboratory. For a skilled technician all that was necessary was that he have available a small spot welder, a vacuum-pump system capable of sustaining a pressure of about 10^{-5} millimeter of mercury, and a high-frequency induction furnace for heating the electrodes during the outgassing process.

The construction and details of the tube are illustrated in Fig. 1. Figs. 1(a) and 1(b) give the general front and side views of the tube. The envelope A is made of pyrex 28-millimeter tubing supplied with a 19-millimeter pyrex electrode press B. The latter carries four tungsten leads imbedded in a uranium glass sleeve C sealed to the press B. Two other similar leads, D, also beaded with uranium glass, protrude through the forward end of the envelope.

Each of the tungsten leads serves as a conductor and support for the tube elements. The filament F (7-mil pure tungsten wire), is kept in position by two nickel prongs 1 and 2 acting as a tension spring, and carrying circular end plates E (6 millimeters in diameter) made of molybdenum, each provided with a hole for the filament.

The oscillating system consists of a pair of semicylindrical anodes G and two yoke-shaped conductors H and J. The anodes G, made of two molybdenum shells facing each other and separated by two slits (usually 0.5 millimeter wide) parallel to the axis, form a hollow cylinder (usual dimensions 8 millimeters long and 4 millimeters in diameter). In order to keep the component parts rigidly together, each shell is welded to one of the legs of the U-shaped nickel yoke H at points within a few millimeters from the ends of the legs. A pair of flexible nickel ribbons I connect the yoke H with the tungsten leads 5 and 6. The latter carry the loop J which terminates the oscillating system. The anode supply is fed through a stiff nickel lead 3 welded to the midpoint of the yoke H, thus serving at the same time as a support for the oscillating elements.

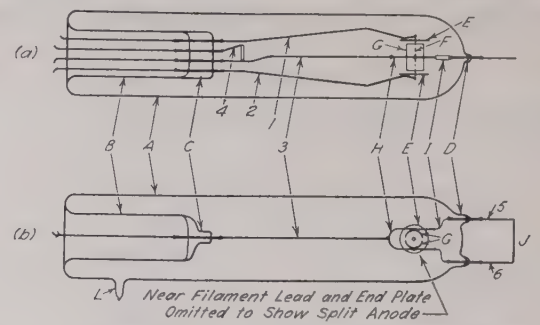

Fig. 1—Magnetron tube with external loop as radiator.

An additional lead 4 serves in conjunction with lead 3 to make connection to a getter element (RCA barium-berylliate).

Construction of Magnetron Tube with Internal Loop (Type II)

The tube described above served well for a range of wavelengths from 8 to 17 centimeters. Below the 8-centimeter wavelength it is not possible to make the external loop J (see Fig. 1) short enough, because the length of the leads I, connecting the external loop J with the anode, cannot be reduced sufficiently. By eliminating the external leads 5 and 6, and by placing the entire loop J within the envelop A, as shown in Fig. 2, this

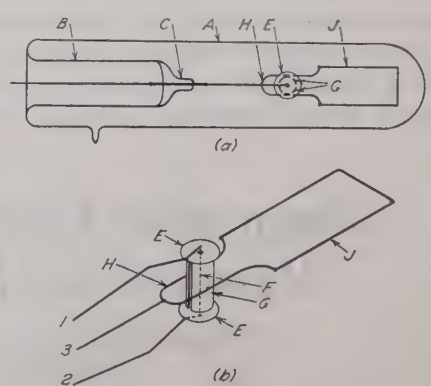

Fig. 2—Magnetron tube with internal loop as radiator.

difficulty is overcome. Besides the simplified construction, economy of tungsten material, elimination of the disturbing capacitances produced at the seals, and better insulation, all add to the increased efficiency of the tube.

An auxiliary view of the electrode structure as shown in Fig. 2(b) indicates the mounting of the electrode elements.

Effect of Length of Radiating Loop

The wavelength emitted by a magnetron tube as well as its efficiency depend not only on the operating

conditions, but also on the constants of the oscillating circuit. These constants are determined by the geometrical dimensions of the split anode *G* and the two adjacent loops *H* and *J* (Fig. 2). At constant diameter and length of the split anode *G*, and at constant frequency, there is for each particular length of the tank loop *H* a corresponding optimum length of the radiating loop *J*. The ratio of these lengths varies with frequency.

Preparation of Magnetron Tubes

In the preparation of a magnetron tube all the precautions applied to the usual thermionic vacuum tube have to be considered. They are especially important in laboratory work where tubes are very often subjected to extreme conditions of operation. Overheating of electrodes occurs quite often, and, if the outgassing has not been properly done, the tube becomes gassy. Also, due to overheating, the electrodes may become warped and cause changes in the tube constants. All these factors are considered in the following procedure.

The split anode is prepared from a sheet of molybdenum[1] from which rectangular pieces are cut, each corresponding in size to one half of the anode. The length of the rectangular pieces is chosen exactly equal to the length of the cylinder, while the width is about 0.5 millimeter smaller than one half the periphery of the circular end of the cylinder.

The anodes are formed and heat-treated in a viselike tool as shown in Fig. 3 where *A* is one of the molybdenum semicylindrical plates. The latter are placed in a groove of the jaw *C*, and subjected to pressure by means of the shaping mandril *B* and the upper jaw *D*. The whole assembly is then tightened by means of the bolts *E*. The core *B* has an extension *F* which serves as a handle for manipulating the vise during the heat treatment.

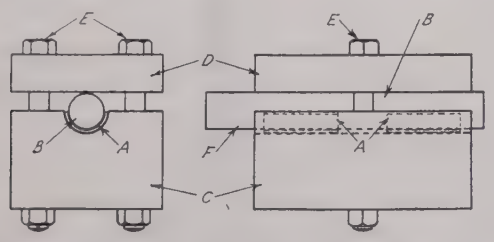

Fig. 3—Vise for heat-treatment of cylindrical split-anodes.

If an electrically heated furnace for the necessary temperature of about 1000 to 1100 degrees centigrade is not available, the vise containing the molybdenum plates may be heated in an oxygen-gas flame of a glassblower's torch. As soon as the entire vise is at a uniform dull-red heat, indicating the appropriate temperature, it is removed from the hot flame and annealed by allowing it to cool gradually to room temperature. The anodes are now removed for mounting.

The two split anodes are then welded to a nickel yoke *H* (see Figs. 1 and 2). Nickel has been chosen for the yoke partly because of the greater ease with which it welds with molybdenum, and partly because it is pliable enough for alignment of the half cylinders.

The four tungsten welds are sealed into the press, and the filament and anode system are mounted by welding. It is important that the two halves of the anode form a regular cylinder with each of the two spacings between them equal in width. The filament is then aligned coaxially with the cylinder. The press assembly is immersed in a solution of sodium dichromate and sulphuric acid for a few minutes to remove grease or other impurities caused by handling, and is finally dipped in distilled water and washed twice in alcohol.

In the case of the tube shown in Fig. 1, the tubular envelope is supplied with openings for the external leads 5 and 6 and is cleaned in the same manner as the press. The press with its entire electrode system is inserted into the envelope *A* and sealed at the base. Finally the protruding tungsten beaded welds carrying the external leads are sealed at the top. If the internal loop is used, as shown in Fig. 2, the latter operation is saved.

Exhaust Procedure

The tube is now ready for the process of outgassing. It is sealed to the vacuum system at the point *L* (see Figs. 1 and 2), and the pumps are turned on.

In order to loosen the gases on the surface of the envelope and the electrodes, an electrical resistance furnace is placed over the tube, the temperature is adjusted to about 350 degrees centigrade and is kept at this point for about half an hour.

The furnace is removed and the electrodes are systematically outgassed one by one. The filament is brought to its normal operating temperature. The getter is then heated to a temperature (orange) just below the flashing point. In the case of the type II tube the induction furnace is applied to the loop to raise its temperature to a red heat. The anode plates are outgassed by applying between cathode and anode a positive potential increasing in steps from 1000 to 4000 volts, first without emission for testing the insulation, and then gradually raising the emission. The electrodes are thereby heated by bombardment of electrons first at red heat and then with increasing plate current until an orange-yellow color temperature is observed. The total time of electron bombardment is usually about 15 minutes.

At this stage, if no signs of a discharge are observable within the tube at anode potentials of about 2000 to 2500 volts and anode current of 20 to 50 milliamperes (15 to 30 watts), the tube is ready for sealing off. In preparation, the constriction is heated with a pointed flame and the tube again pumped for about 10 to 15 minutes. The tube is then sealed off and immediately gettered by applying to the terminals of the gettering element 6 volts at 6 amperes from a storage battery with a 0.4-ohm resistor in series. The tube is now ready for oscillation tests described later.

[1] Nickel may be used instead of molybdenum if the anode temperature is not allowed to exceed dull-red heat (1100 degrees centigrade).

Characteristics

In order to facilitate the operation of the magnetron tube as an oscillator it is useful to have characteristics for typical tubes which show the relation of anode current as a function of applied voltage and magnetic-field intensities. In Figs. 4 and 5 examples of such characteristics are given for a tube whose dimensions are indicated on the curves.

Fig. 4(a) shows the relation $I_b = f(E_b)$; H = constant = 1550 gauss. Also the intensity of radiation is given as measured by means of an antenna and detector at approximately 20 wavelengths distance from the oscillator. The curve (1, 2, 3, 4, 5) shows a rising characteristic with a dip in the region (2, 3).

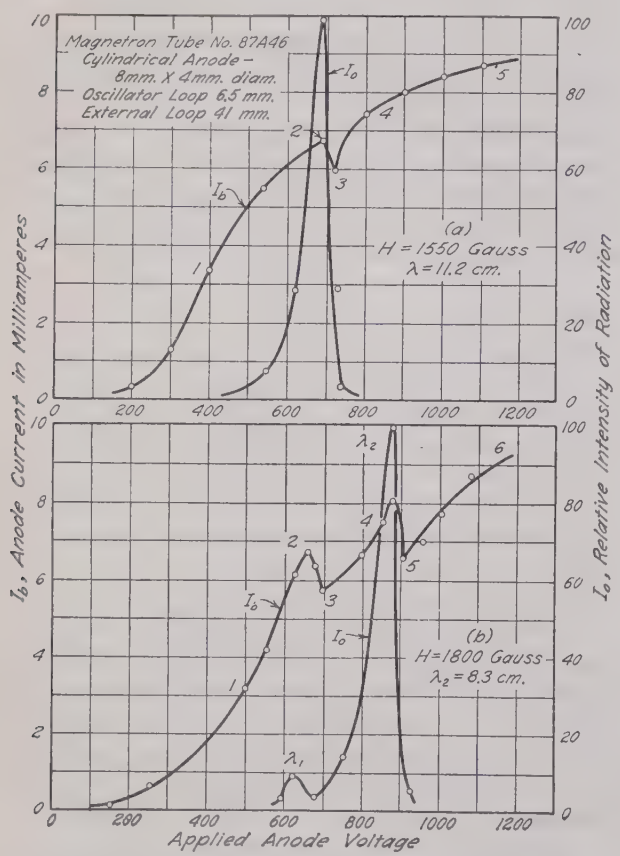

Fig. 4—Relation between plate current and anode voltage.

The maximum of radiation intensity coincides approximately with point 2 where the dip starts. It must be considered that in the region of oscillation (1, 2, 3) the characteristic is not a static one, since the plate current and voltage during oscillation varies above and below certain average values. As the voltage increases to a point 4, at which oscillation ceases, the characteristic returns gradually to its static type (4, 5). The wavelength for $H = 1550$ gauss measured at maximum radiation was $\lambda = 11.2$ centimeters.

Fig. 4(b) shows another characteristic obtained under similar conditions with the exception that the magnetic field was increased by about 15 per cent to $H = 1800$ gauss. The effect is to shift the region 4 of maximum oscillation to higher voltages, namely, from 690 volts to 880 volts. Further, two depressions occur in plate current with corresponding maxima of oscillation at the voltage points 2 and 4. The wavelength of the stronger oscillation decreases from $\lambda = 11.2$ to $\lambda_2 = 8.3$ centimeters. The two curves illustrate the importance of knowing the operating voltages and magnetic fields for specific wavelengths.

Similar but inverse characteristic curves are obtained when anode voltage is kept constant and plate current observed as a function of magnetic field. How the plate current is affected as a function of the magnetic field is illustrated in Figs. 5(a) and 5(b). Here again the region of maximum oscillation coincides with the peak of plate current.

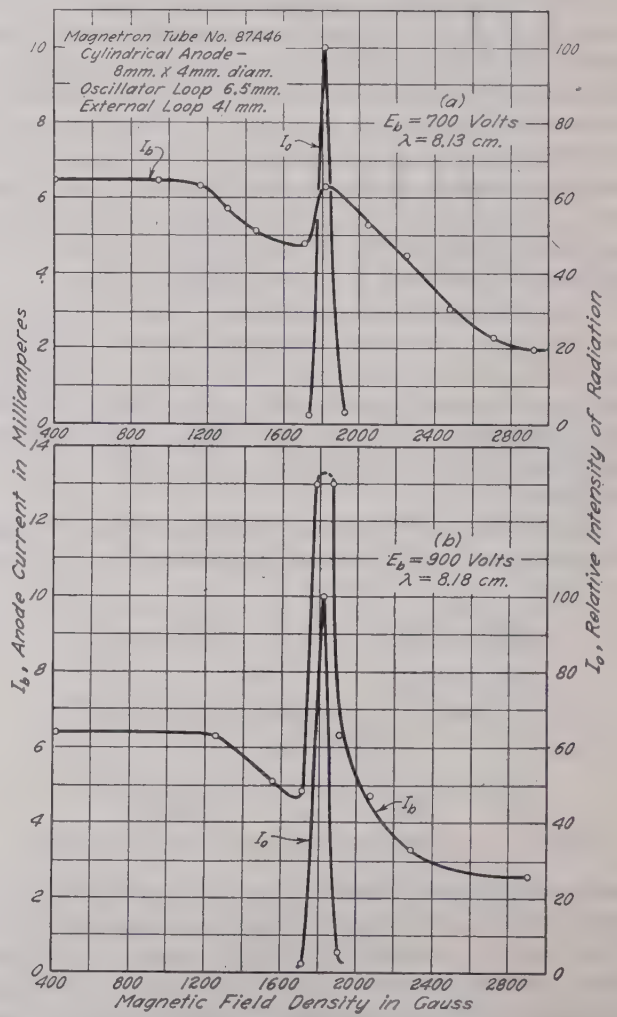

Fig. 5—Relation of plate current to magnetic-field intensity.

Data on Magnetron Tubes

Altogether, 92 magnetron tubes of different types and dimensions have been prepared and investigated. Table I contains data on selected molybdenum, nickel, and graphite split-anode tubes with both internal and external loops that gave continuous usable service in the

TABLE I
DATA ON MAGNETRON TUBES

Tube Number	Type of Radiating Loop	Length of Tank Loop mm.	Dimensions of Radiating Loop in mm.	Magnetic-Field Intensity Gauss	Anode Potential volt	Anode Current ma.	Filament Current amp.	Wavelength for Maximum Power Output λ, cm.	Other Wavelength λ, cm.
			Length × width	1000	450	7	4.8		10.8
21A21	External	6.5	41×12	1200	650	12	5.0	10.2	
				1100	350	10	4.7		13.6
12A12X	External	6.5	41×12	1540	900	4	4.7		8.0
				1800	950	9	4.8	8.14	
				1370	600	8	4.7		8.0
67A37	External	6.5	41×12	1750	1150	8	4.9		7.92
				1840	1100	8	4.7	7.90	
			78×12	1460	900	4	4.9	10.45	
47A28	External	6.5	70×12	1460	800	8	4.9	10.06	
			80×12	1460	900	4	4.9	10.70	
				1800	1300	8	4.7	7.58	
62FG9	Internal	6.5	56×12	1800	1100	8	4.7		7.73
				1660	850	5	4.65		9.50
				1750	950	8	4.95	8.67	
51FG6	Internal	15	35×12	800	400	6	4.90		13.9
				2800	1000	9	4.9		5.9
85J6* (Graphite Anode)	External	6	70×12	900	360	10.5	4.7	16.8	

Constructional details: Anode, length, 8 millimeters; inner diameter 4 millimeters. Filament, length, 10 millimeters, diameter, 7.5 mils.
* Using permanent magnet.

laboratory for instructional and research purposes. As evidenced from the table, wavelengths from about 6 to 17 centimeters ($f = 5000$ down to 1700 megacycles) are obtainable with these tubes.

III. The Magnet

General Requirements and Considerations for Production of Magnetic Field

The magnetron tube differs from all other short-wave oscillators in that it requires a constant magnetic field within the anode cylinder in the direction of its axis. This field forces the electrons to move in trajectories which bring about energy transfers to the adjacent circuit at high frequency. The constancy of frequency requires constancy of the magnetic field. It is therefore quite important to design magnets to suit this requirement. The requirements may be satisfied by using permanent magnets or electromagnets. In cases where a number of frequencies have to be produced by the same tube the range of field intensities which have to be established with a given magnet must be at least in proportion to the range of frequencies. Both permanent magnets and electromagnets of proper design are adaptable for such conditions.

The advantages of the permanent magnet are that its weight is comparatively small and that no external direct-current source is necessary to sustain the field. On the other hand, the aging of permanent magnets presents a serious disadvantage in their use. However, in the laboratory the electromagnet has the advantage of a larger range of magnetic-field intensities. It requires special regulating equipment for preventing variations due to temperature and line-voltage fluctuations. Generally, for instructional purposes, and for most laboratory work, the electromagnet is more serviceable.

Permanent Magnet

A design of a simplified oscillator making use of permanent magnets for producing the necessary magnetic flux through the anode of the magnetron tube is shown in Fig. 6. Two permanent magnets *A* and *B*, made of an aluminum-nickel cobalt alloy (Alnico), or any other alloy having suitable characteristics of high magnetic retentivity, are fixed in a rectangular frame *C*.

This frame consists of four brass bars, two of which are grooved. The magnets are slid into the grooves *E* in such a manner that the like poles face each other.

Thus, the flux passing through the tube *D* from the north to the south poles combines to increase the intensity of the field within the anode cylinder. By using Alnico magnets of the dimensions shown, a resultant field of 860 gauss was obtained. It is possible to use only one magnet in the same frame if the other is replaced by a brass dummy to keep the single magnet in position. In this case, however, the field strength is only about 700 gauss.

The frame *C* fits within a rectangular box *F*. It is supplied with a brass tube *G* for supporting the mag-

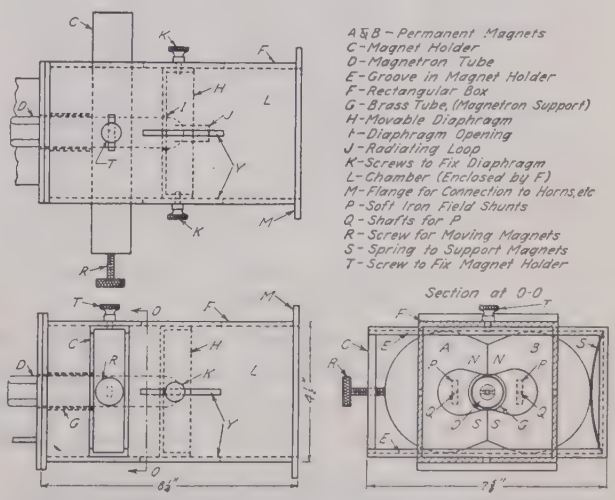

Fig. 6—Magnetron oscillator using permanent magnet.

netron *D*, and with a sliding diaphragm *H*. The latter has a circular opening *I* through which the radiating loop *J* or the tube *D* may pass. Two knobs *K* are provided for adjusting the correct position of the diaphragm along the chamber *L*. A narrow slit *Y* is cut in the wall of the chamber to guide the diaphragm. The chamber is terminated by a flange *M* for connecting to guides, horns, or any other transmission or radiation system. The tube is connected electrically to the external circuit through a system of chokes and condensers in a manner which will be described later.

For many types of experiments it is desirable to vary the field strength through the anode. This may be done by rotating two soft-iron bars *P*, attached to shafts *Q*

(shown in broken lines), so as to shunt a part of the field in each of the magnets. A much simpler method, however, is to move the magnetron along its axis across

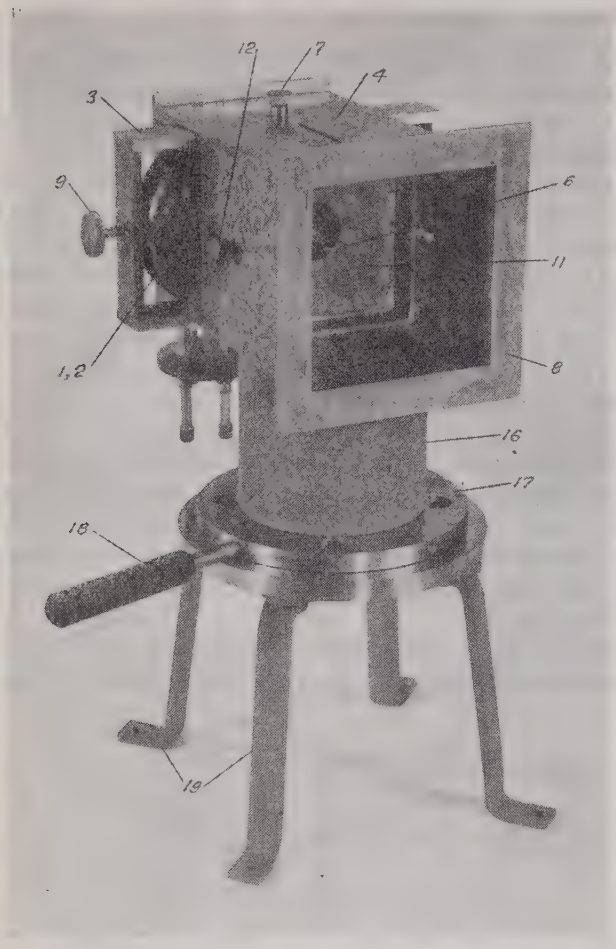

Fig. 7—Magnetron oscillator with permanent magnet and resonance chamber.

the field or to slide the magnets perpendicular to the axis of the tubes; this method is shown in Fig. 6. By means of an adjusting screw *R*, acting against the magnet, and a tension spring *S*, set in the groove *E*, fine

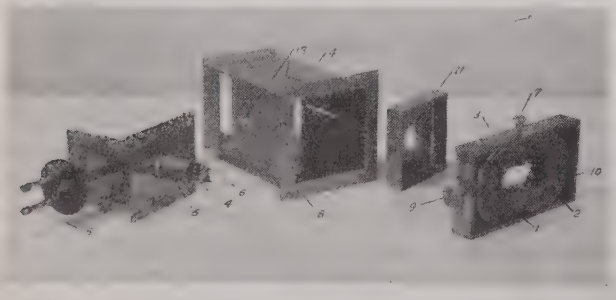

Fig. 8—Details of magnetron oscillator with permanent magnet.

KEY FOR FIGS. 7 AND 8

1, 2. Permanent magnets
3. Frame for permanent magnets
4. Oscillator box
5. Tube holder
6. Radiating loop
7. Knob for adjusting magnet frame
8. Flanges for guide
9. Adjusting screw for magnet
10. Tension spring for magnet
11. Diaphragm
12. Knobs for sliding diaphragm
13. Guiding slots for diaphragm
14. Magnetron tube
15. Condenser and choke assembly
16. Support for oscillator
17. Turntable
18. Handle for turntable
19. Stand

variations may be achieved in the magnetic field passing through the tube. Coarse adjustment is obtained by shifting the frame *C* across the chamber *L*, and locking the frame by means of screw *T*.

Fig. 7 gives a general view of the oscillator mounted on a supporting stand: the main component parts are shown on Fig. 8.

Design and Construction of Electromagnet

The usual electromagnets in connection with magnetrons consist of one or two solenoids supplied with an

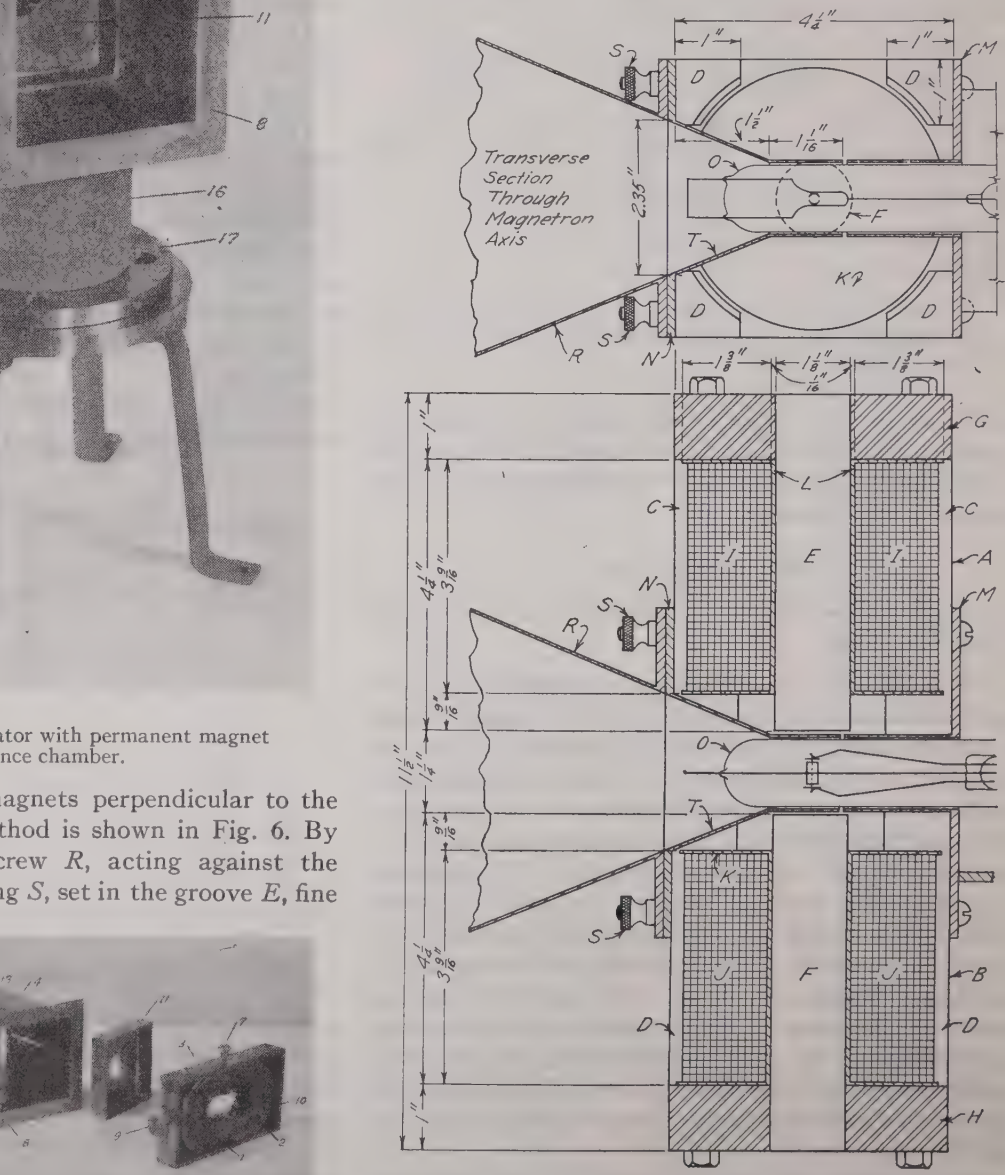

Fig. 9—Magnetron oscillator using electromagnet.

iron core and pole pieces extended towards the tube. It was found that such arrangements produce strong stray fields which cannot be utilized since they by-pass the magnetron anodes. Due to their inefficiency their excitation requires high current densities causing overheating of the coils during continuous use. The new electromagnets were designed with the purpose of

overcoming these difficulties, and for providing convenient adjustable mechanically stable supports, also electrically appropriate coupling of the magnetron tube with various radiating systems.

The magnetic circuit (Fig. 9) consists of two symmetrical parts, *A* and *B*, made of Armco iron, with their ends notched so as to fit one against another. Each part consists of four outside legs *C* and *D* and the cores *E* and *F*. The legs are held together by common plates *G* and *H*. Two methods of turning out each half can be used. One consists in turning each part *A* or *B* out of one solid piece. This method avoids increased reluctance at the connecting surfaces, but requires special tooling. This increased tooling and material may be saved by making the legs, main plates, and cores separately, and joining them by bolting.

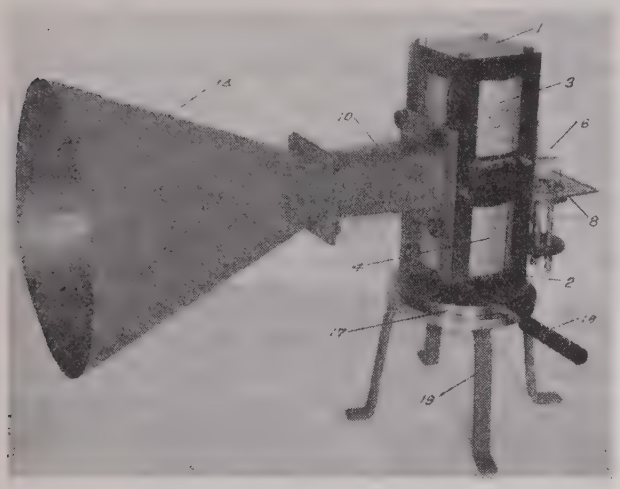

Fig. 10—Magnetron oscillator with electromagnet (mounted vertically), turntable guide, and circular horn.

KEY

1. Upper part of electromagnet
2. Lower part of electromagnet
3. Upper coil of magnet
4. Lower coil of magnet
6. Magnetron tube
8. Terminal board and condenser-choke assembly
10. Guide to horn
14. Round horn
17. Turntable
18. Handle for turntable
19. Stand

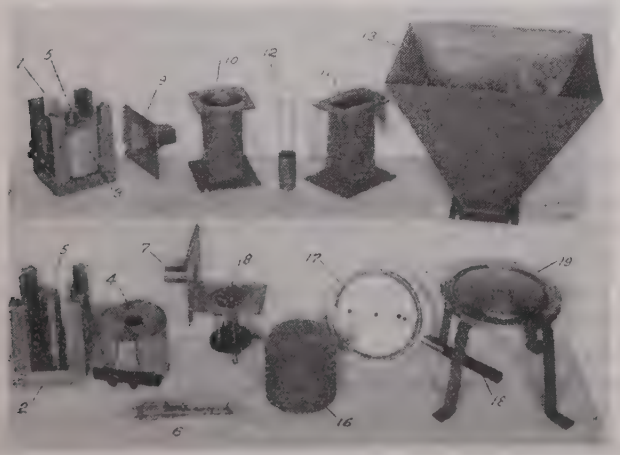

Fig. 11—Details of magnetron oscillator with electromagnet.

KEY

1. Upper part of electromagnet
2. Lower part of electromagnet
3. Upper coil of magnet
4. Lower coil of magnet
5. Inner cores of magnets
6. Magnetron tube
7. Tube holder
8. Terminal board and condenser-choke assembly
9. Coupling attachment
10. Guide to horns
11. Guide to horns
12. Parallel wire attachment
13. Square horn
16. Support for oscillator
17. Turntable
18. Handle for turntable
19. Stand

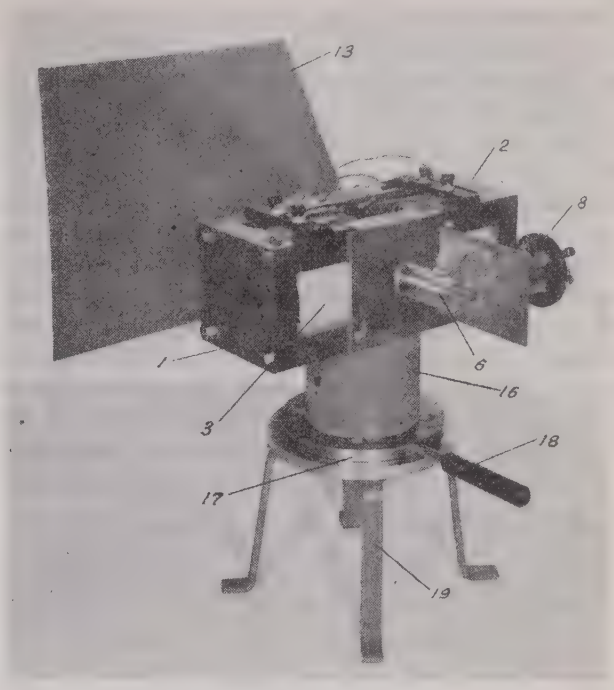

Fig. 12—Magnetron oscillator with electromagnet (mounted horizontally), turntable, and square horn.

KEY

1. Upper part of electromagnet
2. Lower part of electromagnet
3. Upper coil of magnet
6. Magnetron tube
8. Terminal board and condenser-choke assembly
13. Square horn
16. Support for oscillator
17. Turntable
18. Handle for turntable
19. Stand

The coils *I* and *J* wound on brass spools *K* and *L* fit snugly over the cores between the legs of each half of the magnet. The two halves are held together by means of brass plates *M* and *N* which at the same time serve to support the magnetron tube *O* and the radiating system *R*, *T*.

TABLE II

DATA ON ELECTROMAGNET

Material of magnetic circuit	Armco iron
Diameter of core at poles	1½ inches (28.5 millimeters)
Length of air gap	1½ inches (28.5 millimeters)
Field strength at 0.5 ampere	1900 gauss
Number of coils	2
Number of turns per coil	4200
Total number of turns	8400
Ampere turns at 0.5 ampere	4200
Size of copper wire	No. 22 B & S gauge
Insulation of copper wire	enamel single cotton
Resistance per coil	48.5 ohms
Total resistance for series connection	97.0 ohms
Total resistance for parallel connection	24.25 ohms
Energy dissipation at 0.5 ampere	24.25 watts
Temperature rise at 0.5 ampere	13 degrees centigrade
*Weight without support	38 pounds 4 ounces
Weight of support with turntable	13 pounds

* Including tube holder, stubs, and coupling attachment.

The electromagnet is shown in Figs. 10 and 12 as part of the general view of the oscillator, while the details are presented in Fig. 11.

The computation of the dimensions of the magnetic

and electrical circuits is a matter of known procedure.[2] The principal data on the electromagnet are specified in Table II.

Experimental Data

The actual intensity of the magnetic field as a function of the excitation current was measured in the gap by means of a fluxmeter, and is shown plotted in Fig. 13. The curve indicates that intensities of from 0 to 3000 gauss are readily obtainable without exceeding the temperatures prescribed for electromagnets. The values were obtained using the two coils connected in series. Obviously, for parallel connection the line voltage is halved, and the supply current necessary for the same field strengths must be doubled. The maximum temperature at the poles reached under continuous operation at 25 degrees centigrade room temperature are indicated on the curve. The stray fields measured just

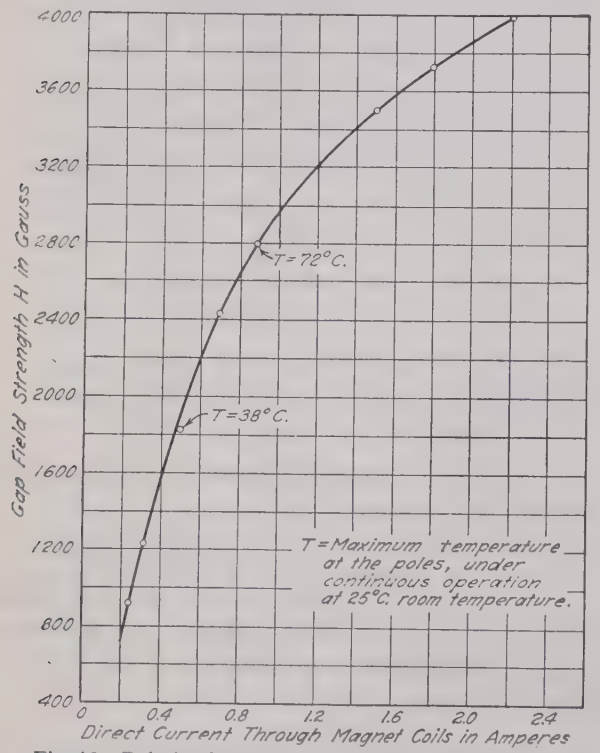

Fig. 13—Relation between current and gap field intensity.

along the periphery passing around the junction line of the legs were so small that they could not be measured with the usual fluxmeter.

IV. Radiators

Magnetron-Tube Oscillator

In order to utilize the ultra-high-frequency oscillations produced by the magnetron tube it is necessary to have the tube properly mounted and wired within the electromagnet. It is also important to provide means of coupling the tube to transmission lines of various forms and to different radiating systems. Further, for investigating radiation patterns it is useful to have the angular position of the radiating system movable along a horizontal or a vertical axis. A complete oscillator must, therefore, contain a variety of attachments which would be flexible enough for the main tasks encountered in the laboratory. A pictorial view of the complete oscillator and of its parts is given in Figs. 10, 11, and 12. A description of the component parts follows.

Arrangement of Magnetron Holder with Choke Stubs

In order to provide a stable support and convenient connections to the power sources a holder has been provided as shown in Fig. 14. It consists of a plate *A*, bolted to the legs of the electromagnet *B*. This plate is supplied with a brass tube *C*, into which the magnetron tube *D* fits, and can be rotated through small angles in

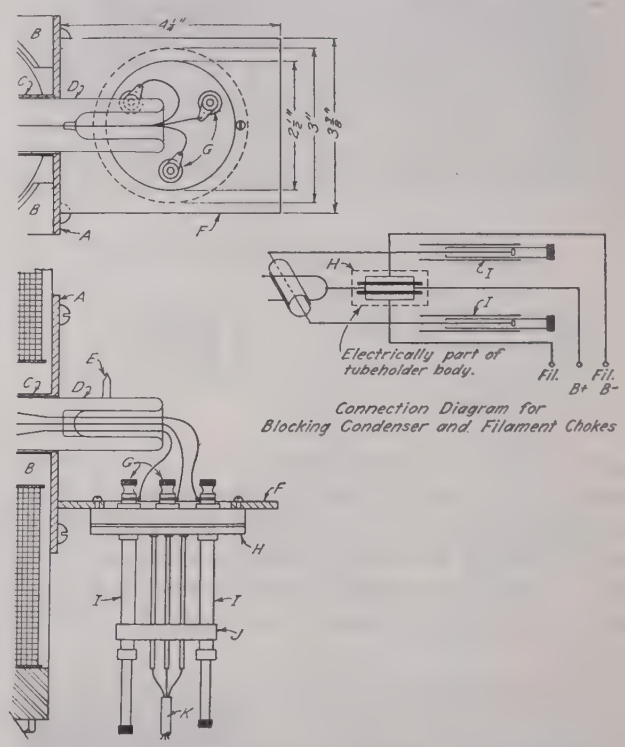

Fig. 14—Magnetron tube holder with choke stubs for filament circuit.

the magnetic field by moving the tip *E*. The plate *A* carries at right angles another plate *F*, provided with a circular opening into which is mounted an assembly carrying binding posts *G*, a blocking condenser system *H*, and a pair of adjustable filament chokes *I* for preventing propagation of radio-frequency waves along the supply line.[3] A bakelite disk *J* keeps the chokes and the leads connecting the binding posts with the power cable *K* firmly in position. How the different circuit elements of the tube are connected with the condenser chokes and power supply is indicated in the connection diagram adjoining Fig. 14.[4] Plates *A*, *F* carry a shield box.

[2] A. D. Moore, "Fundamentals of Electrical Design," McGraw-Hill Book Co., New York 18, N. Y.

[3] The condenser structure *H* can be omitted if a third tuning stub for the anode is added.

[4] The details of construction of a condenser-choke assembly in an ultra-high-frequency system are described by J. G. Brainerd, Glenn Koehler, Herbert J. Reich, and L. F. Woodruff in "Ultra-High Frequency Techniques," D. Van Nostrand Co., New York, N. Y., 1942, p. 302.

Coupling of Oscillating Circuit to Radiating Systems

The oscillation energy developed in the magnetron may be utilized by coupling the radiating loop of the magnetron in various ways.

For studying waves along wires, a Lecher-wire system may be coupled inductively to the tube by means of an attachment, as shown in Fig. 15. It consists of a cylindrical brass tube *A*, which fits snugly over the front end of the magnetron envelop. A pair of brass tubes *B* are soldered to the outer part of the sleeve *A*. Into these can be slid a U-shaped wire *C*, as shown in Fig. 15(a), to complete the closed Lecher system, or two single wires *D* may be inserted to form an open Lecher system, as shown in Fig. 15(b). The inductive coupling can be adjusted by rotating or shifting the sleeve *A* relatively to the loop of the magnetron.

For experiments in which waves in free space are investigated, it is necessary to provide means of directing the radiation by means of horns. How to couple the magnetron to a horn is shown in Fig. 9. For this purpose the Lecher system is replaced by a square or circular intermediate attachment *T*, as shown in Fig. 9. The attachment consists of three parts, a sleeve, a funnel, and

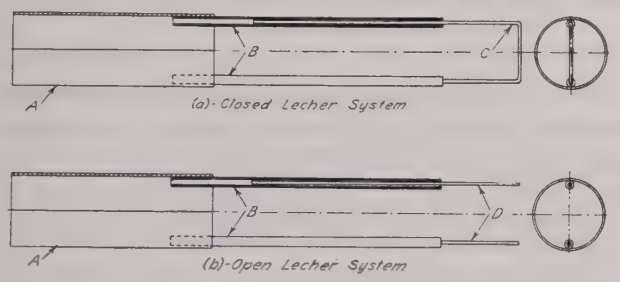

Fig. 15—Attachment for studying standing waves along wires.

a plate *N*. This attachment is inserted between the legs and pole pieces of the magnet, and fastened to the magnet proper by means of thumb screws *S* as shown in Fig. 9. Extensions in form of horns, either square or round, depending upon the shape of the intermediate piece, also may be attached by means of the thumbscrews *S* to the same plate *N*.

Whenever it is necessary to transmit the oscillations along transmission lines or guides, proper chambers can be inserted between the transmission units and the intermediate attachment *T* (see Fig. 9).

Turntable with Stand for Supporting Oscillator

Optical properties of the microwaves in space, such as reflection, refraction, polarization, standing waves, and intensity patterns of beams, may be studied readily by providing means of gradually sweeping the beam in two planes of polarization.

A mechanically simple and convenient arrangement is shown in Fig. 16. The base *A* of the electromagnet rests upon a metal plate *B* which has a circular ridge *C*. The latter fits into a circular groove *D*, cut in a lower plate *E*. A four-legged stand *F* supports the plate *E*. *A* pivot *G* centers the magnet with plates *B* and *E*. By means of a handle *H* the electromagnet may be swiveled, and the angular position indicated in degrees by the pointer *J* upon the dial *I*.

In order to sweep the magnetron oscillator in a vertical plane of polarization the electromagnet is lifted from the turntable and placed on its side as shown on Fig. 12 so that the legs rest on the turntable base. For centering in this new position, pins in the legs of the electromagnet and corresponding holes in the turntable are provided.

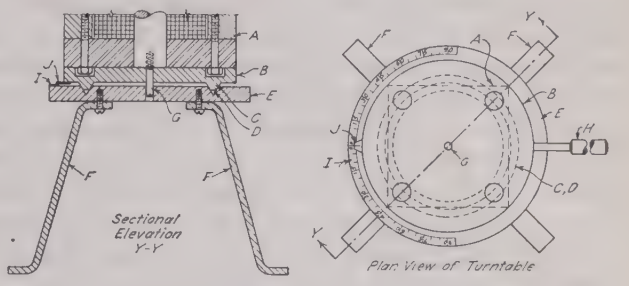

Fig. 16—Turntable with stand for supporting oscillator.

Thus the construction described in the foregoing sections is adaptable to multifarious experiments with microwaves.

V. Operation of Oscillator

General Operating Requirements

For proper operation it must be considered that discrete values of voltage, magnetic field, and space-charge conditions must be established within the tube for definite frequencies of oscillation. Further, the constancy of amplitude of oscillation, most important for all quantitative experiments, requires stable sources of power for anode, filament, and magnetic field. It is desirable that meters be inserted in all the circuits for controlling these conditions.

Magnetron-Oscillator Circuit

The general diagram of connections is shown in Fig. 17. The filament is heated by a transformer *A*, whose output is 6.3 volts at 110 volts input. A variac *B* is

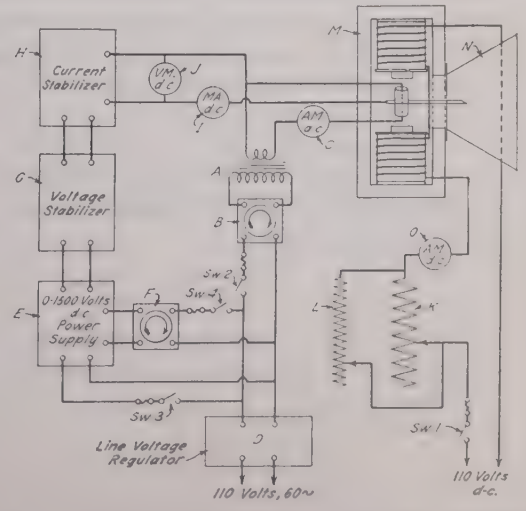

Fig. 17—Diagram of connection for magnetron oscillator.

connected in the primary of the transformer for controlling its output voltage. An ammeter C (0 to 5 amperes) serves to indicate the filament current. The line voltage supplying the variac is usually stable enough for qualitative experiments, if a line-voltage regulator D of the resonance or magnetic-saturation type is inserted in the line. However, it is not sufficient in itself for quantitative experiments. In this case storage batteries are recommended for the filament.

Precise control of the plate voltage and current is necessary for all kinds of experiments because of the danger of damaging the magnetron tube due to sudden overloads peculiar to magnetron oscillators. Such controls are obtained by inserting in the output of the conventional direct-current power supply E, whose input is regulated by a variac F, a voltage stabilizer G in addition to a current stabilizer H of the thermionic type. Examples with detail diagrams of such stabilizing circuits may be found in the literature.[5]

The anode currents and voltage may be measured by means of suitable meters I and J, respectively.

If electromagnets are used for supplying the magnetic field, a simple series circuit using a pair of rheostats K and L, connected in parallel for rough and fine control, may be used for regulating the current. In this case the two magnets M are also connected in series, and an ammeter O is placed in series with the 110-volt direct-current line. Storage batteries are recommended for precise measurements. In the latter case the two magnets may be connected in parallel in order to reduce the required battery voltage to approximately 24 to 30 volts.

Operating Procedure

It is advisable that the operating conditions which are usually given for each magnetron tube be referred to before turning on the power supplies.

Preferably, the current excitation for the magnets is turned on (*Sw* 1, Fig. 17) a few minutes early to allow the coils to heat up to their normal operating temperatures, thus reducing changes in magnetic-field strength due to increased coil resistance produced by temperature rise. It is advisable to adjust the rheostats K and L gradually from maximum resistance down to approximately their normal position.

With the filament variac set to zero voltage, the switch *Sw* 2 is turned on and the variac brought up until the approximate required heating current is observed on the ammeter C. Next, the filaments for the power supply E are turned on by the switch *Sw* 3 and then, with the variac F set to zero, the plate-supply switch *Sw* 4, and also the switches (not shown in the figure) for the filaments of the voltage and current regulators G, H, are turned on. Finally, the variac F is slowly turned up until the voltmeter J and the milliammeter I show approximate operating values.

Before adjusting for oscillation a receiver, consisting of an antenna doublet a few centimeters in length connected through a crystal detector to a microammeter, is placed in front of the horn N or adjacent to any other radiator being used. This receiver serves as an indicator of oscillation. The tube is turned so that the axis of the anode deviates from the direction of the magnetic field from 3 to 10 degrees. If oscillations do not set in, this angle is slightly reset and fine adjustments are made consecutively in filament current, anode current, anode voltage, and magnet current by adjusting controls B, F, and L. This order of adjustment is repeated until an indication of oscillation is observed on the doublet detector receiver. Once oscillation sets in the same order of adjustments are repeated in still smaller steps until the meter of the receiver reaches a maximum deflection.

Results

The magnetron oscillator proved effective for research purposes, testing, and various types of experiments designed to demonstrate the properties of microwaves. The following experiments, performed in the laboratory, may serve as examples of the application of the oscillator:

(1) Testing of about 90 magnetron tubes of different types and dimensions as oscillators.

(2) Determination of static and operating characteristics of oscillators.

(3) Determination of dimensions of circuit elements for definite frequencies.

(4) Study of transmission along parallel-wire systems, coaxial cables, and guides.

(5) Comparative study of various radiating systems.

(6) Determination of wavelength by various methods.

(7) Calibration of crystal detectors and bolometers.

(8) Study of radiation patterns of reflectors, horns, and guides.

(9) Decrease of radiation intensity as function of distance from source.

(10) Polarization, reflection, and refraction of radiated beams.

[5] See page 74 of footnote reference 3.

THE INSTITUTE OF RADIO ENGINEERS

INCORPORATED

SECTION MEETINGS

ATLANTA	CHICAGO	CLEVELAND	DETROIT	LOS ANGELES
May 19	May 19	May 25	May 19	May 16
NEW YORK	**PHILADELPHIA**	**PITTSBURGH**	**PORTLAND**	**WASHINGTON**
June 7	June 1	June 12	June 12	June 12

SECTIONS

ATLANTA—Chairman, Walter Van Nostrand; Secretary, Ivan Miles, 554—14 St., N. W., Atlanta, Ga.

BALTIMORE—Chairman, G. J. Gross; Secretary, A. D. Williams, Bendix Radio Corp., E. Joppa Rd., Towson, Md.

BOSTON—Chairman, R. F. Field; Secretary, Corwin Crosby, 16 Chauncy St., Cambridge, Mass.

BUENOS AIRES—Chairman, G. J. Andrews; Secretary, W. Klappenbach, *La Nacion*, Florida 347, Buenos Aires, Argentina.

BUFFALO-NIAGARA—Chairman, Leroy Fiedler; Secretary, H. G. Korts, 432 Potomac Ave., Buffalo, N. Y.

CHICAGO—Chairman, A. B. Bronwell; Secretary, W. O. Swinyard, Hazeltine Electronics Corp., 325 W. Huron St., Chicago, Ill.

CINCINNATI—Chairman, J. L. Hollis; Secretary, R. S. Butts, Box 1403, Cincinnati 2, Ohio.

CLEVELAND—Chairman, A. S. Nace; Secretary, Lester L. Stoffel, 1095 Kenneth Dr., Lakewood, Ohio

CONNECTICUT VALLEY—Chairman, W. M. Smith; Secretary, R. F. Shea, General Electric Co., Bridgeport, Conn.

DALLAS-FORT WORTH—Chairman, D. J. Tucker; Secretary, P. C. Barnes, WFAA-WBAP, Grapevine, Texas.

DAYTON—Acting Secretary, Joseph General, 1319 Superior Ave., Dayton, 7, Ohio.

DETROIT—Chairman, R. A. Powers; Secretary, R. R. Barnes, 1411 Harvard Ave., Berkley, Mich.

EMPORIUM—Chairman, H. D. Johnson; Secretary, A. Dolnick, Sylvania Electric Products, Inc., Emporium, Pa.

INDIANAPOLIS—Chairman, A. N. Curtiss; Secretary, E. E. Alden, WIRE, Indianapolis, Ind.

KANSAS CITY—Chairman, A. P. Stuhrman; Secretary, R. N. White, 4800 Jefferson St., Kansas City, Mo.

LOS ANGELES—Chairman, L. W. Howard; Secretary, Frederick Ireland, 1000 N. Seward St., Hollywood, 38, Calif.

MONTREAL—Chairman, L. T. Bird; Secretary, J. C. R. Punchard, Northern Electric Co., 1261 Shearer St. Montreal, Que., Canada.

NEW YORK—Chairman, Lloyd Espenschied; Secretary, J. E. Shepherd, 111 Courtenay Rd., Hempstead, L. I., N. Y.

PHILADELPHIA—Chairman, W. P. West; Secretary, S. Gubin, RCA Victor Division, Radio Corporation of America Bldg. 8-10, Camden, N. J.

PITTSBURGH—Chairman, B. R. Teare; Secretary, R. K. Crooks, Box, 2038, Pittsburgh, 30, Pa.

PORTLAND—Chairman, W. A. Cutting; Secretary, W. E. Richardson, 5960 S.W. Brugger, Portland, Ore.

ROCHESTER—Chairman, O. L. Angevine, Jr.; Secretary, G. R. Town, Stromberg-Carlson Co., Rochester, N. Y.

ST. LOUIS—Chairman, N. J. Zehr; Acting Secretary, C. H. Meyer, KFUO, 801 DeMun Ave., St. Louis, Mo.

SAN FRANCISCO—Chairman, W. G. Wagener; Secretary, R. V. Howard, 225 Mallorca Way, San Francisco, Calif.

SEATTLE—Chairman, F. B. Mossman; Secretary, E. H. Smith, Apt. K, 1620—14 Ave., Seattle, 22, Wash.

TORONTO—Chairman, R. G. Anthes; Secretary, J. T. Pfeiffer, Erie Resistor of Canada, Ltd., 128 Peter St., Toronto, Ont., Canada.

TWIN CITIES—Chairman, E. S. Heiser; Secretary, B. R. Hilker, KSTP, St. Paul Hotel, St. Paul, Minn.

WASHINGTON—Chairman, J. D. Wallace; Secretary, F. W. Albertson, c/o Dow and Lohnes, E St. N. W., between 13th and 14th Sts., Washington, D. C.

Institute News and Radio Notes

Board of Directors

March 1 Meeting: At the regular meeting of the Board of Directors, which took place on March 1, 1944, the following were present: H. M. Turner, president; R. A. Hackbusch, vice-president; S. L. Bailey, W. L. Barrow, I. S. Coggeshall, Alfred N. Goldsmith, editor; R. A. Heising, treasurer; L. C. F. Horle, C. B. Jolliffe, F. B. Llewellyn, H. J. Reich, B. J. Thompson, H. A. Wheeler, L. P. Wheeler, W. C. White, and W. B. Cowilich, assistant secretary.

Membership: The following applications for membership were approved: for transfer to Senior Member grade, O. L. Angevine, Jr., Saul Dushman, G. M. Lohnes, J. E. Shepherd, and H. L. Tholstrup; for transfer to Member grade, R. W. Chapman, Harold Goldberg, J. C. O'Shea, and P. W. Spence; for admission to Member grade, F. H. Clarke, F. E. Mauritz, D. H. Preist, and E. G. Sorensen; Associate grade, 115; and Student grade, 44.

Budget: President Turner presented the revised 1944 budget, which had been recommended by the Executive Committee. After a discussion, the revised budget was unanimously adopted.

Committees: Dr. Austin Bailey was appointed chairman of the 1945 Winter Convention.

On the recommendation of Chairman Everitt, Professors A. B. Bronwell and B. R. Teare, Jr., were appointed to the Committee on Education.

President Turner announced that, due to the pressure of other duties, Mr. B. J. Thompson had requested to be relieved of serving on the Board of Editors and the Constitution and Laws Committee. The resignation of Mr. Thompson from these committees was accepted with an expression of regret.

Constitution and Bylaws: In his capacity as chairman of the Constitution and Laws Committee, Treasurer Heising submitted the wording of Sections 1b, c, and d of Article II, given below, as a means of amending the Constitution in a manner that would provide for the proposals recently made by the Montreal Section:

ARTICLE II

Section 1, b—Change the name of "Senior Member" membership to "Member" membership in the Institute and in the Constitution.

c—Change the name of "Member" membership to "Associate" membership in the Institute and in the Constitution.

d—Change the name of "Associate" membership to "Affiliate" membership in the Institute and in the Constitution.

After discussion, the Constitution and Laws Committee was requested to inform the Montreal Section of the suggested method for attempting to amend the Constitution through use of essentially the foregoing wording, the final wording to be subject to approval by General Counsel Zeamans.

As a means of preventing a wholesale demotion of Associates to Affiliate status in the event that the proposed amendments are adopted, Treasurer Heising suggested giving consideration to adding a Section 5 to consist of the following wording, to Article II:

ARTICLE II

Section 5—"An Associate member of record for three years prior to the adoption of this amendment shall not be transferred to Affiliate membership until he shall have been sent a notice of such impending change and shall have been given an opportunity good for a stated period not exceeding six months but depending upon distance, to retain Associate membership, and such Associate member shall be required to show only that he is or has been an engineer or scientist or teacher in radio or allied fields to retain Associate membership."

It was also stated that this additional amendment would facilitate the transfer of Associates to the professional grade of Member and could be sent to the voting membership along with those proposed by the Montreal Section.

The proposed amendment of Section 16 of the Bylaws, which is quoted below, was unanimously adopted:

Bylaws Section 16: "A bill shall be sent to each member not later than December 31 covering his dues for the following year. A second bill shall be mailed on or about March 1, to each member whose dues remain unpaid. Not later than April 1, each member whose dues remain unpaid shall be so notified by the Secretary and informed that, in accordance with Article III, Section 7, of the Constitution, should his dues remain unpaid after April 30, his membership will terminate and he will lose the right to vote and to receive the publications of the Institute. On May 1, the name of each member whose dues remain unpaid shall be removed from the roll of membership and such member shall be sent a notice to the effect that according to Article III, Section 7, his membership in the Institute has in fact terminated. The list of such terminated memberships shall be turned over to the Membership Committee."

Certificate of Incorporation: Treasurer Heising, as chairman of the Investment Committee responsible for making arrangements to amend the I.R.E. charter, reported on the special meeting of the Institute held on January 28, 1944, at which the proposed amendments to the Institute's Certificate of Incorporation were unanimously approved.

Student Chapters: Student Chapters, or Branches were discussed at length.

Institution of Electrical Engineers: The recent letter from Mr. F. S. Barton, junior past vice-president of the Institute, concerning a possible visit from Dr. R. L. Smith-Rose of England, was read by President Turner. It was explained that the intention of Dr. Smith-Rose is to discuss with the Board of Directors the subject of closer cooperation between the I.E.E. and the Institute.

Clark Collection: Professor Alan Hazeltine accepted the appointment to serve as Institute representative on the Engineering Societies Library Committee, organized to catalog and index the George H. Clark collection.

I.R.E. Committee on Professional Recognition: Mr. White, chairman of this committee, stated that, although no recent meeting of his group had been held, considerable correspondence has been carried on with particular reference to studying the actions of other national societies in the field of collective bargaining for engineers.

The procedure for collective bargaining adopted by the American Society of Civil Engineers, the first society to pioneer such a plan, was described and an article on this subject which appeared in *Electrical Engineering* was read. The American Institute of Electrical Engineers recently authorized an investigation of collective bargaining for engineers, and the A.I.E.E. activity in the field will be considered by the Board of Directors from time to time. Mr. White pointed out that the I.R.E.'s approach to the problem was somewhat complicated as a result of the members being in these three widely different classifications: employer, professional, and subprofessional groups. Editor Goldsmith presented to the Board an article "Unionization of Engineers," which appeared in the February 5, 1944, issue of *Electrical World*.

The Institute policy, of preferring general group action to local and of co-operating with other national societies, was reaffirmed. It was suggested that papers on the conflict between professional and labor-union aims and practices be considered for publication in the PROCEEDINGS. The progress report, given by Mr. White, was unanimously accepted.

F. S. Barton: President Turner read the February 5, 1944, letter from Junior Past Vice-President Barton, expressing appreciation of the opportunity of being associated with the Board of Directors and serving the Institute during the past year.

Membership Dues: Two different plans for increasing the membership dues were submitted and discussed at length. A plan providing for a general increase in dues for all grades (except Student) was prepared and proposed by Mr. Coggeshall, as chairman of the special committee on the subject, and another plan providing for increase in dues based on age was submitted by Treasurer Heising.

Following the discussion, the plan offered by Treasurer Heising was referred to the committee with the suggestion that the operations under the plan be projected to 1945 and to ten years thereafter for the purpose of showing the dues income for such periods.

Office Quarters: Both Treasurer Heising, as chairman of the Office-Quarters Committee, and President Turner reported on matters pertaining to the subject of larger quarters for Institute activities. Dr. Heising reported that additional buildings will be inspected by the committee as soon as possible.

President Turner referred to a recent letter from Mr. Van Dyck, suggesting that consideration be given to joining with other societies in the establishment of an engineering-and-science center, which would be a large building and serve as the national headquarters of the sponsoring organizations.

PROCEEDINGS: The action of the Executive Committee in authorizing an assistant to Associate Editor Stote was confirmed.

It was explained that the paper allotment, resulting from the granting of the Institute's recent appeal from the WPB Paper Limitation Order L-344, necessitates continuing the use of lightweight paper in the PROCEEDINGS and limiting the number of extra copies for new members to approximately 500. Editor Goldsmith stated that need existed for a further appeal which may be made later in the year.

Co-operation with Members in Foreign Countries: The October 13, 1943, letter from Mr. Alfred A. Fayers of England, suggesting closer association between American members visiting England and the members residing in the latter country, was read by President Turner.

Attention was called to the existing arrangement with the Wireless Section of the Institution of Electrical Engineers, providing for an exchange of facilities which enables American members to communicate with English members through the headquarters of the latter society.

Executive Committee

February 29 Meeting: The Executive Committee meeting, held on February 29, 1944, was attended by H. M. Turner, president; E. F. Carter, Alfred N. Goldsmith, editor; R. A. Heising, treasurer; F. B. Llewellyn, H. A. Wheeler, and W. B. Cowilich, assistant secretary.

Membership: The following applications for membership were approved for confirming action by the Board of Directors: for transfer to Senior Member grade, O. L. Angevine, Jr., Saul Dushman, G. M. Lohnes, J. E. Shepherd, and H. L. Tholstrup; for transfer to Member grade, R. W. Chapman, Harold Goldberg, J. G. O'Shea, and P. W. Spence; for admission to Member grade, F. H. Clarke, F. E. Maurtiz, D. H. Preist, and E. G. Sorensen; Associate grade, 115; and Student grade, 44.

Budget: Copies of the revised budget for 1944, accompanied by Secretary Pratt's letter of February 29, 1944, were distributed at the meeting. This budget was discussed at length and it was stated that the indicated 1944 surplus compared favorably with that resulting from 1943 operations. Following the discussion, the revised budget was recommended to the Board of Directors for adoption.

Winter Technical Meeting—1944: Mr. Harold A. Wheeler distributed copies of the February 25, 1944, report, along with the financial statement, which had been submitted by Dr. B. E. Shackelford, chairman of the 1944 Winter Technical Meeting. Attention was called by Mr. Wheeler to the surplus of $1416.13 resulting from that meeting. Following a further discussion, the report was accepted.

The Winter Technical meeting was considered to be one of the most successful of its kind held by the Institute, and Dr. Shackelford was complimented for his outstanding work in directing the affairs of the meeting.

Winter Convention—1945: Dr. Austin Bailey was named chairman of the general committee for the 1945 Winter Convention to be held during January, 1945, and was requested to organize the committee by appointing the additional members.

Sections

Fort Monmouth: The Assistant Secretary called attention to a recent inquiry concerning the formation of a Section at Fort Monmouth, New Jersey, and indicated that the information on the steps to be taken had been sent in reply.

London, Ontario: Treasurer Heising, as chairman of the Sections Committee, reported on the recent request for information on the constitutional procedure relative to forming a Section at London, Ontario.

After a discussion, the Assistant Secretary was instructed to supply the information and since the area of the proposed Section is now included in that of the Montreal and Toronto Sections, to communicate with the latter Sections regarding the factors involved in the formation of a London, Ontario, Section.

Connecticut Valley: President Turner read a letter from Mr. W. M. Smith, chairman of the Connecticut Valley Section, suggesting the division of that Section into three separate Sections as a result of traveling difficulties.

Treasurer Heising, as chairman of the Sections Committee, was asked to reply to the letter and to describe the constitutional procedure to be observed in bringing about the proposed division.

Rebates: In his capacity as chairman of the Sections Committee, Treasurer Heising reported that the Chicago, New York, and Washington Sections had requested an increase in the rate of rebate, because of the fact that their expenses exceeded the rebate income received from the Institute.

During the discussion, consideration was given to making the average annual rebate per member (based on those of Fellow, Senior Member, Member, and Associate grades) not less that 60 cents, and to amending By-laws Section 40 accordingly.

Instructions were given to prepare a plan that would provide for an increase in rebates on the order indicated above, and to submit such plan to the Board of Directors for further consideration.

Student Chapters: The subject of Institute activities in colleges was discussed and consideration was given to the advisability of extending such activities, now conducted largely by the appointed Institute of Representatives in Colleges, to include Student Chapters, or Branches. Following the discussion, it was unanimously agreed to recommend the Board of Directors have a committee study the situation and submit recommendations.

Institution of Electrical Engineers: President Turner read a letter from Mr. F. S. Barton, junior past vice-president of the Institute, concerning a possible visit from Dr. R. L. Smith-Rose for the purpose of promoting closer co-operation between the Wireless Section of I.E.E. and the Institute.

PROCEEDINGS: The employment of an assistant to Associate Editor Stote was authorized, subject to approval of the revised budget by the Board of Directors.

It was announced that the Institute's December 21, 1943, appeal from the WPB Paper Limitation Order L-244 was granted but made subject to the minimum ten per cent restriction applicable to all periodicals. By close figuring, the resulting paper allotment will permit publishing 128-page issues during 1944. It was stated that a further appeal may be necessary and accordingly be made later in the year.

Montreal Letter

March 14th, 1944

The Editor
PROCEEDINGS of the I.R.E.
New York, N. Y.

In May and June of 1943 some excellent letters were printed in the PROCEEDINGS concerning a proposal to amend the Constitution.

These discussed at length and with considerable wisdom the possible effects on the Institute of the adoption of new names for the various grades of membership and new qualifications for admission. Unfortunately this correspondence appeared in May and June—the off season—and it is doubtful if anyone read them.

A couple of enthusiasts in Montreal happened to notice them, called the attention of the Montreal Executive, and stirred up enough interest to warrant a special meeting in the heat of July.

However, in spite of our best efforts, the ballots were distributed and a "Yes" vote was carried by a small margin before the 1943–1944 season got under way again.

It is fairly certain that if all those entitled to vote really knew and understood what the issues were, the amendments would have been rejected. After discussion with various individuals in this Section (Montreal) it was not difficult to get sufficient signatures for a petition to the Board of Directors to make yet another amendment that it is believed will put our membership structure on a firm basis.

There is no doubt that some definite action was urgently required insofar as the Associate Grade was concerned. In technical societies, the Associate Grade is generally occupied by the rank-and-file members—the sturdy backbone of the society—and as our history shows, the Institute of Radio Engineers is no exception to this general rule. However, we had an impossible situation. On the one hand, the Associate Grade was open to all comers so long as they were

"interested in radio" and yet on the other hand, Associates were divided into two groups by an entirely artificial barrier—viz., date of admission—before or after March, 1939, the one group having voting rights, the other none at all.

The new qualifications for membership seem to us to have fixed this matter in every respect but one—and that is the all-important matter of names. It might reasonably be expected that the grades of Fellow and Member would stay where they were, that the Associate Grade would be revised to exclude all but professional radio engineers and that these would be given a new name. Instead of this, the change introduces a new and very doubtful title for those previousy called Members and condemns the name Associate to apply to those who cannot qualify as professional men. This can hardly be considered as a help to the prestige and standing of the Institute. The change now suggested by Montreal accepts the qualifications as laid down by the last amendment but proposes the following names:

FELLOW: As before.

MEMBER: As in most other similar societies, a grade to distinguish the more responsible mature and well-established members of the Institute—essentially as it was prior to the 1943 amendment.

ASSOCIATE: Again, as is the custom in other technical societies, this is the name proposed for those who are definitely professional engineers of proved competence who will represent the backbone of the Institute.

AFFILIATE: To designate those individuals who are interested in radio but are not qualified professional radio men.

Some opposition to these proposals may of course appear from those Associates who may be hopefully looking forward, as the outcome of the last amendment, to the exalted title of Member without any further effort on their part.

However, brief consideration on their part will show them that the supposed advantage of the new title is likely to vanish into thin air when it is finally recognized that this title covers the vast majority of the membership and all that will have been accomplished will be a lowering of the prestige of the whole Institute.

For these reasons I am confident that IF THE ISSUES ARE WELL UNDERSTOOD the latest amendment will be passed by an overwhelming majority.

Yours very truly,
L. T. Bird, Chairman,
Montreal Section

Books

The Technique of Radio Design, by E. E. Zepler

Published (1943) by John Wiley and Sons, Inc., 601 W. 26 St., New York 1, N. Y. 305 pages + 8-page index + xii pages. 260 figures. $5\frac{1}{2}\times 8\frac{1}{2}$ inches. Price, $3.50.

This is, to the reviewer's knowledge, the first formal attempt to make available to the technical student, real, down-to-earth information on radio receiver design. While the title indicates that the scope might extend beyond this, it seems, nevertheless, to be the author's intention to confine himself to the particulars of radio receiver design.

The book is invaluable and a major contribution as a text for an academic radio receiver design course. The reason that it is primarily a classroom text is that it is not easy reading as such. The subject matter is done in such a way that it should be supplemented with classroom discussion so as to crystallize the highly intensified nature of the information given in the book. As in any art, this reviewer believes that there is in radio receiver design no substitute for practical experience. However, conscientious classroom textual study of the author's book, complemented by radio laboratory work on complete receiver chassis, would certainly go a long way toward bridging the gap.

The organization and indexing of the book is splendidly done. In fact, this very excellence in indexing points out some of the weaknesses which have practical significance. For instance, the author makes very quick work of the subject of spurious microphonic disturbances, yet any practical designer knows that this difficulty is a major problem in any design. Another omission in the book is in the absence of any reference to electric phonograph technique. This is so much a part of modern radio receiver design that its omission is felt.

This reviewer feels that the art owes to the author a sincere vote of thanks for his courage and painstaking labors in preparing this much-needed and valuable treatise.

DORMAN D. ISRAEL
Emerson Radio and Phonograph Corporation
New York 11, N. Y.

Radio Receiver Design, Part I, by K. R. Sturley

Published (1943) by John Wiley & Sons Inc., 601 W. 26 St., New York 1, New York. 421 pages + 14-page index + xii pages. 187 illustrations. $5\frac{3}{4}\times 8\frac{1}{2}$ inches. Price $4.50.

This is a new book which is intended to cover the fundamentals of radio receiver design. It has been divided into two parts, of which Part I covers radio receiver design from antenna through detection. The coverage or scope of the book can be visualized from the titles of the eight chapters which comprise the manuscript of Part I. These are:

Chapter 1—General Considerations, 17 pages.
Chapter 2—Valves, 40 pages.
Chapter 3—Aerials and Aerial Coupling Circuits, 62 pages.
Chapter 4—Radio-Frequency Amplification, 58 pages.
Chapter 5—Frequency Changing, 63 pages.
Chapter 6—Oscillators for Superheterodyne Reception, 48 pages.
Chapter 7—Intermediate-Frequency Amplification, 51 pages.
Chapter 8—Detection, 65 pages.

Audio-frequency amplifiers, power supplies, receiver measurements, television, and frequency-modulation receiver design, are dealt with in Part II, which is not covered in this review. The order of treatment is probably open to objection on the ground that the student would undoubtedly follow a somewhat different order than that employed by the author. However, the author recognizes this limitation and mentions it in the author's preface. This difficulty has been largely overcome by a detailed contents section, covering some six pages. The titles of the various paragraphs are highly descriptive and in sufficient detail that they may be used for ready reference by the reader who wishes to skip about in the book or follow a more logical sequence in reading it. As an example of this detail, Paragraph 8.2 in Chapter 8 relating to diode detection, is listed as follows in the contents section:

8.2 Diode Detection
1. Introduction
2. Characteristic Curves
3. The Effect of the Coupling Impedance from Diode to Audio-Frequency Amplifier
4. Input Circuit Damping
5. Equivalent Damping Resistance Due to Diode with a Linear I_aE_a Characteristic
6. Equivalent Damping Resistance for Conduction Current Beginning at a Negative Anode Voltage
7. Conduction Current Beginning at a Positive Anode Voltage
8. Equivalent Damping Resistance Due to a Diode with a Parabolic I_aE_a Characteristic Curve
9. Conduction Current Beginning at a Negative Anode Voltage
10. Damping and the Preceding Radio-Frequency Amplifier Stage
11. Effect of the Capacitance in Shunt with the Load Resistance
12. Detection Efficiency and Effective Resistance for a Linear Diode with no Shunt Capacitance
13. Effect of Shunt Capacitance on Detection Efficiency
14. Amplitude Distortion Due to a Large Value of Shunt Capacitance
15. Frequency Distortion Due to the Shunt Capacitance
16. The I_mE_a Characteristic Curves for a Linear Diode Conducting at $E_a=0$.

While the order of the book may not be ideal from the standpoint of the student, it is entirely satisfactory for reference work. From the standpoint of the student the subject matter is well chosen and comprehensive. The author appears to have covered the planned scope of the text rather amply. One criticism which might be leveled at the book lies in the choice of topics, which are to be treated in detail at the expense of other important topics. It is this reviewer's opinion that automatic volume control, squelch circuits, and limiters for noise

reduction in amplitude-modulated receivers deserve considerably more space than the author has given to them. It is believed that this will be particularly noticeable if the text is used as a reference book. From the view of the student this deficiency is not so apparent, and could perhaps be eliminated entirely by use of the bibliographical material supplied at the end of each chapter. While these bibliographies are all brief, the author has shown excellent discrimination in picking some of the most pertinent art in the English language for reference purposes. It might be expected that an American reader would have some difficulty with English terminology and terms. However, the author has used commonly accepted terminology generally used in the technical press of this country throughout the book.

The expression $E_{\cos\omega t}$ for a voltage of sinusoidal wave shape is used in the text nstead of the sine expression because it eads to a simpler mathematical analysis. For similar reasons the author expresses grid-bias voltage as $-E_b$, where E_b represents an arithmetic rather than algebraic value of bias.

The book is reasonably comprehensive, interestingly written, and appears to be free of errors. While there is a considerable amount of mathematics in the book, all of it is very readable, and should be understood by any student with a knowledge of the calculus. In fact, a knowledge of algebra and plane trigonometry would be entirely sufficient for reading most of the book. The book was written in 1942, and as a result is reasonably up-to-date and includes a great deal of modern information not generally available in textbook form.

This reviewer was particularly impressed with the choice of material and the logical presentation. The chapters on "Aerial and Aerial Coupling Circuits" and "Diode Detection" are both impressive in choice of subject matter and detail of coverage. Both of these sections include material not generally available to the student in textbook form.

This information given in the book is presented in clear and readable fashion. The order of presentation is not the most appropriate from the standpoint of some readers, but this defect is largely overcome by the detailed index and contents section. There appear to be no inconsistencies between sections nor any serious repetitions of subject matter in the book. It is this reviewer's opinion that this book should fill a need as a reference book because of its simplified and logical discussions, as well as because of the author's choice of topics for emphasis. Some of the topics treated most fully by Mr. Sturley have received very little consideration in recently published books, and some of them have not been treated fully in the technical press.

F. X. Rettenmeyer
Radio Corporation of America
Camden, New Jersey

Contributors

James J. Adams (A'36) was born on July 7, 1912, in Sioux Falls, South Dakota. He received a B.S. degree in electrical engineering from the University of Colorado in 1934 and the M.S. in electrical

J. J. Adams

engineering from the same school in 1935. From 1936 to 1938 he was employed as a radio engineer with the Philco Radio and Television Corporation. Since 1939 he has been with the Zenith Radio Corporation.

❖

Louis R. Bloom was born in May, 1914, at Chicago, Illinois. He received the B.S. and M.S. degrees from the University of Illinois in 1938 and 1941, respectively. During 1939–1943 he was a member of the research staff of the electrical engineering

Louis R. Bloom

Experiment Station of the University of Illinois. He assisted in the development of photoelectric tubes and electronic equipment. He has recently taken a position with the special development division of the RCA-Victor Division, Lancaster, Pa. Mr. Bloom is a member of the American Association for the Advancement of Science, and Sigma Xi.

❖

Milton Dishal (A'41) was born on March 20, 1918, in Philadelphia, Pennsylvania. He received the B.S. degree from Temple University in 1939, and the M.A. degree in physics from Temple University in 1941. From 1939 to 1941 Mr. Dishal was a Teaching Fellow in physics at Temple University. In 1941, while taking graduate courses in electrical engineering at Columbia University, he was employed by the Research Mission Federal Telephone and Radio Laboratories where he now is assistant engineer engaged in the development of wide-band, ultra-high-frequency receivers.

Milton Dishal

❖

Gabriel Krøn was born on July 23, 1901, in Hungary. He received the B.S. degree in electrical engineering from the University of Michigan in 1924 and the Honorary M.S. degree in 1936. Mr. Kron has engaged in design, research, and development work with Robbins and Myers, Lincoln Electric, Westinghouse, and several other electrical companies both in this country and abroad. Since 1934, he has been with the General Electric Company, serving in the capacity of consulting engineer since 1938.

GABRIEL KRON

❖

Humboldt Walter Leverenz was born in Chicago, Illinois, in 1909. He received a B.A. degree in chemistry from Stanford University in 1930. During 1930–1931 he studied physics and chemistry at the University of Munster, in Westphalia, Germany, as an exchange fellow of the Institute of International Education. Since 1931, Mr. Leverenz has conducted chemicophysical research on sensitive materials, responsive to light and electrons, for the Radio Corporation of America. He is a Fellow of the American Physical Society, and a Member of the American Chemical Society, the Franklin Institute, Sigma Xi, Alpha Chi Sigma, and Phi Lambda Upsilon.

❖

Simon Ramo (A '38) was born in Salt Lake City, Utah on May 7, 1913. He received the degrees of B.S. in E.E. from the University of Utah in 1933 and Ph.D. from California Institute of Technology in 1936. Since that time Dr. Ramo has been with the General Electric Company in Schenectady where he is now a member of the electronics laboratory.

❖

David L. Shapiro was born in New York City, on August 25, 1921. He received the

DAVID L. SHAPIRO

B.S. degree in electrical engineering from Massachusetts Institute of Technology in June, 1941. He was with the United States signal Corps for one year and has been with Hazeltine Electronics Corporation since, working on apparatus development.

❖

Joseph T. Tykociner (M'21-SM'43) was born in Vloclavek, Poland, on October 5, 1877. He was graduated from the Higher Technical Institute at Coethen in 1901 and studied in Berlin and Goettingen, Germany. During 1902–1903 he was with the Marconi Wireless Telegraph Company at Chelmsford, England; 1904, research engineer with the Telefunken Wireless Telegraph Company in Berlin; in 1905 he organized a radio department in Russia for the Russian Siemens Company in St. Petersburg; was engineer-in-chief of this department from 1905 to 1908 and manager of the same department including a research laboratory from 1908 to 1918; during 1904–1918 he was active in developing and installing radio equipment for the Russian Navy, Army, and the Ministry of Posts and Telegraphs; research work at the Radiological Laboratory in Warsaw, expert for Radiocommunication at the State Department of Posts and Telegraphs, Warsaw, Poland, 1919; and research engineer at the Westinghouse Electric and Manufacturing Company, 1920–1921. Since

❖

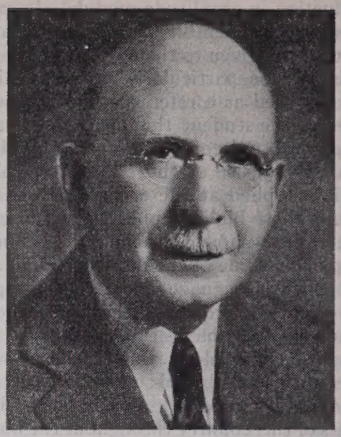

JOSEPH T. TYKOCINER

1921 he has been research professor of electrical engineer at the Engineering Experiment Station of the University of Illinois, Urbana, Ill., and professor of the Graduate School since 1929. His investigations include sound motion pictures, antenna models, high-frequency measurements, dielectrics, piezoelectricity, photoelectric tubes, and microwaves. Professor Tykociner is a Fellow of the American Physical Society, American Society for the Advancement of Science, Active Member of Sigma Xi, and a member of Engineering Societies.

❖

Alan Watton, Jr., (A'43) was born on August 9, 1915, in Seattle, Washington. He received the B.S. degree in electrical engineering with a minor in physics from the University of Washington in 1939. From 1939 to 1942, he was employed in a civilian capacity by the Army Air Forces at the propeller laboratory, engineering division, Wright Field, Dayton, Ohio, engaging in the development of electronic apparatus used in propeller-vibration stress measurements. Since 1942, he has been on active duty with the Army Air Forces, stationed at Wright Field, engaged in similar work.

Lieutenant Watton is a member of the American Institute of Electrical Engineers and the Acoustical Society of America.

H. W. LEVERENZ

SIMON RAMO

ALAN WATTON, JR.